Emerging Technologies in Optical Sciences

ETOS 2004

University College Cork, Ireland

JULY 26-29, 2004

REPORT DOCUMENTATION PAGE

Form Approved OMB No. 0704-0188

1. REPORT DATE *(DD-MM-YYYY)*
12-09-2006

2. REPORT TYPE
Conference Proceedings

3. DATES COVERED *(From – To)*
26 July 2004 - 29 July 2004

4. TITLE AND SUBTITLE
Proceedings of the Conference on Emerging Technologies in Optical Sciences

5a. CONTRACT NUMBER
FA8655-04-1-5067

5b. GRANT NUMBER

5c. PROGRAM ELEMENT NUMBER

6. AUTHOR(S)
Guillaume Huyet and Jerome Moloney, Eds.

5d. PROJECT NUMBER

5d. TASK NUMBER

5e. WORK UNIT NUMBER

7. PERFORMING ORGANIZATION NAME(S) AND ADDRESS(ES)
University College Cork
Kane Building
Cork
Ireland

8. PERFORMING ORGANIZATION REPORT NUMBER
N/A

9. SPONSORING/MONITORING AGENCY NAME(S) AND ADDRESS(ES)
EOARD
PSC 821 BOX 14
FPO 09421-0014

10. SPONSOR/MONITOR'S ACRONYM(S)

11. SPONSOR/MONITOR'S REPORT NUMBER(S)
CSP 04-5067

12. DISTRIBUTION/AVAILABILITY STATEMENT
Approved for public release; distribution is unlimited. (approval given by local Public Affairs Office)

13. SUPPLEMENTARY NOTES

14. ABSTRACT
The Final Proceedings for Conference on Emerging Technologies in Optical Sciences, 26 July 2004 - 29 July 2004

Dilute Nitrides, Generation and Propagation of Short Pulses, High Power Semiconductor Lasers , Microcavities, Photonic Crystals, Photonic Crystal Fibers, Photonic Systems, Quantum Dot Based Devices, Simulations of Photonic Devices

15. SUBJECT TERMS
Semiconductor lasers, photonics, photonic devices, EOARD

16. SECURITY CLASSIFICATION OF:			17. LIMITATION OF ABSTRACT	18, NUMBER OF PAGES	19a. NAME OF RESPONSIBLE PERSON
a. REPORT	b. ABSTRACT	c. THIS PAGE			BARRETT A. FLAKE
UNCLAS	UNCLAS	UNCLAS	UL	117	19b. TELEPHONE NUMBER *(Include area code)* +44 (0)20 7514 4285

Standard Form 298 (Rev. 8/98)
Prescribed by ANSI Std. Z39-18

Dear Participants

We are delighted to welcome you to the first conference on Emerging Technologies in Optical Sciences at University College Cork. We hope that you will enjoy your time in Cork and benefit greatly from the oral and poster presentations.

We wish to thank the following for their contribution to the success of this conference: Science Foundation Ireland, Enterprise Ireland, European Office of Aerospace Research and Development of the USAF, the Physics Department of University College Cork, Butler Technologies and Rohde & Schwarz.

This conference would not have been possible without the dedicated efforts of Natasha Pokrovskii, Thomas Busch and Robin Gillen and we express our sincere thanks to them. We would also like to acknowledge Olwen Carroll, Martina Connolly, Stephen Hegarty, John Houlihan, David O'Brien, Shane O'Donoghue, Tomasz Piwonsky and Yann Tanguy.

We also thank and acknowledge Brian Corbett, David Cotter, Gabriel Crean, John McInerney and Eoin O'Reilly for their help on the scientific committee.

Guillaume Huyet and Jerome Moloney

Our Sponsors

University College, Cork

sfi

science foundation ireland

fondúireacht eolaíochta éireann

ENTERPRISE

IRELAND

Butler

TECHNOLOGIES

ROHDE&SCHWARZ

Modeling and Simulation of Polarization and Spatial Effects in Broad-area Vertical-Cavity-Surface-Emitting Lasers

T. Ackemann[1], M. Sondermann[1], T. Rössler[2], and J. V. Moloney[2]

[1] *Institut für Angewandte Physik, Westfälische Wilhelms-Universität Münster, Correnstraße 2/4, 48149 Münster, Germany*

[2] *Department of Mathematics, University of Arizona, Tucson, Arizona 85721, USA*

The spatial and temporal coherence of broad-area semiconductor lasers is typically rather limited due to spatio-temporal instabilities with a very complex phenomenology. Modeling of these phenomena is a challenging and computationally expensive task due to the complicated processes influencing the dielectric polarization of semiconductors and the large span of spatial and temporal scales involved. Compared to edge-emitting devices, the complexity is even enhanced in vertical-cavity surface-emitting lasers (VCSELs), since polarization degrees of freedom are easily excited.

In this contribution, a microscopically-based dynamical model for a VCSEL is introduced that consistently accounts for the vector nature of the field, includes the quantum well gain dispersion and spin degrees of freedom, and realistically treats the losses arising due to reflection of the fields from the distributed Bragg reflectors (DBRs). It considers the conduction band, the heavy-hole band and the light-hole band (including the spin degeneracy) in a free-electron approximation.

The polarization anisotropy of the DBRs at nonzero transverse wave vectors is identified as the principal cause for the field polarization preference near threshold. In numerical simulations of native-oxide confined broad-area VCSELs with a square aperture, the polarization is found to be orthogonal to the wave vector of the single-frequency stripe-like standing-wave pattern emerging at threshold. At higher pump levels a polarization instability sets in. Modes with both the orthogonal polarization and orthogonal wave vector appear. After the bifurcation the two polarization modes have about the same average amplitude. The time averaged total intensity shows a square pattern. The spectral features associated with the instability are investigated.
These findings are in very good agreement with experimental observations in broad-area square VCSELs [1].

Motivated by the experimental results discussed in [2], the formation of flower-like patterns in circular VCSELs is studied. The influence of the radial shape of the pump profile and of spatial noise in the pump profile is discussed.

[1] Hegarty et al., Phys. Rev. Lett. **82**, 1434 (1999)
[2] Ackemann et al., J. Opt. B. **2**, 406 (2000)

Effect of dot shape and size on ground state optical matrix element in InAs/GaAs quantum dots

A. D. Andreev[(1)] and E. P. O'Reilly[(2)]
[(1)] *Department of Physics, University of Surrey, Guildford, GU2 7XH, U.K.*
[(2)] *NMRC, University College Cork, Lee Maltings, Cork, Ireland.*

We present a theoretical analysis of the optical matrix element between the electron and hole ground states in InAs/GaAs quantum dots (QDs) modelled with a truncated pyramidal shape. We use a plane-wave expansion method based on an 8-band **k·P** Hamiltonian to calculate the QD electronic structure, with strain and piezoelectric effects fully taken into account through Green's function and Fourier transform techniques. We found for many dots that the **k**-dependence of the bulk optical matrix element is the main physical reason for the reduction in optical matrix element compared to that initially expected in an ideal QD. We demonstrate that the ground state optical matrix element is very sensitive to variations in both the QD size and shape. For all dot shapes, the matrix element initially increases with increasing dot height, as the electron and hole wavefunctions become more localised in k-space (extended in real space). Depending on the QD aspect (base to height) ratio and on the degree of pyramidal truncation, the matrix element then reaches a maximum for some dot shapes at intermediate dot size beyond which it decreases abruptly in larger dots, where piezoelectric effects lead to a marked reduction in electron-hole overlap. However, for some QD aspect ratios, the matrix element continues to increase with dot height even to relatively large heights. It should therefore be possible to engineer the size and shape of QDs with the aim to increase and optimize the optical gain in QD lasers and optical amplifiers. In particular, "flat" QDs with a large aspect ratio have a larger optical matrix element. We conclude that, depending on the QD geometry, the piezoelectric field may either have little noticeable effect on the ground state matrix element or else will markedly reduce the matrix element, effectively switching off the ground state optical transition in some QDs. This work was supported by Science Foundation Ireland and by EPSRC (U.K.)

Radiative recombination in InAs-based Quantum Dot Lasers: dependence on carrier density and dot parameters

A. D. Andreev[1] and E. P. O'Reilly[2]

[1] *Department of Physics, University of Surrey, Guildford, GU2 7XH, U.K.*

[2] *NMRC, University College Cork, Lee Maltings, Cork, Ireland.*

The aim of this paper is to study theoretically the radiative recombination rate in InAs/GaAs QDs and its dependence on the carrier density and QD shape and size. Our analysis is based on an 8-band **k.p** model using a plane wave expansion method. Three-dimensional strain and piezoelectric field distributions are fully taken into account through a Green's function and Fourier transform-based technique. We define the radiative recombination coefficient as $B(N)=R/N^2$, where R is the total radiative recombination rate. We consider InAs QDs with a truncated pyramidal shape. We show for InAs quantum dots that, in contrast to quantum well and bulk samples, the radiative recombination coefficient B usually depends strongly on the carrier density N. The coefficient B is also sensitive to variations in the quantum dot shape and size, and to the amount of inhomogeneous broadening in the sample. We demonstrate that these effects occur because the optical matrix element for an interband transition between the ground state electron and hole levels in a quantum dot is usually larger than the matrix element between the excited electron and hole states (see Fig.1). This means that the conventional approximation that the total radiative recombination rate varies as B_0N^2 does not work for QD laser structures.

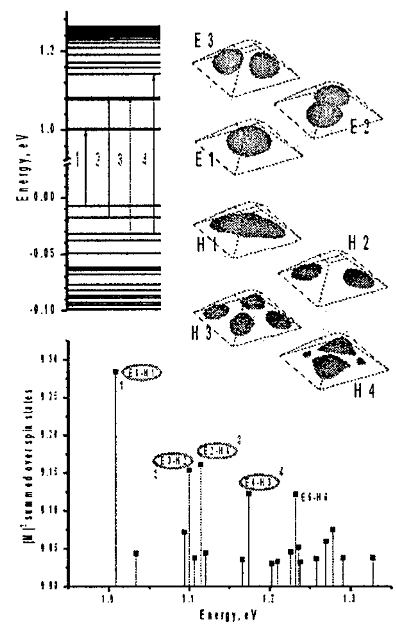

Figure 1: Calculated energy spectrum, wave functions and optical transition matrix elements for an InAs truncated pyramid QD in a GaAs matrix, with QD height 5.5 nm, base length 16 nm and top length 4 nm. The arrows between the electron and hole energy levels show the four strongest electron-hole transitions, with the corresponding matrix elements highlighted in the lower part of the figure. We also show calculated surfaces of constant probability density $|\psi|^2$ for the first few electron and hole states.

Recent progress on semiconductor photonic crystal devices

Toshihiko Baba
Yokohama National University

This talk presents recent theoretical and experimental studies on semiconductor photonic crystal devices. It covers the observation of Purcell effect in single defect nanocavity, lasing action in quasiperiodic structures, efficient light extraction in (O-)LEDs by easy process, high power single-mode VCSELs, group delay and dispersion control device based on chirped waveguides, integration with high index contrast waveguides, active waveguides, tuning of transmission characteristics, superprism filter with optimized interfaces and so on.

Development of ultra-short pulse sources for high-speed photonic system

Liam Barry
Dublin City University, Dublin, Ireland

The development of ultra-short optical pulse sources is vital for the future implementation of high-speed optical communication systems using Wavelength Division Multiplexing and Optical Time Division Multiplexing technologies. This talk will focus on recent work that has been undertaken to develop optical pulse sources that have sufficient spectral and temporal purity to be used in practical optical communications systems operating at data rates in excess of 100 Gbit/s.

On the noise properties of quantum dot optical amplifiers

Alberto Bilenca and Gadi Eisenstein

Electrical Engineering Dept., TECHNION - Israel Institute of Technology, Haifa 32000 ISRAEL
bilenca@tx.technion.ac.il

Abstract: We describe a theoretical study of noise in quantum-dot optical amplifiers. We consider nonlinear (FWM-like) noise-signal interactions and examine the impact of fast carrier dynamics and inhomogenous gain on optical noise and RIN spectra. The results are consistent with published noise saturation spectra.

The unique properties of quantum dot (QD) based optical gain media: inhomogeneous gain broadening, fast carrier dynamics and a low α parameter are known to affect the static and dynamic characteristics of QD optical amplifiers[1, 2] (QD-SOA). The same basic QD characteristics also determine the noise properties which are intimately related to gain and saturation. However, noise in QD amplifiers has not received much attention to date. Of special interest is the noise of nonlinear QD amplifiers because of the potential advantages of QD optical amplifiers as broadband all-optical switches[3].

This paper describes a theoretical study of noise in QD-SOAs. We address the optical noise (ASE) as well as the RIN and examine the roles played by operating conditions and various physical parameters. Our noise spectra calculations show a good qualitive fit to published measurements of saturated ASE spectra in QD amplifiers[1, 2]. We also examine the effect of the wetting layer (WL), which serves as a carrier reservoir, on the effective rate of the carrier pulsation process which is responsible for the FWM-like interaction between the saturating signal and the noise[4].

The model considers a QD-SOA consisting of inhomogeneously broadened M ground states (having resonance frequencies ω_j^{GS}, $1 \leq j \leq M$) which interact with an applied electric field ($\hat{E}$ centered about ω_s) via the nonlinear polarization and with a carrier reservoir by a detailed balance of carrier capture and escape. The carrier dynamics of the reservoir (eq. (1)) and the ground state of the j-th dots group (eq. (2)) are governed by the following set of coupled rate equation derived of the density-matrix formalism

$$\frac{\partial N_W}{\partial t} = \eta_j \frac{J}{qd} - \frac{V_D'}{V_W} N_W \sum_{j=1}^{M} G_j \frac{1-P_j}{\tau_{cap}^0} + \sum_{j=1}^{M} N_j \frac{D_W}{D_g N_D} \frac{V_D}{V_W} \left(1 - \frac{N_W}{2D_W}\right) \frac{1}{\tau_j^{esc}} - \frac{N_W}{\tau_W} \tag{1}$$

$$\frac{\partial N_j}{\partial t} = N_W G_j \frac{1-P_j}{\tau_{cap}^0} - N_j \frac{D_W}{D_g N_D} \left(1 - \frac{N_W}{2D_W}\right) \frac{1}{\tau_j^{esc}} - \frac{N_j}{\tau_{GS}} - \frac{\Gamma\gamma}{\hbar\omega} g_j^{peak} \mathrm{Re}\left\{ \bar{E} \cdot \left[\bar{E}^* \otimes e^{-\left(i\left(\omega_s - \omega_j^{GS}\right)+\gamma\right)t} u(t) \right] \right\} \tag{2}$$

where G_j is the fraction of the j-th QD group type within an ensemble of different dot size populations (assumed to be Gaussian distributed), $P_j = N_j / 2D_g N_D G_j$ the occupation probability of the ground state of the j-th QD group and $g_j^{peak} = 2a_j^G(\omega)(N_j - D_g N_D G_j)$ its gain coefficient peak value. All others parameters have their common physical meaning. The field ($\bar{E}$) evolution is calculated from a typical propagation equation containing a Langevin noise term[4] describing the spontaneous emission process. Using first-order perturbation analysis, we derive the optical and intensity noise spectra at the output of the amplifier due to the injection of a single CW signal. The results shown hereon use practical physical parameters which are based on experimental data taken from the literature.

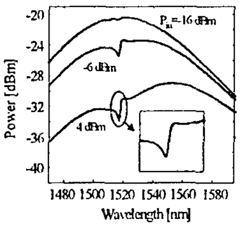

Fig. 1 – Optical spectra for different input powers, λ_{peak}=1517 nm and α=1.5

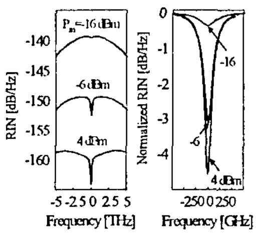

Fig. 2 – RIN spectra for different input powers, λ_{peak}=1517 nm and α=1.5.

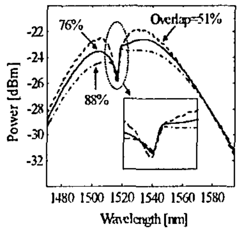

Fig. 3 – Optical spectra for several spectral overlaps

Fig. 1 and 2 show calculated optical noise and RIN spectra, respectively, for a signal injected at the gain peak, λ_{peak}=1517 nm, and for several input powers. The shift of the gain peak towards long wavelength is due to state filling while the asymmetry near λ_{peak} is due to the Bogatov effect[5] and diminishes when the α parameter becomes zero (α=1.5 in the example shown). These spectral effects were reported in ref. [1] and [2]. The RIN suppression near λ_{peak} exhibits two slopes, one is determined by the spectral hole burned in an inhomogeneously broadened medium and the second is due to the mixing between noise and signal[4]. The noise reduction increases with power and extends over ~1 THz due to stimulated emission and the fast carrier dynamics of the QD gain medium.

Different QD groups are coupled via the WL and by the spectral overlap between their respective homogeneously broadened gain spectra. Fig. 3 describes the optical noise spectrum for several degrees of overlap between energetically close QD groups. The burned spectral hole is more pronounced for low overlap values (i.e., for a more inhomogeneously broadened gain medium) and, as seen in the insert, the efficiency of the population pulsation dynamics increases due to the discrete nature of the dot states.

The role of the WL itself and is examined in Fig. 4. As expected, a smaller WL causes a carrier injection bottleneck which results in a longer response time and hence a narrower bandwidth of the nonlinear signal – noise interaction.

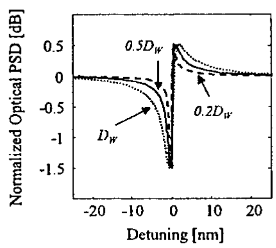

Fig. 4 – Optical spectra normalized to the broadband optical noise spectra for several number of states of the WL (D_W).

To conclude, we presented a theoretical noise analysis of QD-SOAs. Nonlinear noise-signal interaction, gain inhomogeneuity, fast carrier dynamics, WL size and injected power levels have been considered. The calculated optical spectra are consistent with published noise saturation spectra of QD-SOAs.

- This work was partially supported by the BigBand project within the fifth framework of the EU.

[1] Bakonyi et al., IEEE JQE, 34, p. 1409, 2003.
[2] Nambu et al., Jpn J. Appl. Phys., 38, p. 5087, 1999.
[3] Sugawara et al., Meas. Sci. Tech., 13, p. 1683, 2002.
[4] Shtaif and Eisenstein, IEEE JQE, 32, p. 1081, 1996.
[5] Bogatov et al., IEEE JQE, 11, p. 510, 1975.

Microsphere Laser made from Erbium doped ZBLALiP and optical proprieties of an array of microspheres

Mohamed Boustimi*, Ruth Carey and Síle Nic Chormaic

Department of Applied Physics and Instrumentation, Cork Institute of Technology, Rossa Avenue, Bishopstown, Cork, Ireland.

For miniaturising microelectronic and optoelectronic devices, a lot of theoretical and experimental work had been devoted to mesoscopic systems such as microspheres, micro-rings, micro-cylinders etc. [1-3]. Among them, microspheres are used more because it is easy to produce and manipulate them.

Here, we are interested in two new types of microspheres: fluoride glasses, ZBLAN and ZiBLaLiP, doped in Er3+ or Yb3+ ions, which we fabricate in collaboration with the Optronics Laboratory, ENSSAT, France. The microspheres are pumped with laser light at either 975 nm or 1480 nm and emit light in the 1550 nm region. The pump laser and the microspherical laser emission are coupled into and out of the microsphere modes using a tapered fibre, obtained by heating and stretching a standard single mode optical fibre. When the taper is suitably close to the microsphere an overlapping of the evanescent field of a phase-matched optical waveguide with the evanescent field of the whispering gallery modes (WGMs) within the microsphere occurs.

The WGMs are strongly confined electromagnetic waves, which propagate around the internal surface of the sphere. Photons remain trapped for a long time within the microsphere (a few hundred µs) and this offers very high quality factors (Q > 108) for this type of resonator. This property makes such microspherical lasers very interesting and explains why numerous works in both applied and fundamental research has appeared in recent years.

Some experimental results will be presented here for such fluoride glass microspheres. This will show the laser emission for different concentrations of erbium or ytterbium ions (from 0.05% at 0.8% by mole). The microsphere lasers which have the highest efficacy, i.e. the optimal concentration in erbium or ytterbium, are used to study the mutual influence due to the evanescent wave overlap between two microspheres situated in proximity to each other and how this affects the optical transmission of these systems. These results will help us to study the optical proprieties of a sequence of periodically spaced microspheres taking into account the coupling effect of whispering gallery mode lasing.

[1] S. Gianordoli, L. Hvozdara, G. Strasser, W. Schrenk, K. Unterrainer and E. Gornik, Appl. Phys. Lett. 75, 1045-1047 (1999)

[2] T. A. Ibrahim, W. Cao, Y. Kim, J. Li, J. Goldhar, P. T. Ho and C. H. Lee, J. Lightwave Tech. 21, 2997-3003 (2003).

[3] Z. P. Cai, H. Y. Xu, G. M. Stephan, P. Feron, M. Mortier, Opt. Commun. 229, 311-315 (2004).

*mboustimi@cit.ie

Planar microcavities: Physics and recent applications

Louise Bradley
Physics Department, Trinity College Dublin

Microcavity structures, through modification of the density of photon modes, provide a means for enhancing light-matter interaction. Control of this interaction can result in a myriad of phenomena. For example, modified spontaneous emission far field patterns and decay rates, enhanced non-linear phenomena and Rabi splitting in the strong coupling regime. Some of this physics has been exploited in resonant cavity light emitting diodes and photo-detectors. The presentation will review recent work, in particular the development of two-photon-absorption enhanced microcavity photo-detectors. These novel devices are of particular interest for autocorrelation and optical-time-division-multiplexing applications

Waveguide devices for biosensor and chemical applications using Refractive Index changes.

D.Brennan[1], N.Freeman[2], D.Hoffman[1], J.O'Brien[1], M.Loughran[1],G. Crean[1]

[1]Biophotonics Team, NMRC, Lee Maltings, Prospect Row, Cork, Rep. Of Ireland

[2] Farfield Sensors Ltd, Unit 51, Salford Business Park, Leslie Hough Way

Salford, Manchester, M6 6AJ.

email: dbrennan@nmrc.ie http://www.nmrc.ie/

Abstract

We outline the fabrication, integration and test of a sensor based on waveguide technology [1]. The device is fabricated using standard CVD techniques to deposit thin layers of varying refractive index. The device is composed of two waveguides which act as a coherent source when exposed to radiation an interference pattern can be observed in the Farfield, these fringes are observed to change position as refractive index changes in the sensor window.

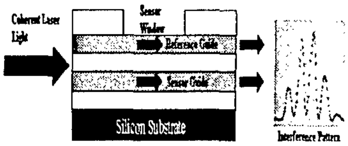

Figure 1: *Outlined is the sensor layout with a typical Farfield interference Pattern.*

The fabrication of the sensor device has two stages the deposition of waveguide layers and the opening of a sensor window in the top clad layer using a plasma etch process. The device wafer is diced and cleaved along optical interfaces to give individual devices.

A microscope objective (x10) is used to couple light into the wave guide from a He-Ne laser source. The interference pattern from the two waveguides is captured on a CCD array (255 pixels) linescan camera, where changes in fringe position are recorded. The flow of liquids with varying refractive index in the sensor window results in a phase shift in the interference pattern.

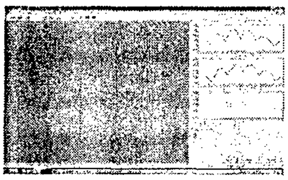

Figure 2: *Outlined is the image recorded on a CCD camera in the Farfield with a waveguide device.*

The sensor system can also monitor thin films deposited on the sensor surface (e.g Biolayers). Changes in structure or size of the biolayer will present a change in refractive index. The micro fluidic system was designed to present nano-litre volumes to the sensor from a capillary separation column [3].

The integration of fluidic and optical components present a challenge from material and bonding approaches [2].

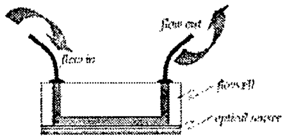

Figure 3: *The optic and fluidic components are integrated using a polymer bond technique.*

Two integrated Microsystems were tested with cell volumes of 5.6nl and 30nl respectively. The liquid delivery system was as outlined in section 2. Prior to system test the flow-cell was allowed to "wet " for one hour, once primed the flow through the fluidic system was stable and impact from air bubbles was minimal. The first test carried out was to determine the response of the integrated system to changes in R.I and compare it to a conventional measurement set-up with 1.5μl volume flow-cell, the response on this standard system is 93 radians for water to IPA transitions.

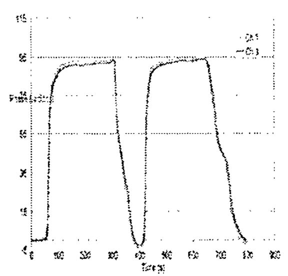

Figure 4: *The sensor response on the 3nl cell with transitions of IPA to DI water in the fluidic system.*

Figure 4, illustrates the phase change from DI water to IPA on the 5.6nl flow-cell, the measured response of 24 radians, was obtained for the sample transition. The second device tested was a micro-system with 30nl cell volume the response was 92 radians, to the same test. The performance of the larger micro-system compares well to the standard system while the performance of the smaller cell degrades by a factor of three. This could be explained by the effect of stray light in the smaller cell volume, alignment of smaller windowed chips with low volumes is more critical than larger windowed chips with high volumes.

Conclusion

The design and fabrication of an integrated microfluidic platform has been demonstrated using microelectronics technology. The materials and methods used for integration are compatible with existing fabrication techniques. Three bond approaches were tested, anodic bonding proved unsuitable due to material issues, the teflon gave a low pressure seal that degraded over time. With further work it seems possible these approaches could be improved and successfully implemented. The third bonding approach, polymer bonding provided a fluidic seal suitable for integration of the fluidic and sensor components. The integrated polymer bonded system, was tested with a standard HPLC test mixture to determine the seperation performance of the integrated system. The impact of dead volume on HPLC performance has been shown to be minimal and tailing of fluidic plugs due to corner effects has also had little impact on the HPLC performance. The integrated device was evaluated for optical performance with a refractive index measurement system, Farfield Analight ®BIO250. The response of the microsystem was tested with water to IPA transitions and the performance

compared to a standard system. In the case of the 30nl flow cell the response compares well to the response in the standard system. For the 5.6nl flow cell there was a less favourable response compared to the standard. Initial injections were carried out with the capillary separation system, but more work is required to determine the response of the performance of the microsystem to HPLC separations.

Acknowledgements

This work was carried out with the support of the E.U IST programme, project number IST-2001-35050.

References

[1] Graham H. Cross, Andrew A. Reeves, Stuart Brand, Jonathan F. Popplewell, Louise L. Peel, Marcus J. Swann, N.J Freeman: A new quantitative optical biosensor for protein characterisation, Bioelectronics, In press Corrected proof, Available online 29 August 2003,

[2] Kruger J, O'Brien P, Morrissey A, Alderman J, O'Neill A: Materials, Processing, Component Integration, Assembly and Packaging Issues, Microtech IMAPS, 2001.

[3] Steven A. Soper, Alyssa C. Henry, Bikas Vaidya, Michelle Galloway, Musundi Wabuyele and Robin L. McCarley: Surface modification of Polymer based microfluidic devices Analytica Chimica Acta 11 October 2002, Pages 87-99

To investigate dielectric microspheres as tools for ICT

Ruth Carey*, Mohamed Boustimi and Sile Nic Chormaic

Department of Applied Physics and Instrumentation, Cork Institute of Technology,
Rossa Avenue, Bishopstown, Cork, Ireland.

Microcavity lasers are of interest in telecommunications as industry strives towards miniaturisation. These lasers provide attractive qualities such as low mode volumes and high quality factors, as light is confined efficiently in whispering-gallery-modes of microspheres. These high quality factors of microspheres have led to very low threshold lasers. Another important feature is the ability to narrow the linewidth of lasers. This project intends to study the behaviour of microspheres doped with rare earth ions. Once this is completed the emitted light from the laser will be coupled into neighbouring microspheres to look at the signal transmission.
An overview of the experiments is as follows: The experiment will use a taper fibre to excite the microspheres. The advantage of this method over others is that it is an easier coupling regime. The primary disadvantage of this method is that the tapered end of the fibre is very delicate. Light from a pump laser will be coupled to the fibre. A pump laser at 980 nm will be used to achieve laser action at around 1.5 μm, (the telecom wavelength). The fundamental mode will have an evanescent wave, which, at the taper region, will propagate in free space. This evanescent wave will be used to excite the microsphere. The microsphere will be attached to the tip of an optical fibre for easy manipulation and entrance into the set-up. The distance between sphere and taper will be controlled using micro-positioning and a piezoelectric actuator. The taper can be used to both couple light into the sphere and collect light from it for investigation. After the characterisation of such spheres is made, another sphere will be introduced into the set-up and so on until an array of spheres is created and studied.

* rcarey@cit.ie

Carrier induced refractive index in quantum dot semiconductor lasers

Olwen Carroll, Jan Muszalski, John Houlihan, Guillaume Huyet
Physics Department, National University of Ireland, University College Cork

Carrier induced refractive index changes in semiconductor lasers strongly influence device characteristics e.g. spectral linewidth, self-focussing and filamentation in broad area devices and wavelength chirp under modulation. The degree to which changes in the carrier density alters the refractive index of the active layer is often characterised by the linewidth enhancement factor (LEF) or alpha-factor and is currently the subject of much experimental investigation. Values of alpha of 2-3 have been recorded for QW devices, with higher values measured for devices emitting in the telecommunications bandwidth. The superior lasing characteristics of QD semiconductor lasers has led to an increased interest in their development as practical devices for telecommunications applications. A symmetric gain spectrum yields an alpha-factor of zero at the peak gain as the refractive index does not change with carrier density at this point (Kramers - Kronig relation). Due to their delta like density of states, the gain spectrum for a QD is expected to satisfy this condition resulting in a significantly lower value for alpha.

We measure the gain and change in refractive index of InAs/GaAs QDs emitting at 1310nm using the Hakki-Paoli method. By analysing devices with different lengths operating at different injection currents, we are able to show that the alpha factor increases with carrier density and is not wavelength dependant. We obtained typical values for alpha of 1-3.

We will also show that the analysis of the optical spectrum above threshold can provide further information on the effect of the off resonance carriers on the refractive index.

Photonic Crystal Vertical Cavity Lasers

Kent D. Choquette
Electrical and Computer Engineering
University of Illinois-Urbana-Champaign
Urbana, IL 61801

Photonic crystal confinement in vertical cavity surface-emitting lasers (VCSELs) is a robust and reliable technology for achieving operation in the fundamental lateral mode and is potentially applicable to a variety of materials systems and operating wavelengths. We demonstrate photonic crystal VCSELs operating in a single transverse mode with over 30 dB side mode suppression and over 3 mW of output power. These lasers have been subjected to a post-process technique to introduce the etched holes making up the photonic crystals that surround a centralized defect in which lasing occurs. In addition to control of lateral modes, we find that the beam sizes can be compressed, producing enhanced lateral confinement over oxide apertures. In fact, the additional confinement creates lower optical loss, which will benefit microcavity phenomena in VCSELs. Finally, we also show that coupling between adjacent defects in a photonic lattice is possible, providing a means for coherent coupling in large element arrays.

Characterisation of Picosecond Pulses Propagating through a Semiconductor Optical Amplifier using Frequency Resolved Optical Gating

A.M. Clarke[1], P. Anandarajah[1], L.P. Barry[1] and D.A. Reid[2]
[1]Research Institute for Networks and Communications Engineering,
School of Electronic Engineering, Dublin City University, Dublin 9, IRELAND.
Phone : + 353 1 7005883, Fax :+ 353 1 7005508 E-mail: liam.barry@eeng.dcu.ie
[2]Physics Department, Auckland University, Auckland, NEW ZEALAND

ABSTRACT

The phenomenal growth in information and communications technology (ICT) over the last decade can be largely attributed to research and development of optoelectronic technologies, which enable the enormous capacity of optical fibre to be exploited. Today, optical fibre communication systems operate at aggregate bit rates in excess of 100 Gb/s. Achieving such high-speed optical communication systems would involve using Wavelength Division Multiplexing (WDM) and Optical Time Division Multiplexing (OTDM) technologies or possibly even a combination of these techniques to form hybrid WDM/OTDM. A vital requirement for such high-speed networks would involve the development of ultrashort, transform-limited pulses that exhibit high Side Mode Suppression Ratios (SMSR) and broad wavelength-tunability. In addition to the development of these pulse sources, it will also be vital to ensure that optical amplifiers used in the transmission systems can correctly amplify the optical data signals, which are represented using picosecond optical pulses.

In this paper we carry out extensive investigations to characterise picosecond pulses propagating in a Semiconductor Optical Amplifier (SOA). Although much work has been undertaken in this domain using simulations, there has not been the same extensive work experimentally to complement this. The usual technique in characterising the output pulses involves using a separate time and frequency domain measurements consisting of an optical intensity autocorrelator and an optical spectrum analyser. A more recent method called Frequency Resolved Optical Gating (FROG) can overcome the limitations of the existing methods and allows the complete characterisation of the intensity and phase of any arbitrary ultra-short pulse. The FROG measurement is a spectrally resolved autocorrelation. Iterative techniques are then applied to the measurements to reconstruct quantitative information about the electric field and the phase.

Using a self-seeded, gain switched laser diode to generate picosecond optical pulses with low timing jitter and good SMSR, we investigate the propagation of a pulse through an SOA. The resulting temporal and spectral distortions induced on the pulse due to propagation through the amplifier are very important for the use of these devices in long haul and high-speed optical communication systems. This paper will analyse the pulse shape and spectrum of the pulse propagating through an SOA after applying a chirped gain switched input pulse. We will show experimentally from results obtained using a FROG how the input power and the bias current affect the properties of the amplified output pulse such as spectral broadening, pulse shape, chirp, and time-bandwidth product (TBP).

Numerical Simulation of Semiconductor Optical Amplifiers

Michael Connelly
University of Limerick

The Semiconductor Optical Amplifier (SOA) will play an increasing role in emerging optical transmission systems, both as a general gain element and also as a central component in functional subsystems such as optical switches and wavelength converters. Numerical models of SOAs are necessary in order to predict device performance and enable optimization of their use in optical subsystems. This paper will present a wideband numerical model of a homogeneous buried ridge stripe SOA with a bulk active region and a parameter extraction algorithm based on the Levenberg-Marquardt method. A numerical solution to the modified Schrödinger equation for prediction of pulse propagation in SOAs will also be presented.

Interference Effects of Supercontinuum Filaments

K Cook*, A K Kar, M Taghizadeh, R J McGeorge
Physics, School of Engineering and Physical Sciences, David Brewster Building, Heriot-Watt University, Edinburgh EH14 4AS, Scotland
* *K.Cook@hw.ac.uk*

R A Lamb
Optronics Department, QinetiQ, Malvern WR14 3PS, England

We report an investigation using cylindrical lenses focusing into water. With this geometry a line focus is produced resulting in a one dimensional array of stable filaments, allowing interference effects between neighbouring filaments to be studied directly. A Ti: Sapphire laser is used with a regenerative amplifier to produce 1mJ, 120fs pulses with a centre wavelength of 800nm. A 170mm focal length cylindrical lens focuses the beam into a cell of de-ionised water. The line focus of the lens was in the horizontal plane and a number of white-light filaments were observed along the line focus depending on the pulse energy.

At a pulse energy of 780μJ only two filaments appeared. Images of these filaments allowed the separation and diameter to be deduced for the 700nm and 600nm wavelengths respectively. After removal of the imaging lens a white light interference pattern was observed. The fringes were perpendicular to the line focus of the cylindrical lens and were similar to those produced by a pair of slits illuminated by spatially coherent light, i.e. $\cos^2$ interference fringes within a sinc^2 diffraction envelope (Young's slits). Young's theory predicts values for the fringe spacing and filament width that are in good agreement with experimental results.

We also demonstrate the interference of multiple white-light supercontinuum (SC) filaments in B 270 crown glass through the use of an array of diffractive optical elements (DOE's). Each DOE has a focal length of 7mm and is square in shape. The focal plane is placed 1mm in front of the 2mm thick glass sample to avoid damage. On passing through this glass, the diverging beam of each DOE is shown to generate between 1 and 6 filaments regularly arranged in a rectangular pattern. Again, interference is observed between adjacent filaments when only two DOE's are illuminated by the input beam. Furthermore, it is found that the introduction of a π phase delay between neighbouring DOE's causes a shift of one fringe in the interference pattern This coherence property combined with control over interferogram position suggests a wide variety of possible applications such as optical information processing.

Metal selection for GaN devices

Brian Corbett, Pleun Maaskant, Mahbub Ahkter, Brendan Roycroft, Mark Walshe,
Liam Lewis, Nicolas Cordero.
Photonics Group, NMRC, Lee Maltings, Cork, Ireland.

GaN is well established as a material for visible opto-electronic devices. As the list of potential applications grows each aspect of the device structure needs to be optimised. Areas for improvement include the maximisation of the extraction and the wall-plug efficiency. These properties can be simultaneously improved by making a low resistance ohmic contact to p-type GaN, which has a high reflectivity and is optimised in phase to extract the maximum amount of light through the transparent sapphire substrate. The further use of flip-chip mounting provides improved heat sinking for higher output power.

We investigated a number of p type metallisation schemes based on Ag, Pd/Ag, Pt/Ag, NiAu/Ag and Ni/ITO. While NiAu/Ag provides good contact resistivity, there is poor adhesion between the oxidised NiAu and the silver. Pd/Ag yielded epitaxial contacts without thermal annealing with a specific contact resistance of ρ_c=4x10^{-3} Ω.cm^2 determined using the circular TLM method (c-TLM). An advantage of the c-TLM patterns over rectangular TLM patterns is that the c-TLM patterns do not require mesa etching to eliminate edge effects. The I-V curves measured between the inner and outer Pd-Ag contacts are all linear, provided that the bias is kept low. We will discuss the limitations of this technique.

Using a custom resonator consisting of a 1λ cavity on top of a PECVD deposited SiN/SiO_2 distributed Bragg reflector the cavity with the metal. From the fitting to the spectral reflectivity using the known properties of the dielectrics we determine that the magnitude of the reflectivity to GaN is 68% and phase of 104^0 for PdAg metallisation.

We will discuss the importance and relevance of these results in the applications of data communication using resonant LEDs and in high power devices.

Comparative study of active quench and reset circuits for photon counting detectors

Donal Cronin, Alan P. Morrison
Department of Electrical and Electronic Engineering
University College Cork

March 3rd, 2004

Email: *a.morrison@ucc.ie*

Abstract

A comparative study of three different Active Quench and Reset circuits (AQRC) is presented. The AQRC is an essential component to enable the high speed photon counting capability of geiger-mode avalanche photodiodes (GMAPs). It's purpose is to turn off the detector once a photon has been detected, to register the photon count, and to reset the device after a preset interval by restoring the bias on the detector. The circuits used [1],[2],[3] were implemented on printed circuit boards for testing and analysis. The parameters of interest are the quench-time, the reset time, the controllability of the hold-off time, the ability to gate the detector and the maximum achievable count rate.

Initial tests on various GMAPs were carried out using a simple passive quench arrangement [4] to determine their dark count-rate. With the simple passive quench arrangement there exists a limit to the maximum achievable count rate due to the long passive reset time (microsecond range) of the GMAP [1]. This long reset time is due to the RC time constant formed by the junction capacitance of the diode and the large ballast resistor required to quench the device. The AQRC overcomes this limitation by minimising the recharge time and increases the allowable count-rates into the Mcounts/sec range. Comparative measurements of the AQRC quench and reset times, in addition to maximum achievable count rate were made using an integrating sphere with a calibrated commercial detector, a monochromatic light source and a single GMAP under test connected to the various AQRC designs. These measurements allow the determination of the detection efficiency, and quantum efficiency of the GMAP and how these measurements vary with the various quench circuit designs used to control the GMAP.

Keywords

Active Quench and Reset Circuit (AQRC), Geiger Mode Avalanche Diode (GMAP), photon detection, quantum efficiency, integrating sphere, afterpulsing, dark-count

References

[1] F. Zappa, M. Ghioni, S. Cova, C. Samori, and A. C. Giudice. An Integrated Active-Quenching Circuit for Single-Photon Avalanche Diodes. *IEEE Transactions on Instrumentation and Measurement*, 49(6):1167–1175, December 2000.

[2] Vasileios Serafeim Sinnis. *Technology Development for Resonant Cavity Enhanced Single Photon Counting Detector.* PhD thesis, NMRC, University College Cork, January 1999.

[3] Donnchadh Joseph Phelan. *Geiger Mode Avalanche Photodiode Microarray System.* PhD thesis, Department of Experimental Physics, NUI Galway, August 2002.

[4] W.J. Kindt, N.H. Shahrjerdy, and H.W. van Zeijl. A silicon avalnache photodiode for single optical photon counting in the Geiger mode. *Sensors and Actuators*, A(60):98–102, 1997.

Polarization Switching in VCSELs with Noise and Feedback

D. Curtin, S.P. Hegarty, D. Goulding, J. Houlihan, Th. Busch, C. Masoller and G. Huyet

It is well known that the polarization dynamics of VCSELs in the bi-stable regime with intrinsic or external noise is a realization of Kramers hopping problem. The residence time distribution, describing the statistics of the polarization switches, is then found and calculated to be an exponential function, which demonstrates the Markovianity of the dynamics.

Applying feedback to a VCSEL changes the polarization dynamics dramatically. The fedback light represents a memory function for the laser and correlations between the current state and the delayed state become important. This in particular leads to a dynamics that is non-markovian.

Here we present an experimental investigation into a VCSEL with opto-electronic feedback and measure its residence time distribution and its autocorrelation function. We find strong modifications of the exponential shape of the residence time distribution and periodic features in the autocorrelation function. All of the results can be very well explained within a double-well model with feedback and we numerically confirm the observations. Using a simplified non-linear two-state model, we also derive analytic expressions for the residence time distribution.

SEMICLASSICAL MODEL OF LIGHT GENERATION IN 1-D PHOTONIC CRYSTAL LASER WITH FABRY-PERROT RESONATOR.

Pawel Czuma[a*], Paweł Szczepański[a,b]
[a]*Institute of Microelectronics and Optoelectronics, WUT, Koszykowa 75 Street, 00-662 Warsaw, Poland*
[b]*National Institute of Telecommunications, Szachowa 1 Street, 04-894 Warsaw, Poland*

Photonic crystal (PC) structures have been the subject of intense research activity since Eli Yablonovitch pioneer work written in 1987 (Physical Review Letters, 58, pp. 2059-2063). The PC, a periodic structure consisting of alternating arranged dielectric materials, provides an intriguing stage for controlling radiation fields. It exhibits several properties, that are important of view of optical applications, such as integrated photonic and optoelectronic integrated circuits or optical telecommunication networks. Especially, the existence of a spectral gap, anomalous frequency v.s. wave-number dispersion near the band edge and related to it high density of state observed in this region open up many potential applications such as high-efficient amplifiers, thresholdless lasers or high-efficient light emitting diodes. In particular, the experimental results on laser oscillation in active photonic crystals have been reported together with a discussion of the threshold. Moreover, it was found that optical gain is extremely intensified in the vicinity of the photonic band edge in the photonic crystals. The study of its origin suggest, that it is caused by reduction in part in light velocity near the band edge. Because this phenomenon shows up in PCs, i.e., periodic structures consisting of materials with different dielectric constants, the most basic origin should undoubtedly exist in the disparity of the dielectric constants. Thus, it seems to be still important to break down this origin into the specific factors that account for the gain enhancement.

In this paper, for the first time, we present the semiclassical model of light generation in 1D photonic crystal laser with F-P resonator. We use the semi-analytical Transfer Matrix Method (TMM) to obtain small signal gain coefficient, taking into account semiclassical model of active medium. In this method electric field E(r,t), which propagate through active medium, induces microscopic dipole moments (p_i) according to the laws of quantum mechanics. Sum of these moments give us the macroscopic polarisation of the medium P(r,t), which acts as a source in Maxwell's equations. The condition of self-consistency requires that the assumed field E equal the reaction field E' (see Fig.1 for details).

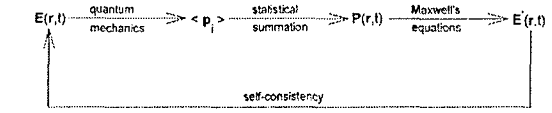

Fig. 1 The self- consistency diagram.

More generally, polarisation of the matrix defined by Fourier components of the susceptibility has the form:

$$\vec{P} = \varepsilon_0(\chi' + j\chi'')\vec{E}.$$

The real part of polarisation results in dispersion due to the medium. The imaginary part results in gain and loss of the medium.

Combination of TMM with semiclassical theory give us the lasers characteristics of small signal gain as a function of parameters: period of the structure, contrast of the refractive indices, geometry of the primitive cell as well as the number of the primitive cells creating the photonic crystal.

*pczuma@elka.pw.edu.pl, Project granted by the State Committee for Scientific Research (KBN), project nr 1281/T11/2003/25

Adaptive Optics

Christopher Dainty
National University of Ireland Galway

Adaptive Optics (AO) is an active optical technique in which a wave front is sensed and corrected in near real time. Historically, the main application has been in astronomy, where AO is used to compensate the deleterious effects of atmospheric turbulence. More recently it is finding application in other areas and in this talk I shall describe its application in vision science, where it can be used to produce better images of the retina or to enhance vision.

Spectroscopy of microspheres and photonic molecules

John Donegan
Trinity College, Dublin, Ireland

We have made a study of microsphere formed with melamine formaldehyd espheres with cadmium telluride quantum dot layers on the surface. We observe very strong whispering gallery modes from the stucture indicative of a high Q cavity. We have observed Raman scattering and anti-Stokes emission from only a single quantum dot layer on the sphere surface. Coupling between two microspheres to form a photonic molecule has been studied. We observe bonding and anti-bonding states from the photonic molecule when exciting along the axis. Off-axis detection, we observe an fine structure splitting of the bonding and anti-bonding states due to the removal of the degeneracy with respect to the azimuthal quantum number. We will discuss the potential of such microcavity structures in photonic applications.

Recombination Processes in GaInAsN/GaAs Quantum Wells and their Influence on Optoelectronic Devices

R. Fehse, S.J. Sweeney, E.P. O'Reilly, S. Tomić, A.R. Adams and H. Riechert

University of Surrey, ATI, Guildford, Surrey, GU27XH, UK
NMRC, University College, Lee Maltings, Prospect Row, Cork, Ireland
Infineon Technologies AG, Corporate Research, 81730 Munich, Germany

The dilute III-V alloy GaInAsN is of great interest for its use in optoelectronics. It can be grown lattice-matched on GaAs substrates and due to its unusually strong bowing the band gap can cover the range 0.8 eV < E_g < 1.4 eV, even with N content less than 4%. This makes GaInNAs-based devices ideal for application in the 1.3μm-1.55μm communication window. However, the detailed band structure of GaInAsN remains relatively unexplored and is the subject of some controversy.

To understand and improve the performance of optoelectronic devices, knowledge of the magnitudes of the various recombination processes is a key factor. In this paper we show that an operating semiconductor laser provides an ideal tool to experimentally determine the required information right up to the carrier density n required for lasing operation.

The absolute variations of monomolecular (defect-related, ~An), radiative (~Bn^2) and Auger recombination (~Cn^3) were determined from 130K to 370K by studying the spontaneous emission from normally operating ~1.3μm GaInAsN/GaAs-based lasers. Importantly we found that defect-related recombination (⑩ n) can contribute up to 50% of the total current at lasing threshold, in stark contrast with previously studied InGaAsP/InP-based lasers, where this contribution is negligible.

Theoretical calculations of n as a function of temperature were also performed using a 10-band $k{\cdot}p$ Hamiltonian. This enabled us to determine the individual magnitudes of A, B and C and their temperature variation. At 300K values of A ~ $1\times10^{8}\,s^{-1}$, B ~ $1\times10^{-10}\,cm^3s^{-1}$ and C ~ $4\times10^{-29}\,cm^6s^{-1}$ were obtained. Interestingly, C is within the range $1\text{-}8\times10^{-29}\,cm^6s^{-1}$ reported for 1.3μm InGaAsP-based devices. This indicates that Auger recombination is also an important intrinsic recombination mechanism in GaInAsN despite its unusual band structure. The influence of the growth conditions and laser structure on the magnitudes of the recombination processes and potential device performance will be discussed.

Quantum dot photonic nanodevices

Andrea Fiore
Institute of Quantum Electronics and Photonics
Ecole Polytechnique Federale de Lausanne (EPFL)
CH-1015 Lausanne, Switzerland

Single semiconductor quantum dots can provide single photons on demand, however much work is needed to realise practical single-photon sources for quantum cryptography systems. Main issues are emission wavelength, electrical injection, efficient coupling to optical fibres and temperature of operation. I will report on the progress towards the realisation of compact and efficient single quantum dotlight-emitting diodes with integrated nanocavities, emitting at 1300 nm.

Cavity Solitons: Status, Potential, and Applications

William Firth
Department of Physics, University Of Strathclyde

Cavity solitons are self-localized structures generated through nonlinear light-matter interaction within an optical resonator, bistable elements which can be switched on and off by means of laser pulses. They form in cavities hosting a variety of nonlinear media, in particular semiconductors. They are sensitive to parameter gradients, whether intrinsic or imposed, leading to interesting and potentially useful transverse motion and interactions. They could thus act as malleable, re-configurable optical pixels, opening the way to novel and efficient control and diagnostic techniques. The talk will assess the state of the art, briefly reviewing the various kinds of cavity soliton so far proposed and demonstrated. Some potential applications will be outlined, and relevant advantages and potential drawbacks of cavity solitons will be considered. One obvious drawback is the need for a holding beam to sustain the solitons against losses, but there are exciting possibilities of making them self-excited, i.e. a cavity soliton laser. This and other new concepts for cavity soliton developments and applications will be discussed.

Dual semiconductor optical amplifier polarisation diversity wavelength conversion using four-wave mixing with electronic feedback

David I. Forsyth and Michael J. Connelly.
Optical Communications Research Group, Dept. of Electronic and Computer Engineering, University of Limerick, Limerick, Ireland.
e-mail: david.forsyth@ul.ie

Abstract

A key function in future high capacity dense wavelength-division multiplexed (DWDM) optical networks will be the ability to convert data from one wavelength channel to another at very high bit rates. Semiconductor optical amplifiers (SOAs) have numerous advantages at present, and can utilise non-linear effects to produce high speed wavelength conversion by the process of *four-wave mixing* (FWM) with continuous wide-range tuning. Efficient four-wave mixing can be achieved when SOA pump and input signals are co-polarised, as newly-generated conjugates can fluctuate by > 10 dBm (or even completely disappear) with changing signal input polarisation states.

Semiconductor optical amplifiers have been arranged with the aim of obtaining polarisation-free wavelength conversion, using four-wave mixing. Two similar SOAs are used in a one-pump polarisation-diversity arrangement, with a third SOA used as a pre-amp to improve receiver sensitivity. Pump and modulated SOA input signals are coupled into a system consisting of two polarising beamsplitters/combiners and two SOAs. The pump is polarised at 45° to a polarisation beam splitter's principal axes, so that half of its power goes to each SOA. The input to each SOA is a pump field and the co-polarised component of the signal field which mix in each SOA to produce a conjugate signal with the same polarisation. These orthogonally-polarised conjugates are recombined by a polarisation combiner. The scheme is polarisation independent, if each SOA has identical gain and conversion efficiencies. In practice the gain and conversion efficiencies are not equal. An optoelectronic feedback loop

was used to control the gain of one of the SOAs such that the power level in the converted signal was kept constant. The polarisation sensitivity of the wavelength-converted signal was monitored over periods of up to 12 hrs. As the polarisation of the input signal was changed over all possible states in this time period (by a scanning polarisation controller) with no feedback, the output power of the corresponding wavelength-converted signal changed as much as 2.0 dB for a 622 Mb/s data bit rate, and 1.5 dB at 2.488 Gb/s. With feedback, the change was less than 0.5 dB at both data rates. Initial results therefore indicate that the technique achieves a polarisation dependence of < 0.5 dB (with feedback) and < 2.5 dB maximum (without feedback) in the wavelength-converted signal. We conclude that the work shows the potential of a simple polarisation-diversity wavelength conversion scheme, based on four-wave mixing in semiconductor optical amplifiers, and achieves an improved level of polarisation sensitivity utilising gain feedback.

Three-dimensional Photon Confinement in a Spherical Microcavity with CdTe Quantum Dots: Raman Spectroscopy

M. Gerlach[1], Yu.. Rakovich[1], J.F. Donegan[1], N.Gaponik[2] and A. L. Rogach[3]

[1] *Semiconductor Photonics Group, Department of Physics, Trinity College, Dublin 2, Ireland*
[2] *Institute of Physical Chemistry, University of Hamburg, 20146 Hamburg, Germany*
[3] *Department of Physics and CeNS, University of Munich, 80799 Munich, Germany*

Spherical particles of 2-100 μm in diameter can act as three-dimensional optical resonators providing the feedback required for nonlinear-optical processes such as enhanced Raman scattering. Polymer latex microspheres containing semiconductor quantum dots (QDs) are promising candidates for the development of advanced Raman sources, which can extend the available range of semiconductor microlasers. In this work, we have studied the Raman spectra of a microcavity-QD system consisting of CdTe colloidal QDs coated onto a polystyrene (PS) microsphere of 70 μm diameter. A layer-by-layer deposition technique has been utilized to provide the controllable coating of the microsphere by a shell of close-packed quantum dots.

The measured Raman spectrum of a single PS microsphere covered by a monolayer of CdTe QDs at resonance with excitation by an Ar^+-laser (514.5 nm) shows a number of peaks which are intrinsic to the PS (620, 759, 793, 1001 and 1031 cm^{-1}). Moreover, in addition to these lines, the cavity-induced enhancement of the Raman scattering allows also the observation of LO phonon mode from only a monolayer of CdTe QDs (164 cm^{-1}), redshifted due to confinement of optical phonons.

A periodic (ripple) structure with very narrow regular peaks in the Raman spectra of a PS/NCs microsphere corresponding to the whispering gallery modes (WGM) was detected with strong scattering into selected modes at high pump intensity. This effect can be attributed to the strong field enhancement at the microcavity resonances. The shape, position and separation between the WGM peaks were theoretically analyzed in a wide spectral region taking into account material dispersion of PS.

Using low intensity non-resonance excitation by a He-Ne laser (632.8 nm) strong coupling between photonic states of spherical microcavity and electronic states of CdTe QDs was achieved resulting in enhanced luminescence contribution to the Raman signal simultaneously in both Stokes and anti-Stokes spectral regions. This effect was analyzed in terms of photon energy up-conversion and can once again be attributed to the optical feedback via the microcavity with WGM structure which leads to an increased probability of energy transfer to the emitting species.

Inhibition of modulational instabilities and novel localized structures using intracavity photonic crystals

Damià Gomila, Roberta Zambrini, and Gian-Luca Oppo
Department of Physics, University of Strathclyde
107 Rottenrow East, Glasgow,
G4 0NG, United Kingdom
Phone: +44 141 548 3354 Fax: +44 141 552 2891,
e-mail: damia@phys.strath.ac.uk

Spatial structures are studied in a nonlinear cavity with a photonic crystal. Pattern formation is inhibited via the creation of a photonic band-gap. A novel mechanism of light localization due to defects is described.

We study the effects of a photonic crystal in the formation of spontaneous patterns on a nonlinear dissipative system driven out of equilibrium. In particular we show how the linear phenomenon of photonic band-gap affects the selection of a nonlinear spatial structure, allowing for the complete inhibition of the off-axis emission associated with modulation instabilities (MI) and pattern formation.

We consider an optical cavity containing a self-focusing Kerr medium and a linear medium with spatially varying refractive index, i.e. a photonic crystal. In the mean field approximation, the dynamics of the slowly varying amplitude of the paraxial electric field E can be described by

$$\partial_t E = -\{1 + i[\theta + f(x)]\}E + i\partial_x^2 E + E_0 + i|E|^2 E, \tag{1}$$

where θ is the average detuning between the frequency of the pump and the frequency of the cavity, $f(x)$ accounts for the modulated refractive index in the transverse direction of the photonic crystal and E_0 is the input field.

In the absence of any modulation of the refractive index, above a certain threshold, the homogeneous steady-state solution E_s becomes modulationally unstable leading to the formation of a stripe pattern.

In presence of a photonic crystal the pattern forming instability is inhibited for a range of detuning values. For detuning values within the band-gap, the fundamental solution regains stability. Outside the band-gap, the fundamental solution is unstable leading to the formation of a high amplitude pattern. The final spatial structure has a combined periodicity of the pattern that would appear without photonic crystal and of the photonic crystal.

The inhibition of MI due to photonic crystals can then be used to control the transverse properties of light in nonlinear optical cavities in a novel way analogous to light control in holey waveguides. For example we consider a profile of the refractive index represented by the grey line in Fig. 1. We see how the large amplitude pattern is inhibited in the modulated regions where the system is anchored to the fundamental solution, while a strong localized structure is observed in the defect.

An important potential application of this effect is in the case of subcritical patterns where the delaying of the MI may dramatically increase the region of coexistence between the fundamental and patterned solutions. The immediate benefit is to increase the region of existence of cavity solitons thus simplifying their utilization in information processing. Other potential applications are the use of the localization of light due to defects as a tool for diagnostic of photonic crystals or to obtain peculiar output intensity structures by engineering the defects.

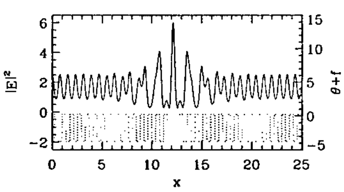

FIG. 1: Localized structure formed inside a defect 1.5 photonic crystal wavelengths long. For this figure $f(x)$ is a step function between -2.0 and 2.0. Here $I_s = 1.8$ and $\theta = -1.75$. For these parameter values the band-gap is found for detuning values $-2.0 < \theta < -0.38$.

Quantum key distribution in the first fibre telecommunications window

Karen J. Gordon, Veronica Fernandez, Gerald S. Buller
Sergio D. Cova*, Simone Tisa* and Paul D. Townsend†

School of Engineering and Physical Sciences, Heriot-Watt University, Edinburgh, Scotland
**Dipartimento di Elettronica ed Informazione, Politecnico di Milano, Milano, Italy*
†Photonic Systems Group, Department of Physics, University College Cork, Cork, Ireland
p.townsend@ucc.ie

Quantum cryptography [1] or quantum key distribution (QKD) as it is more accurately known is the result of a synthesis of ideas from basic quantum physics and classical encryption that offers a fundamentally new approach to the business of protecting sensitive information. The technique exploits the fundamental principles of quantum measurement, as embodied in the Heisenberg uncertainty principle, to permit users of communication channels to exchange messages with provable security.

In the last decade progress towards practical, optical fibre-based QKD systems has been rapid [2-4], with recent demonstrations reaching transmission distances of around 100km at a wavelength of 1550nm. However, the key exchange rate in these systems remains low (typically around 100bits/s) due mainly to the count rate limitations imposed by the deleterious effects of afterpulsing in the cooled germanium or InGaAs/InP single photon avalanche diode (SPAD) detectors that are required for operation at the fibre transparency wavelengths. An alternative approach that is applicable for short distance applications is to work in the so-called first fibre telecommunications window at a wavelength of 850nm. Although the fibre loss is relatively high at this wavelength (~ 2.2 dBkm^{-1}) it is nevertheless possible to obtain enhanced system performance through the use of silicon SPADs, which offer high detection efficiencies (>50%) and do not suffer from afterpulsing limitations. For applications in campus- or metropolitan-scale networks, for example, at distances of up to 10km silicon SPAD-based QKD systems can offer the highest key exchange rates currently attainable. This talk will describe the realisation of such a system, which utilises polarised VCSEL sources, state-of-the-art silicon SPADs and mode-selective launch techniques to achieve QKD over standard telecommunications fibre [5]. The system exhibited a low quantum bit error rate (QBER) of 1.4%, and an estimated net bit rate (NBR) greater than 100 kbits^{-1} for a 4.2 km transmission range, and a QBER of 2.1%, and estimated NBR greater than 7kbits^{-1} for a 10km range. The performance of this system in both point-to-point and multi-user network configurations will be discussed and some conclusions about the general applicability of the approach will be drawn.

[1] C.H. Bennett, and G. Brassard, "Quantum cryptography: Public key distribution and coin tossing," *Proc. Int. Conf. Computer Systems and Signal Processing*, Bangalore, Kartarna, pp. 175-179, 1984.

[2] C. Marand, P.D. Townsend," Quantum key distribution over distances as long as 30 km," *Opt. Lett.*, vol. 20, pp. 1695-1697, 1995.

[3] D. Stucki, N. Gisin, O. Guinnard, G. Ribordy, H. Zbinden, "Quantum key distribution over 67 km with a plug&play system," *New. J. Physics*, vol. 4, article 41, 2002.

[4] H. Kosaka, A. Tomita, Y. Nambu, T. Kimura, K. Nakamura, "Single-photon interference experiment over 100 km for quantum cryptography system using balanced gated-mode photon detector," *Electron. Lett.*, vol. 39, pp. 1199-1201, 2003.

[5] K. J. Gordon, V. Fernandez, P. D. Townsend, and G. S. Buller, "A short wavelength gigaHertz clocked fiber-optic quantum key distribution system" *(submitted to IEEE J. Quant. Electron. January 2004)*

(GaIn)(NAsSb) and the Challenges for Long Wavelength Communications Devices

James Harris
Department of Electrical Engineering,
University Of Stanford

The major limitations for rapid expansion of the information highway to provide high-speed access to the desktop/living room are the bottlenecks at the switching points (on/off ramps) and the feeder networks. While the critical optical device parameter for the fiber backbone was performance, the critical parameter for metro area and local area networks (MANs and LANs) is COST, with lasers and optical amplifiers being particularly critical elements as the cost must be reduced about 500X over the current cost of these devices in the fiber backbone. A second critical issue is functional integration of components as their numbers will be 10s-100s of millions of units compared to current requirement of 10s of thousands where assembly of discrete components is acceptable. Dilute nitride-arsenide alloys (GaInNAs) have been actively pursued for the development of low cost, directly modulated 10 GHz, 1.3_m single mode vertical cavity surface emitting lasers (VCSELs) for transmitters. However, a significantly broader range of devices will be required to achieve the end goal of high-speed direct access to the fiber network. Key components in expanding the accessible fiber bandwidth to the full low loss region from 1.2-1.6_m will not only require VCSELs, but semiconductor optical amplifiers (SOAs), high power pump lasers for Raman amplifiers and non-linear and waveguide elements for full functionality. These are rather dramatically different requirements that no single materials technology has yet been able to address. The limitations are both fundamental and technological and dependent upon finding a material, growth and processing technology to meet these challenges. There has been a major push to find suitable solutions to these problems and a number of approaches have been pursued over the past five years. Recent research has shown that MBE growth of GaInNAsSb with a near lattice match to GaAs has both a suitable bandgap energy, prospective optical characteristics, including low threshold current density, high temperature and high power CW operation and high T_0 over the entire wavelength range of 1.2 to 1.6_m plus the highly developed processing advantages of AlAs/GaAs for high index contrast DBR mirrors and AlAs/AlO oxidation for integrated photonic crystal waveguides, resonators, etc. These results suggest that GaInNAsSb may be the winning technology in this development of much lower cost communications optoelectronic components and ICs. As attractive as the dilute nitride-arsenides appear, there are many difficult challenges to realize a useful technology because all of these materials must be grown at low temperatures under metastable conditions because of the fundamental miscibility gap in the alloys. This results in generation of many defects and possible stability problems. A major challenge for GaInNAs is avoiding phase segregation and maintaining good 2-D epitaxial growth for materials operating beyond 1.3_m. We have developed a new structure using GaInNAsSb quantum wells (QWs) with strain compensating GaNAs barriers which has produced 1.5_m lasers with threshold currents of 1kA/cm2 and the first 1.5_m VCSELs. By adding a small amount of Sb to the QW growth, we are able to incorporate higher concentrations of In and N with thicker active layers and avoid 3-D nucleation and phase segregation. This material is grown by solid source MBE with a RF plasma source and both growth temperature and ion damage from the plasma source have turned out to be critical issues and MBE may be the only technology that can produce the range of devices and reliability required for optical networks. I will review some of the materials requirements which must be met for the above applications and then focus on the successes to date on long wavelength lasers and the challenges which remain to make this a viable technology for next generation high speed optical networks.

Four Wave Mixing in the Visible using a Photonic Crystal Fibre

J.D. Harvey, R. Leonhardt, K.L. G. Wong, R. Kruhlak
Physics Department, University of Auckland, Private Bag 92019, Auckland, New Zealand
Tel +6493737999, FAX +6493737445, e-mail j.harvey@auckland.ac.nz

J.C. Knight, W.J. Wadsworth and P.St.J. Russell
Optoelectronics Group, Department of Physics, University of Bath, Claverton Down, United Kingdom

Photonic crystal fibres (PCFs) can now be constructed exhibiting a wide range of dispersion profiles and nonlinearities, which have enabled the demonstration of many nonlinear optical phenomena. Recently it has been shown that the strong waveguide contribution to the dispersion curve can give rise to scalar modulation instability in the normal dispersion regime when using a photonic crystal fibre[1], where the process is phase matched for the generation of sidebands widely separated from the pump. This effect can be explained as arising from the contribution of the higher order terms in the expansion of the propagation constant. The conventional analysis of scalar MI [2] shows that MI gain is only obtained in the anomalous dispersion regime where the wavevector mismatch is balanced by SPM. Using this theory, the MI gain vanishes in the normal dispersion regime. Extending the expansion to fourth order shows that gain can be obtained when:

$$\beta_2 + \beta_4\Omega^2/12 < 0$$

and this condition can be satisfied even in the normal dispersion regime for a range of wavelengths close to the zero dispersion wavelength. In our experiments we have used a range of fibres with varying zero GVD points around the visible red pump wavelength. The resulting upshifted sidebands which can be generated, span the entire visible range from the blue to the red, whilst the corresponding downshifted sidebands range from approximately 750 to 1000nm. The development of pump lasers tunable over a modest range (10nm) and highly uniform fibres would enable this process to be used to be used to generate an all solid state tunable laser in difficult to access regions of the visible spectrum.

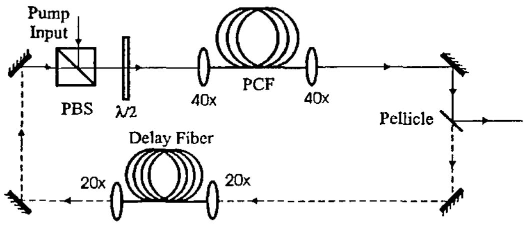

Fig. 1 Schematic of experimental arrangement, when operating as an OPO, a fraction of the upshifted output signal wave is fed back through a delay line

The experimental setup (Figure 1) also enabled the cavity to be operated as a singly resonant fibre optic parametric amplifier, and in this configuration (with feedback provided by an 80m single mode fibre delay line), the system provided up to 25% energy conversion to a blue upshifted sideband. The efficiency of this process is greatly assisted by the associated large frequency shifts as the blue photon has about twice the energy of the downshifted photon.

References

1. J.D.Harvey, R.Leonhardt,K.L.G.Wong J.C.Knight,W.J.Wadsworth and P. St. J. Russell "Scalar modulation instability in the normal dispersion regime using a PCF" Opt. Lett. **28**, 2225-2227 (2003)
2. G. P. Agrawal *Nonlinear Fibre Optics* Academic Press, London (2001)

Multimode Interference Couplers Utilizing WGM Bends for both visible and infra-red optical applications

M. Hayden, C. Gallagher, P. Lambkin, A. P. O'Neill, P. J. Hughes
NMRC, UCC, Cork

Photonic couplers and their integration represent key components for optical applications ranging from wavelength management in telecommunication networks to emerging bio-analytical optical based systems. In this paper, 1x2 splitters based on multimode interference (MMI) coupler with additional 'S'-bends were designed and fabricated for both visibl (633nm) and infra-red (1550nm) wavelength operation. For optimal MMI performance, Whispering Gallery Mode (WGM) were added to the 'S'-bend designs at each output arm of the device. Using this approach, low loss devices with minimum uniformity and excess loss are reported.

Index Terms— Multimode interference, whispering gallery modes, effective index, optical waveguides, splitters, parallel analysis.

Experimental investigation of quantum–dot laser phase amplitude coupling and feedback sensitivity.

S.P. Hegarty
Physics Department, University College, Cork, Ireland

The performance of quantum dot devices is presently the subject of great interest. Several studies have concentrated on the sensitivity of quantum dot semiconductor lasers to the influence of optical feedback. We present experimental results on quantum dot lasers at 1.3 microns under feedback conditions and explain an anomalously high threshold for coherence collapse. As the sensitivity of semiconductor lasers to feedback is governed to a large extent by the non–zero value of the alpha factor, this parameter is worth detailed consideration. Some studies have reported very low values for this parameter which has brought the possibility of designing directly modulated semiconductor lasers operating without optical isolators and therefore reducing the cost of these devices. We present measurements of the line–width enhancement factor at the ground–state transition and also below bandgap. We then consider the origin of the a factor in a system comprised of an ensemble of symmetric linewidth oscillators. Crucial to understanding this effect is appreciation of the role of the different carrier populations in the quantum dot laser.

Fabrication and Optical Identification of Barcode Labelled Micro-Beads in a Micro-Fluidic environment

Daniel Hoffmann, Des Brennan, Alan O'Neill, Michael Loughran, Gabriel Crean
NMRC, Cork, Ireland, 2004

Corresponding author: e-mail Michael.loughran@nmrc.ie

A novel micro-bead encoding and detection technology platform is presented. This platform will provide new opportunities for environmental monitoring and clinical diagnostics.

The optical ID tags consist of photo-lithographically defined micro-barcodes that can be identified by a laser detection system integrated onto the micro-fluidic platform.

Figure 1 shows a typical smart-bead with encoded micro-barcode.

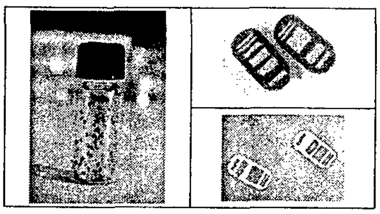

Figure 1: *Micro-Beads tagged with an optical ID*

The dimensions of these barcode tagged micro-beads are in the range of sub millimetre. Micro-beads with dimensions reaching down to 600 μm by 300 μm by 80 μm have been successfully fabricated. The technology used is capable of fabricating beads with dimensions 100 μm by 50 μm by 50 μm.

Customized software developed with LabView identifies each unique micro-barcode. This approach will enable us to visualize biological reactions e.g. antigen – antibody binding events.

The developed identification system consists of an optical laser detection system (**Figure 2**) that provides input to a data acquisition system.

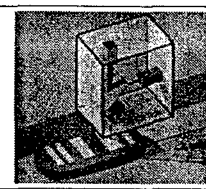

Figure 2: *Optical detection system*

The optical detection system uses laser-diode technology to identify the ID tag of the smart micro-beads providing a clear detection pattern (**Figure 3**).

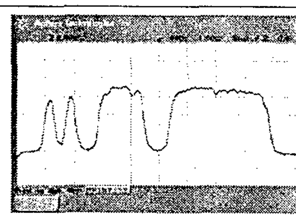

Figure 3: *Detection pattern of a Micro-Bead ID*

The smart micro-bead technology provides the advantages of reproducible, low cost fabrication. The microfluidic platform also enables specific micro-bead interactions to be performed in different aqueous solutions and liquid suspensions. This flexible approach enables rapid creation of large micro-bead libraries in a small volume for different clinical and chemical analyses.

Alignment-free CPM FROG based on a microstructure optical fiber

P. Honzatko, J. Kanka, B. Vrany

Institute of Radio Engineering and Electronics, Academy of Sciences of the Czech Republic, Chaberská 57, 182 51 Praha 8, Czech Republic

A microstructure optical fiber (MOF) with a high nonlinear coefficient and low dispersion was used as a nonlinear medium in an alignment-free cross phase modulation frequency-resolved optical gating device (CPM FROG). To prepare mutually orthogonal linearly polarized probe and reference pulses, the alignment-free set-up uses a fiber-pigtailed polarization beam splitter, two Faraday mirrors, and a fiber stretcher employed as a delay line. The robust optical fiber based device allows unambiguous measurement of the amplitude and phase of picosecond low-energy optical pulses around the important communication wavelength of 1550 nm. There is a trade-off between the sensitivity and bandwidth of the fiber CPM FROG, as the length of the nonlinear fiber L should satisfy the condition $0.05L_D > L > 0.1L_{NL}$, where L_D is the dispersion length and L_{NL} is the nonlinear length. Compared to the set-up with a conventional fiber, the use of MOF with a high nonlinear coefficient and low dispersion increases the range of the measurement to shorter or lower energy pulses. The CPM-FROG measurement of pulses from the fiber laser will be presented as well as the reconstruction algorithm based on a combination of the simulated annealing and beam propagation method. The algorithm can cope with the dispersion in the nonlinear fiber enabling us to go beyond the aforementioned limit and achieve higher sensitivity by using a longer fiber even when its dispersion is not negligible any longer.

Increase functionality for vertical-cavity lasers by monolithic integration of wavelength-scale diffractive structures

John Justice, Paul Lambkin, Brendan Roycroft and Brian Corbett
NMRC, Prospect Row, Cork. Ireland

Vertical Cavity surface emitting lasers (VCSELs) are now a well established technology with existing applications in datacom and sensors. Increased applications can be made if additional functionality is provided by the VCSEL. One way of doing this is to integrate diffractive optics elements (DOEs) with the VCSEL. Previous work has placed diffractive elements on the substrate emitting side of VCSEL or used an external DOE. While these methods allow the beam to expand permitting more complex diffractive patterns to be realised, they also requiring complex processing and/or alignment of external optics.

Modification of the surface of a VCSEL has been utilised in the promotion of transverse modal control and polarization stabilization. Here we examine its capabilities for increasing device functionality by changing the output beam though the use of phase diffraction gratings. We show that simple diffractive patterns can be etched into the surface of a VCSEL using Focussed Ion Beam (FIB) etching. While FIB is not so amenable to high volume production, the scales involved are well within the capabilities of modern lithographic processing equipment.

The DOEs were etched directly on the mirror surface of red (660 nm) single and multimode VCSELs. A number of structures were investigated including linear and two-dimensional gratings. A one dimensional, "linear" grating acts as a 2x beam-splitter when the phase depth is π. The two-dimensional "chessboard" grating acts as two crossed linear gratings creating a 4x beam-splitter. Output beam angles are given by $\lambda=\Lambda \operatorname{Sin}(\theta)$, where, θ is diffractive angle of first order emission, λ is the emission wavelength in air and Λ is the grating pitch. Both these structures showed excellent suppression of the original beam (zero order diffraction). The maximum coupling efficiency, of unetched VCSEL power into the total first order power, for π etch depth "chessboard" and "linear" gratings were approximately 12% and 22% respectively assuming (unrealistically) the incident beam is unaffected. No polarization dependence was found for grating pitches to 1λ ($0.67\mu m$) and rotational angles of 90^0. Threshold current increases of 35%- 40% were measured.

Effect of Coulomb-induced nonlinearities on the excitonic optical Stark effect in II-VI semiconductor quantum wells

A. K. Kar, G. Papageorgiou, R. Chari, C. Bradford, K. A. Prior and I. Galbraith
Physics, School of Engineering and Physical Sciences, David Brewster Building, Heriot-Watt University, Edinburgh EH14 4AS, United Kingdom
A.K.Kar@hw.ac.uk

H. Kalt
Institut für Angewandte, Physik, Universität Karlsruhe, D-76128 Karlsruhe, Germany

Abstract:

The role of Coulomb-induced nonlinearities in the description of the optical Stark effect in semiconductors has attracted considerable attention not only due to fundamental interest in semiconductor physics but also because of the potential applications of the effect in ultrafast optical switching [1].

Their importance is investigated in polarization selective pump-continuum probe experiments by studying the Stark shift dependence on the pump pulse detuning for same (SCP) and oppositely (OCP) circularly polarized pump and probe pulses at 4 K during below-gap excitation by an ultrafast pulse. A range of ZnSe-based multiple quantum wells with different heavy-hole (HH) to light-hole (LH) separation is examined, including novel ZnSe/MgS quantum well structures [2]. ZnSe-based quantum wells provide an ideal material for the study of Coulomb interactions due to their increased exciton binding energy. Moreover, their large HH-LH energy separation allows the investigation of the Stark effect independently at both HH and LH resonances.

The excitonic optical Stark shift is a result of contributions from phase-space filling (PSF), first-order Coulomb interactions, higher order Coulomb correlations and the coupling between the HH and the LH excitons [3]. Considering a range of pump pulse detuning and HH-LH splitting combinations and exploiting the polarization dependence of PSF and first-order Coulomb interactions, we identify the effect of Coulomb correlations to the observed Stark shift and we find that their significance depends critically on the pump detuning to splitting ratio Γ. For the multiple quantum wells studied, higher order Coulomb correlations play a strong role when Γ is less than 2.

At the HH resonance, their contribution results to an increase in the Stark shift with increasing detuning when the pump and probe pulses are of opposite circular polarization and therefore there is no PSF contribution. The observed behaviour for OCP stems from the competition between the Pauli blocking term, due to the influence of light-holes on heavy-holes, and higher order Coulomb correlations. The first produce a blue shift, whereas the latter are known to cause a red shift of the HH resonance [4]. In spite of the relatively high biexciton binding energy in the ZnSe-based quantum wells studied, the origin of the increase of the shift cannot be associated directly with bound biexcitons. Our conclusion is derived from

measurements at T >150 K where bound biexcitons do not form, and is in agreement with studies in $In_xGa_{1-x}As$ quantum wells, where the red shift was attributed to Coulomb memory effects [5].

At the LH resonance, the influence of Coulomb correlations can be realized by comparing the spectral dependence of the Stark shifts for the two circular polarization configurations at the same Γ regime. PSF produces higher shift for OCP than SCP at the LH, however the observed Stark shifts turn out to be equal. Therefore, the polarization dependence of the shift manifests the significance of the Coulomb induced nonlinearities at the LH resonance as well. The Stark shift behaviour at both resonances for higher Γ ratios, where Coulomb interactions become less prominent, supports the above conclusions.

References:

[1] M. Shimizu, and T. Ishihara: Subpicosecond transmission change in semiconductor-embedded photonic crystal slab: Toward ultrafast optical switching, Appl.Phys.Lett, **80**, 2836 (2002)
[2] C. Bradford, C. B. O'Donnell, B. Urbaszek, A. Balocchi, C. Morhain, K. A. Prior, B. C. Cavenett: "Growth of zinc blende MgS and MgS/ZnSe quantum wells by MBE using ZnS as a sulphur source, J. Crys. Growth, **227/228**, 634 (2001)
[3] S. W. Koch, C. Sieh, T. Meier, F. Jahnke, A. Knorr, P. Brick, M. Hubner, C. Ell, J. Prineas, G. Khitrova, and H. M. Gibbs, "Theory of coherent effects in semiconductors", J. Lumin, **83-84**, 1 (1999)
[4] P. Brick, C. Ell, S. Chatterjee, G. Khitrova, H. M. Gibbs, T. Meier, C. Sieh, and S. W. Koch, "Influence of light holes on the heavy-hole excitonic optical Stark effect", Phys. Rev. B, **64**, 75323 (2001)
[5] C. Sieh, T. Meier, F. Jahnke, A. Knorr, S. W. Koch, P. Brick, M. Hubner, C. Ell, J. Prineas, G. Khitrova, and H. M. Gibbs, "Coulomb Memory Signatures in the Excitonic Optical Stark Effect", Phys. Rev. Lett. **82**, 3112 (1999)

Photon twins and quantum entanglement in a quasi-phasematched down-conversion sources

Anders Karlsson
Department of Mathematics,
Royal Institute of Technology, Stockholm

Quantum correlated (entangled) photons are crucial for quantum communications, being needed, as a starter, for protocols such as quantum teleportation and for some quantum key distribution protocols. A good source for entangled photons should be compact, easy to use and feature high brightness in the number of entangled photons. In this talk we will, following a general introduction to the subject, describe our recent work on the generation of polarization entanglement created by spontaneous parametric downconversion in quasi-phase matched KTP crystals. The crystals are periodically poled for quasi-phase matching, providing collinear and non-degenerate output at 810nm and 1550nm in a single spatial mode. This source is thussuitable for fiber-based long-distance quantum communication.

Re-examining the 2-D and 3-D Scaled Optical Fourier Transform

D. Kelly[a], J. T. Sheridan*[a], W. T. Rhodes[b]
[a] Department of Electronic and Electrical Engineering,
University College Dublin,
Belfield, Dublin 4, Republic of Ireland.

[b] Department of Electrical and Computer Engineering,
Georgia Institute of Technology,
Atlanta, Georgia, USA.
**Corresponding author:* e-mail: John.Sheridan@ucd.ie
Tel: +353-(0)1-716-1927 Fax: +353-(0)1-283-0921

ABSTRACT

The Optical Fourier Transform (OFT) is the most fundamental operation in Optical Signal Processing (OSP). The Scaled Optical Fourier Transform (SOFT) is one widely used method for implementing OFT. This method has the attractive feature of allowing the Fourier transform distribution to be scaled in size dependant only on the distance between the object and the lens. In the analysis of the SOFT it is generally assumed that the lens produces a perfect converging spherical wave that fully illuminates the object. However, the wave nature of light will give rise to diffraction effects, which will cause deviations from perfect spherical wave illumination. The phase deviations from the ideal cylindrical and spherical wave produced by wave effects were examined for the 2-D and 3-D cases. It can be shown that for both cases the extrema in phase, and the maximum phase deviations in each object plane lie along well defined curves. Although the identification of sources of the phase deviation is clearly of some interest, fluctuations in the illumination intensity, can change the appearance of the resulting Fourier transform distribution even when a ray-optics analysis

shows the object to be fully illuminated by the converging cone of light. To this end, the intensity deviations that occur in the Fourier plane, when an aperture is illuminated are examined for both the 2-D and 3-D cases. The aperture is placed at a variety of object plane positions and the size of the aperture is varied. The locations and sizes of the aperture that result in larger intensity deviations in the Fourier plane are noted. It was observed that the locations where the larger intensity deviations occur are related to the well defined curves derived from the analysis of phase deviations. This goes some way to allowing the cautious user to identify an operational region where the SOFT can be carried out so as to minimise effects due to diffraction from the finite extent of the lens aperture.

Analysis of holographic grating formation in photopolymer

John V. Kelly[a], Michael R. Gleeson[a], Feidhlim T. O' Neill[a], John T. Sheridan*[a],

[a]Department of Electronic and Electrical Engineering, Faculty of Engineering and Architecture,

University College Dublin, National University of Ireland, Belfield,

Dublin D-4, Republic of Ireland.

*Corresponding author: john.sheridan@ucd.ie; phone +353-1-716-1927; fax +353-1-283-0921

ABSTRACT

Holography has become of increasing interest in recent years with developments in many areas such as data storage and interferometry. Photopolymer materials such as acrylamide-based photopolymers are ideal materials for the recording of holographic optical elements, as they are inexpensive and self-processing. A model describing grating formation in photopolymer is proposed. The Non-local Polymer Driven Diffusion model (NPDD) accounts for high spatial frequency cut-off by the inclusion of a non-local spatial response. Polymer chain termination mechanisms are also examined. Assuming a primary termination mechanism dominates the chain formation process, a quadratic relationship is shown to exist between the monomer concentration and polymerization rate. Using a multi-harmonic expansion we examine the predictions of the model. An automated fabrication system, which enables efficient recording and testing of high-density holographic 2-D grating arrays has also been developed. Predictions of the NPDD model are fitted numerically to growth curves of experimentally monitored diffraction efficiencies of the gratings recorded and physical parameters such as diffusion constant and polymerization rate are extracted and compared to the literature. This technique allows bulk recording and testing. The bulk testing of these materials leads to a better understanding of holographic recording processes and therefore also leads to material improvements. It has been noted, that under certain recording conditions, the recording beams are seen to modulate in intensity during fabrication of the grating. In this paper we also investigate this modulation in the recoding beams as the grating is being formed and propose an explanation for this behaviour. Also approximations to the absorption coefficient of the photopolymer material and the vibrational effects caused by the system components and surrounding noise are extracted giving rise to a broader explanation of the recording process.

Measurement of the chirp introduced to a picosecond pulse injected into an SOA as a function of input polarization angle.

B.F. Kennedy[1], S. Philippe[2], M. Martinez-Rosas[2], A.L. Bradley[2], P. Landais[1]
1) School of Electronic Engineering, Dublin City University, Dublin 9, Ireland.
2) Physics Department, Trinity College Dublin, Dublin 2, Ireland.

Abstract

The semiconductor optical amplifier (SOA) has huge potential for use in wavelength division multiplexing (WDM) and metropolitan networks [1]. In these systems the signal is generally transmitted through conventional single mode fibre, where the polarization state varies in a random manner. The polarization dependence of signals injected into the SOA is therefore of key importance in order to assess its viability for use in such systems.

The device under test is commercially available. It is a bulk amplifier structure with a 300μm central active waveguide terminated by two 150μm lateral active tapered regions and 50μm lateral passive regions. The polarization state of the injected beams is selected with a linear polarizer immediately before injection into the SOA, which is biased at 200mA [2].

Two techniques were used to study the polarization dependence of signals injected into the SOA. The first technique uses second harmonic generation (SHG) frequency resolved optical gating (FROG), which is based on spectral resolution of the output from an autocorrelator [3]. Using this technique the instantaneous frequency variation, i.e. the chirp, can be measured. Fig.1 shows the instantaneous frequency variation for several angles of linear input polarization. It can clearly be seen that the chirp changes for different polarizations. From this plot it is possible to determine the penalty or improvement in the chirp introduced by the SOA as a function of the polarization state.

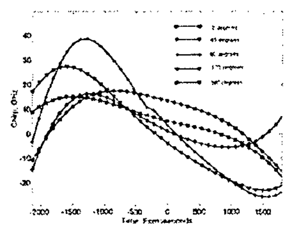

Fig. 1 Chirp as a function of the angle of a linear polarization input signal

The second technique is based on the gated-delayed self-homodyne (GDSH) technique. [4]. The pump and the probe signals are injected into the SOA with a linear polarization state at a given angle. A gain switched laser whose modulation frequency is gated by a 2x3.5μs square signal generates the pump signal. At the output of the SOA, the probe signal is selected by a band-pass filter and passes through a Mach-

Zehnder interferometer, where one arm is delayed by 3.5μs. The average chirp is measured directly from a reading on an RF Spectrum analyzer. Using this technique we are able to measure the chirp introduced to the probe signal as function of pump power and the injected polarization state of the probe.

Acknowledgement

The authors would like to thank Dr L.P. Barry and Dr. D. Reid for their helpful discussions.

References

[1] M. Asghari, I.H. White and R.V. Penty,"Wavelength conversion using semiconductor optical amplifiers", J. Lightwave Tech., vol. 15, no. 7, 1181-1190 (1997)
[2] S. Diez, C. Schmidt, R. Ludwig, H.G. Weber, P. Doussiere, and T. Duceiller, "Effect of birefringence in a bulk semiconductor optical amplifier on four-wave mixing", J. Photonics Tech. Letters, vol. 10, no. 2, 212-214 (1998)
[3] J.D. Harvey, M.D. Thomson, B.C. Thomsen, P.G. Bollond, and R. Leonhardt, "Complete characterization of ultrashort pulse sources at 1550nm", J. Quantum Electronics vol. 35 no. 4, 441-450 (1999)
[4] D.M. Baney, W.V. Sorin, "Measurement of a modulated DFB laser spectrum using gated delayed self-homodyne technique", Electronic Letters, vol. 24, no. 11, 669-670 (1988)

Equilibrium and Nonequilibrium Gain and Luminescence in Semiconductor Laser Structures

Stephan Koch
Philipps-Universität, Marburg

The gain/absorption, refractive index, and luminescence properties of semiconductor laser structures are analyzed using a microscopic approach. Optical spectra are computed for quasi-equilibrium and selected non-equilibrium situations. Implications for device analysis and optimization are discussed.

The optimization of MBE growth conditions of InAlGaAs strained layers

Kamil Kosiel*, Kazimierz Regiński, Michał Kosmala, Anna Szerling, Tomasz Piwoński, Dorota Wawer, Anna Wójcik-Jedlińska, Tomasz Ochalski, Maciej Bugajski
Institute of Electron Technology, Al. Lotników 32/46, 02-668 Warsaw

The potential applications of the strained InAlGaAs material as the active layer of semiconductor laser states the motivation of this work. While the quaternary material system presents greater challenges in materials growth, it offers the interesting features comparing to standard AlGaAs and InGaAs lasers. This is due to the combined effect of indium alloy (InGaAs) known for lattice stability and larger thermal conductivity of aluminium alloy (AlGaAs). As a result InGaAlAs/GaAlAs quantum well lasers offer the prospect of highly reliable power devices operating at 810 nm. Indium containing alloys, however are widely known as easily segregating this element during their crystallisation. This effect being especially strongly pronounced in the case of InAlGaAs. That is why the conditions of InAlGaAs growth play the crucial role during the epitaxy of laser structures. However, the knowledge of the growth conditions of InAlGaAs quaternary is so far very limited.

Structural as well as optical properties of deposited strained InAlGaAs were investigated as a function of epitaxial growth conditions. The influence of crystal surface temperature, As/III group flux ratio and quaternary alloy growth rate on the properties of InAlGaAs layers and InAlGaAs/AlGaAs quantum wells were studied. The result of interrupting the epitaxy process, just before the InAlGaAs growth, as an alternative for the continuous deposition was investigated. Investigated quantum well structures had the nominal composition of $In_{0.25}Al_{0.19}Ga_{0.56}As$ and the nominal thickness of 8 nm and were optimized for 810 nm band lasers.

Solid source MBE technique was used for growing the structures. Crystal surface temperature was measured by pyrometer. The materials growth rate was determined from pyrometric oscillations. The structures were optically characterised by means of photoluminescence measurements. PL spectra were obtained at room temperature with excitation line of 514 nm from Ar laser. Atomic force microscopy (AFM) was used for crystal surface structure characterisation. In particular the smoothness of InAlGaAs straight and reverse interfaces was investigated. AFM measurements were performed in contact mode or alternatively tapping mode and with scanning frequency from the range of 1-3Hz. For this case the Scanning Probe Microscope, Nanoscope IIIa of Digital Instruments was applied. As a result we have found optimum growth conditions of strained InAlGaAs/GaAs system.

* Correspomnding author, e-mail:kosiel@ite.waw.pl

Deeply etched tunable filters in InP-based material

Maria V. Kotlyar, Thomas F. Krauss.

email: mvk@st-and.ac.uk

School of Physics and Astronomy, University of St Andrews, North Haugh, Fife, KY169SS, U.K.

In optical telecommunications, wavelength division multiplexing has become a key technique. Tunable optical filters are necessary components for the realization of these systems. In this work we propose and fabricate tunable filters realised in high-contrast InP-air Bragg gratings. To achieve tunability the Quantum Confined Stark Effect is used. QSCE is widely used in optical intensity and phase modulators [1]. The speed of reverse-biased devices is potentially much higher then carrier injection devices because as it is not necessary to sweep out carriers from the device.

One dimensional photonic crystals were etched in InP using Chemical Assisted Ion-Beam Etching. An etching regime using a high beam voltage-current ratio was developed to overcome the many etching problems posed by InP [2]. High quality features with smooth vertical walls were etched to depths up to 5.5um, see fig.1.

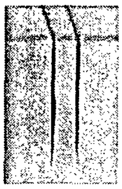

Figure 1: An example of an etched feature in InP. The depth is 3.5 μm.

An active material with 10 InGaAsP/InGaAsP quaternary quantum wells was designed. The waveguide width was chosen to be large (1.6 μm) in order to minimize diffraction losses. A passive filter was realized by using two third-order Bragg-mirrors with 100 nm air-sections on both sides of a 20 μm long cavity. 5 μm access waveguides were shallow etched to produce a single mode passive filter. Fig. 2 shows an experimental filter peak at a wavelength of 1318 nm. The achieved full width at half maximum was less than 2 nm.

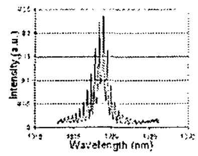

Figure 2: The spectrum transmitted by a passive filter.

Metal contacts were then evaporated on the top/bottom of the sample. Applying an electric field perpendicular to the plane of the quantum wells causes the e1-hh1 exciton absorption peak to red shift, accompanied by a reduction in the peak absorption and a broadening of the absorption linewidth. Changes to the exciton absorption naturally give rise to changes in refractive index via the Kramers-Kronig relations. For an applied electric field of strength up to 20 V the filtered peak was shifted between 0.5-5 nm. The closer to material absorption peak at 1250 nm, the bigger the shift.

In conclusion, a high-selective deeply etched InP-based tunable filter was designed and fabricated. The maximum achieved Stark-shift was 5 nm at this stage. A new CAIBE regime was developed for etching high-aspect ratio air-slots in InP-hetersostructure. A better filter performance and greater shift could be achieved by optimizing filter model and material design.

References

[1] M. S. Tobin and J D. Bruno, *J. of App.Phys.*, vol 89, pp. 1885-1889, (2001).

[2] M. V. Kotlyar, L. O'Faolain, R. Wilson and T. F. Krauss, submitted *J. of Vac. Sci. Tech.* 2003.

Pulse propagation in photonic crystal waveguides

Thomas Krauss
Department Of Physics & Astronomy,
University Of St Andrews

Some of the most exciting aspects of photonic crystal waveguides are their dispersive properties, which allow us to control the wavelength-dependent propagation of optical pulses. Different aspects of pulse propagation in photonic crystal waveguides will be discussed, amongst them the observation of pulse compression, the propagation of very slow modes and the propagation of modes with negative phase but positive group velocity. Furthermore, using a pump-probe geometry, we have seen large, optically induced shifts in photonic resonances.

Two-photon absorption based microcavity detector

T.Krug, M.Lynch, A.L. Bradley and J.F.Donegan
Semiconductor Photonics Group, Physics Department, Trinity College, Dublin 2, Ireland
T: 00353-1-6082167, F: 00353-1-6082680, E: krugt@tcd.ie

H.Folliot
Laboratoire de Physique des Solides, INSA, Rennes Cedex
Herve.folliot@insa-rennes.fr

L.P. Barry
Department of Electronic Engineering, Dublin City University, Dublin 9, Ireland
Liam.barry@dcu.ie

J.S. Roberts and G. Hill
Department of Electronic and Electrical Engineering, University of Sheffield, Mappin Street, Sheffield, S1 3JD, England

We have designed semiconductor microcavity structures for the enhancement of the two-photon absorption (TPA) photocurrent. It has been demonstrated that the TPA photocurrent can be hugely enhanced, by four orders of magnitude, by placing the active material in a microcavity structure [1], [2]. TPA in semiconductors is an attractive alternative to second harmonic generation for autocorrelation, because of lower cost and increased sensitivity. A GaAs/AlAs microcavity device has been used as a photodetector in an autocorrelator for measuring the temporal pulse width of 1.5 μm optical pulses created by an optical parametric oscillator system.

In optical telecommunication, where there is a requirement to measure low peak powers, our 1.5 μm TPA microcavity device is an excellent candidate for a detector. The enhancement of the TPA-induced photocurrent due to the cavity finesse greatly improves the sensitivity of the autocorrelation measurement. Enhancement of the two-photon absorption photocurrent results in an autocorrelation (average-power times peak-power) sensitivity of 9.3×10^{-4} $(\text{mW})^2$ at 1 Hz, which represents an improvement by two orders of magnitude when compared with commercially available SHG devices. In order to determine the sensitivity of the cavity to optical alignment, we have made depth of field and angular dependence measurements. Our measurements indicate these TPA microcavity detectors are also potential candidates for optical switching and sampling in time division multiplexed communications systems.

[1] H.Folliot, M.Lynch, L.P.Barry, A.L.Bradley, L.A.Dunbar, J.Hegarty, J.F.Donegan, J.S.Roberts, G.Hill, "Two-photon absorption photocurrent enhancement in bulk AlGaAs semiconductor microcavities", Appl. Phys. Lett., 80, 2002, pp. 1328-1330.

[2] H.Folliot, M.Lynch, A.L.Bradley, T.Krug, L.A.Dunbar, J.F.Donegan, L.P.Barry, "Two-photon-induced photoconductivity enhancement in semiconductor microcavities: A theoretical investigation", J. Opt. Soc. Am. B, Vol.19 No.10, 2002, pp. 2396-2402.

Phase correlation due to four-wave mixing in self-pulsating distributed Bragg reflector semiconductor lasers

P. Landais[a], Ciara Mulligan[a], J. Renaudier[b] and G.-H. Duan[c]

[a]School of Electronic Engineering, Dublin City University, Glasnevin, Dublin 9, Ireland

[b]Département Communications et Electronique, Ecole Nationale Supérieure des Télécommunications, 46 rue Barrault, 75634 Paris Cedex 13, France

[c] Alcatel Research & Innovation, Route de Nozay, 91460 Marcoussis, France

Keywords: Distributed Bragg reflector, self-pulsating laser, clock recovery, four-wave mixing and phase correlation.

ABSTRACT

All-optical regeneration at 40 Gbit/s and beyond appears to be a crucial element for future transparent networks. One solution to achieve the regeneration is an all-optical clock recovery element combined with a Mach-Zehnder interferometer. In this respect truly all-optical clock recovery is of very high interest as it would supersede the complicated optoelectronic schemes including a high speed photo-receiver, a high-Q filter, a power amplifier and a high speed laser or an integrated laser modulator. Among the different approaches investigated so far, a scheme based on a single self-pulsating distributed Bragg reflector laser is of particular interest from practical and cost viewpoints. In this structure at least two longitudinal modes beat together, generating power oscillation even though the laser is DC biased. The oscillation frequency is given by the free spectral range of the structure. However, in the case of a self-pulsating laser, the RF signal linewidth is smaller than the sum of the linewidth of the lasing modes, benefiting from the correlation of the phase of the optical modes through the interband four-wave mixing (FWM) non-linearity. The FWM results as a modulation of the carrier population, leading to a nonlinear gain and refractive index modulation, affecting both the amplitude and the phase of the cavity modes. Based on a four-wave mixing formalism we present a study of the origin of the RF oscillation in a 3 longitudinal mode self-pulsating DBR laser. From this model, a stability analysis is derived; the phase correlation of these modes is calculated. The modeling results provide design criteria for high performance self-pulsating lasers for all-optical clock recovery.

Tilted Cavity Laser

Nikolai Ledentsov
Electrical Engineering University of St.Petersburg

The concept of a tilted cavity diode laser [1] as proposed to combine advantages of an edge-emitting laser, such as high power operation, and a surface-emitting aser such as wavelength-stabilized operation. The tilted cavity laser comprises a resonant cavity confined by at least one multilayered interference reflector (MIR). The cavity has a narrow dip in the reflectivity spectrum at a tilted incidence of light, and the spectral position of the dip is, naturally, a function of the tilt angle. The multilayered interference reflector has a narrow stopband in the reflectivity spectrum and the spectral position of the stopband maximum is also a function of the tilt angle. The device is designed such that the spectral positions of the cavity dip and of stopband maximum coincide at only one tilt angle, and therefore the resonant conditions for low-loss operation are realized at one wavelength. As the angle deviates from the optimum value, the cavity dip and the stopband maximum of the mirror shift at different rates and thus run away from each other and the Q-factor of the cavity decreases. In this concept no distributed feedback (DFB) grating, or coupling to fiber grating is needed to achieve wavelength stabilization, and conventional as-cleaved or coated facets can be used. By proper adjustment of the design, one can realize positive, zero or even negative wavelength shift with temperature, as opposite to both conventional DFB and vertical cavity lasers, where the wavelength shift is always positive, being defined by the refractive index dependence versus temperature.

Depending on the particular design, the tilted cavity laser can operate as:

- an edge-emitting laser where the laser light comes out through the facet;
- as a tilted cavity surface emitting laser (TCSEL), if the tilt angle of the resonant optical mode is below the total internal reflection angle at the semiconductor/air interface;
- as a TCSEL where the laser light comes out through a patterned top surface;
- in a closed optical mode which propagates within the laser and exists outside the laser structure only in the form of evanescent field. Such design allows efficient direct outcoupling of the laser light via direct adjustment of an optical fiber or via dielectric rod deposited on the surface.

Experimental results on high-performance tilted cavity lasers based on quantum well and quantum dot active media emitting at 1-1.3_m in the wavelength-stabilized mode and a broad temperature range will be presented.

[1] N.N. Ledentsov, V.A. Shchukin *"Novel concepts for injection lasers"* SPIE Optical Engineering, 2002, 41, pp. 3193-3203.

Feedback Resistance and Linewidth of Quantum Dot DFB Lasers

Luke Lester, H. Su, L. Zhang, R. Wang, and A. L Gray
University of New Mexico

External optical feedback effects in quantum dot (QD) laterally-loss-coupled (LLC) distributed feedback lasers (DFB) are reported. The critical external feedback ratio that causes coherence collapse of the QD DFB is measured to be -14 dB. No spectral broadening at this feedback level is observed within the 0.06 nm resolution of the optical spectrum analyzer (OSA). Self-homodyne measurements also confirm that the re-broadened linewidth of the QD DFB under -14 dB feedback is still much smaller than the feedback-free linewidth. Under 2.5 Gbps modulation, eye-diagram measurements show that the signal to noise ratio (SNR) starts to degrade at a feedback ratio of -30 dB in the QD LLC-DFB, about 20 dB higher than a typical quantum well (QW) DFB at the same output power and extinction ratio. The linewidth of these QD DFB lasers is also investigated. A linewidth-power product less than 1.2 MHz-mW is achieved in a device of 300 _m cavity length for an output power up to 2 mW. Depending on the gain offset of the DFB grating from the QD ground state gain peak, linewidth rebroadening or a floor is observed at a cavity photon density of about 1.2-2.4x10^15 cm^-3, which is much lower than in quantum well (QW) lasers. This phenomenon is attributed to the enhanced gain compression observed in QDs.

Wavelength-Tunable Transform-Limited Optical Pulse Generation using External-Injection of Two Fabry-Perot Gain-Switched Laser Diodes at 10GHz

P.J.Maguire, A.M. Clarke, C.Mulligan, P.M. Anandarajah,
and L.P. Barry,
Research Institute for Networks and Communications Engineering,
School of Electronic Engineering,
Dublin City University, Dublin 9,
IRELAND.
Email: maguirep@eeng.dcu.ie

Due to the continued growth of the Internet and the introduction of new broadband services such as video-on-demand and mobile telephony, there will be a need to develop new optical techniques that can handle extremely high capacities and better utilise the enormous bandwidth that optical fibre offers within the network. However in a basic optical communications network comprising a laser transmitter, an optical fibre transmission medium, and a receiver, the capacity is essential limited by the speed of the available electronics (e.g. the modulation speed of the transmitter). To overcome this problem it is possible to implement optical multiplexing techniques such as Optical Time Division Multiplexing (OTDM), Wavelength Division Multiplexing (WDM), or a combination of the two to form a hybrid WDM/OTDM.

In order to operate at these high-speeds, the development of an ultra-short, transform-limited pulse source with broad wavelength-tunability is vital. There are a number of different ways in which ultra-short optical pulses can be generated. One of the simplest, cost effective and reliable techniques involves the gain-switching of a Fabry-Perot (FP) laser. However, this technique has a number of disadvantages including chirp, timing jitter and a multi-moded laser output. There are a number of techniques available that can overcome these problems, with the most promising being self and external injection seeding of a gain-switched FP laser. Not only do these methods reduce the frequency chirp and timing jitter, but they also allow wavelength tuning and enhancement of the Side Mode Suppression Ratio (SMSR). Unfortunately self-seeding suffers from the fact that the repetition rate must be kept at an integer multiple of the round trip frequency which is determined by the external cavity length. This introduces instability as the external cavity length would have be continually altered for continuous wavelength tunability. External injection seeding of a gain switched FP laser on the other hand, has the advantage that the repetition rate can be set at an arbitrary value.

Current trends and technology maturity favour the deployment of optical communication systems, operating at line rates of 10 Gb/s and beyond, thereby making the development of optical pulse sources at high repetition rates ($\geq$10GHz) to be extremely important. We demonstrate external injection seeding of a gain-switched source containing two FP lasers. Using such an integrated dual laser source we have shown it is possible to generate pulses that exhibit very high (previously unreported) SMSR (>50dB) and tunability over a very large wavelength range (>50nm). Furthermore, using this technique it may be possible to develop a wavelength tunable pulse source exhibiting high SMSR with wavelength tunablility from S to L band.

Study of phase-locking in arrays of index-guided Tapered Lasers for high-brightness applications

D. Masanotti, F. Causa, J. Sarma
Department of Electronic and Electrical Engineering,
University of Bath, Bath BA2 7AY, UK

High output powers are essential for a variety of applications, especially where bulky systems have to be replaced with more compact and versatile laser diodes. To achieve high output powers from semiconductor lasers it is necessary to increase the active (gain) volume and reduce the risk of catastrophic optical mirror damage. However, to increase the device brightness it is necessary to develop semiconductor optical sources with high beam quality also. Tapered geometry lasers have been developed to achieve relatively high output power and high brightness. In particular, two categories of tapered devices have been developed: MOPA (Master Oscillator Power Amplifier) sources, e.g., [1-3], where a system of lenses is used to achieve high brightness from a gain-guided optical source; and index-guided tapered lasers where the high brightness can be achieved without the use of lenses, [4], [5]. The latter category of devices has the added attraction of being suitable for low cost applications.

To further increase the output power arrays of a large number of stripes have been first developed, [6]. Although producing large output powers, such devices generally have poor beam quality. The out-of-phase mode is in fact typically favoured in these devices because of the better overlap with the gain distribution (especially in index-guided arrays) which produces the undesired multi-lobed far field profile. The ideal case is when the array operates in the fundamental array-mode with constant phase across the facet, producing the desired single lobe, narrow far field, [6]. Various designs have been proposed to achieve effective mode selection in such arrays but at the cost of sophisticated device fabrication, e.g., [7]. The relatively few papers that discuss arrays of tapered lasers are specifically either on arrays of MOPAs, [8], [9], or on uncoupled, linearly tapered lasers, [10]. The devices of interest in this paper are arrays of index guided parabolic tapered lasers designed to achieve a longitudinally non-uniform coupling between the elements with weak coupling along the length of the device and strong coupling at the output of the device, to promote overall coherence, [11]. Such devices have been demonstrated to be suited for high-brightness with output powers in excess of 2.5W/facet in a ~1deg. beam (corresponding brightness ~ $275MWcm^{-2}sr^{-1}$).

The scope of this paper is to present a theoretical and experimental study on phase-locking in arrays of index-guided tapered lasers developed and fabricated in-house. Useful comparisons between the operational characteristics of arrays of different geometries are going to be discussed and interpreted using models based on the diffraction theory, [12], and on the coupled mode theory, [13], taking into account also the optical gain, [11]. Preliminary results are presented in Fig. 1, where the Far Field intensity profiles measured from Arrays of five Parabolic Bow-Tie Lasers (PBTL), [1], [2], [13], at threshold (a) and at twenty-two times the threshold (b) are compared with those calculated considering the elements out of phase at threshold and in-phase at high currents.

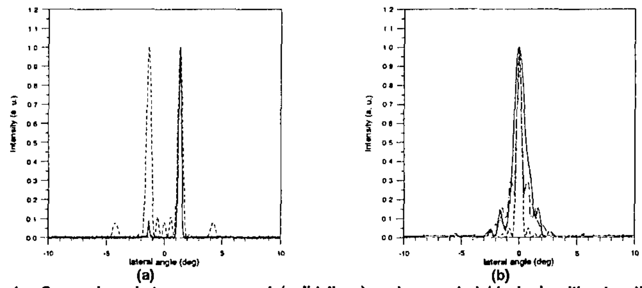

Fig. 1: Comparison between measured (solid lines) and computed (dashed: without optical gain; dash-dot: with optical gain) Far Field Intensity profiles for 5-element Parabolic Bow-Tie Laser Arrays.

References

[1] J. N. Walpole, E. S. Kintzer, S. R. Chinn, C. A. Wang, L. J. Missaggia, *High-power, strained-layer InGaAs/AlGaAs tapered travelling wave amplifier*, Appl. Phys. Lett., vol. 61, p. 740, 1992

[2] S. O'Brien, R. J. Lang, R. A. Parke, J. Major, D. F. Welch, D. Mehuys, *2.2-W continuous-wave-diffraction-limited monolithically integrated master oscillator power amplifier at 854nm*, IEEE Photonics and Technology Letters, vol. 9, n. 4, pp. 440, 1997

[3] A. Egan, C. Z. Ning, J. V. Moloney, R.A. Indik, M. W. Wright, D. J. Bossert, J. G. McInerney, *Dynamic Instabilities in master oscillator power amplifier semiconductor lasers*, IEEE J. Quantum Electronics, vol. 34, n. 1, pp. 166, 1998

[4] D. Masanotti, F. Causa, J. Sarma, *Design optimisation of high power high brightness parabolic Bow-Tie laser diodes*, IEE Proceedings - Circuits, Devices and Systems, vol. 150, n. 6, pp. 537, 2003

[5] D. Masanotti, F. Causa, J. Sarma, *High brightness, index-guided parabolic Bow-Tie laser diodes*, accepted (October 2003) for publication in IEE Proceedings - Optoelectronics

[6] *Diode Laser Arrays*, ed. D. Botez and D. R. Scifres, Cambridge University Press (1994)

[7] A. Bhattacharya, L. J. Mawst, M. P. Nesnidal, J. Lopez, D. Botez, *0.4W CW diffraction limited beam Al free 0.98μm wavelength three core ARROW-type diode lasers*, Electron. Letters, vol. 31, n. 7, p. 657, 1996

[8] J. S. Osinski, D. Mehuys, D. F. Welch, K. M. Dzurko, R. J. Lang, *High-power, spectrally coherent array of monolithic flared amplifier-master oscillator power amplifiers (MFA-MOPAs)*, IEEE Photonics and Technology Letters, vol. 6, n. 10, p. 1185, 1994

[9] M. Mikulla, A. Schmitt, M. Walther, R. Kiefer, W. Pletschen, J. Braunstein, G. Weimann, *25-W CW High-brightness tapered semiconductor laser-array*, IEEE Photonics and Technology Letters, vol. 11, n. 4, p. 412, 1999

[10] F. J. Wilson, J. J. Lewandowski, B. K. Nayar, D. J. Robbins, P. J. Williams, N. Carr, F. O. Robson, *9.5W CW output power from high brightness 980nm InGaAs/AlGaAs Tapered Laser Array*, Electronics Letters, vol. 35, n. 1, p. 43, 1999

[11] D. Masanotti, F. Causa, J. Sarma, *Bright parabolic bow-tie laser arrays*, Paper CC6-2-WED (oral presentation), CLEO EUROPE EQEC 2003, Munich ICM (Germany), 22-27 June 2003

[12] D. R. Scifres, W. Streifer, R. D. Burnham, *Experimental and analytical studies of coupled multiple stripe diode lasers*, IEEE J. Quantum Electronics, vol. QE-15, n. 9, p. 917, 1979

[13] D. Botez, *Array-mode far-field patterns for phase-locked diode-laser arrays: coupled mode theory versus simple diffraction theory*, IEEE J. Quantum Electronics, vol. QE-21, n. 11, p. 1752, 1985

Differential lifetime measurements of spontaneous emission in self-assembled Quantum Dots

Daniel R Matthews, Huw D Summers, Peter M Smowton, and Peter Blood

School of Physics and Astronomy, Cardiff University, 5, The Parade, Cardiff, Wales,

U.K. CF24 3YB

Paul Rees

School of Informatics, University of Wales Bangor, Bangor, Gwynedd, Wales, U.K.

Mark Hopkinson

EPSRC Centre for III-V Technologies, University of Sheffield, Sheffield, U.K.

Understanding carrier capture, relaxation and re-excitation dynamics in strain-induced quantum dots in the high carrier density regime is essential for advancing the performance of semiconductor lasers. In this paper we report on time-resolved luminescence measurements of InGaAs quantum dots within a p-i-n diode laser structure. A key feature of this experimental work is the design of the sample architecture, where window in the p-contact metallization allows both the measurement of spontaneous without the influence of a lateral waveguide and injection of a short duration optical pulse which is tuned to generate carriers in the barrier material of the structure. CW electrical injection to the sample establishes a carrier population in the quantum dots, a pulse of photo-generated carriers is added to the system and by monitoring the temporal evolution of the spontaneous emission the differential lifetime of the dots can be obtained for varying levels of occupation. By analysing the spontaneous emission we are able to simultaneously measure the time response across the whole spectrum and hence study the temperature dependent cross coupling between localised dot states in the high carrier density regime. We find strong evidence that the temporal evolution of the luminescence is correlated across the emission spectrum indicating that the individual spectral contributions are due to multiple states within dots rather than the existence of bi- or even tri-modal distributions of dots within the sample. Capture of the photo-generated carriers into the dots occurs within 30 ps, even at low temperature (50 K) or high carrier density indicating that a capture bottleneck due to insufficient scattering mechanisms does not occur. Although the intrinsic response time of the dots is rapid the effective speed of the system can be extremely slow in response to modulation of the wetting layer population since these high energy states maintain the supply of carriers to the dots. This carrier relaxation bottleneck can produce a decay lifetime in excess of 1ns. Lifetime measurements in the presence of an external reverse biased, dc electric field show a pronounced temperature dependence which indicates that the dot states couple to the wetting layer via phonon absorption.

External Optical Feedback Effects on Semiconductor Lasers

David McInerney,J.F.Donegan

Semiconductor Photonics Group, Physics Department, Trinity College, Dublin 2,Ireland

The spectral characteristics of a semiconductor laser can be strongly affected by optical feedback. Unwanted optical feedback can cause serious problems in practice, which leads to the performance of the diode laser being degraded. These effects are investigated on the output characteristics of a Slotted Fabry Perot (SFP) laser, a DFB laser, and on a widely tunable laser. The feedback is coupled back into the front facet of the laser by an external mirror of high reflectivity at a distance of approximately 10cm from the laser.
The output spectrum of the SFP and DFB with feedback present, are shown below. Our measurements show that the feedback has an obvious detrimental effect on the output of the both the SFP and DFB. The presence of unwanted side modes reduces the SMSR in the SFP by 10dB to –25dB. The feedback causes a splitting of the main mode in the DFB, which results in the presence of other side modes. Feedback work on the widely tunable lasers was also performed in order to get a comparison between the three different lasers.

Figure 1: Graph of Power vs Wavelength for SFP at 79.2mA with arrows indicting additional side modes due to the feedback.

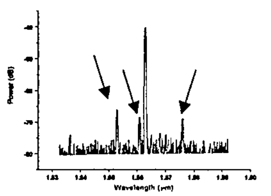

Figure2: Graph of Power vs Wavelength for DFB at 55.2mA.

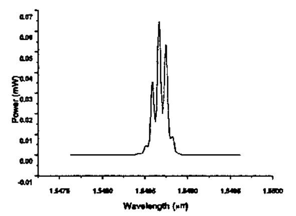

Carrier capture dynamics in quantum dot lasers and the implications for modulation bandwidth

S. Melnik, D. O'Brien, S.P. Hegarty, G. Huyet and A. Uskov.
Physics Department, National University of Ireland, University College, Cork, Ireland

April 2, 2004

1 Abstract

We investigate the behavior of quantum dot lasers in the frequency domain and how this behavior deviates from conventional semiconductor laser behavior. We use a rate equation model for quantum dot lasers in which the laser dynamics are described in terms of three equations. The active medium is described by an equation describing the carrier occupation probability in the quantum dots. This carrier population is maintained by carrier capture from the wetting layer of the quantum dot laser structure. The population of carriers in the wetting layer is described in terms of a second equation. A third equation describes the light field interacting with this active medium. From this model we derive the transfer function for the system and describe the relative importance of the different parameters for the high frequency operation of these devices.

The frequency behavior of laser diodes is generally characterized by a 2 pole transfer function. The model presented above for quantum dot lasers is described by a three pole transfer function. This has implications for the maximum modulation bandwidth of lasers based on this active medium. Isolating the relevant parameters responsible for this third pole provides insight into the limitations of quantum dot laser operation in high speed applications. The appearance of a third pole in the transfer function of quantum dot lasers is in agreement with recent experimental small signal transfer function results. We show how this model for quantum dot lasers reduces to the familiar two pole transfer function in two limiting cases. One of these cases is that of very fast carrier capture from the wetting layer into the ground state of the dots. The mechanism responsible for carrier capture into the dots and subsequent inter-dot relaxation to the lasing ground state has previously been highlighted as a limitation on the maximum bandwidth achievable by quantum dot lasers. The predicted effect was referred to as the phonon bottleneck. Other relaxation

mechanisms such as Auger carrier capture have been put forward as an alternative relaxation mechanism, although there is still some debate over the rate of carrier capture/relaxation in the dots. Some experimental schemes have already been put in place to speed up carrier transport to the quantum dot ground state such as tunnel injection. Quantum dot lasers using tunnel injection have shown modulation bandwidths of up to $15GHz$. The effect of fast carrier capture and other techniques such as gain levering in two-section lasers on the modulation bandwidth of the quantum dot laser is also explored.

Ultrafast Gain Dynamics in Multiple Quantum Well Semiconductor Optical Amplifiers

Alan Miller and Alvaro Gomez-Iglesias
School of Physics and Astronomy
University of St Andrews
Scotland

Ultrafast switching is essential for all-optical processing applications. In this context, the last decade has seen a substantial progress in the use of semiconductor optical amplifers (SOAs). Interferometric switches, such as the Terahertz Optical Asymmetric Demultiplexer (TOAD) or Mach-Zehnder interferometers can be operated at rates faster than the interband gain recovery time of the material. However, despite the work carried out to date, there is still much to be understood on the implications of the subpicosecond refractive index changes associated with the gain dynamics in switching operation. Previous pump-probe experiments and some theoretical models stress the role of carrier heating in the SOA response when femtosecond pulses are involved. Here we present the results of gain and refractive index dynamics including interferometric three-beam pump-probe experiments with a SOA.

A High Speed, High Multiplication Gain CMOS Avalanche Photodiode

Aoife M. Moloney, J. Carl Jackson[†], Alan Mathewson[†], Alan P. Morrison

§

Department of Electrical and Electronic Engineering,
University College Cork, Cork
IRELAND

[†]*National Microelectronics Research Centre,*
"Lee Maltings", Prospect Row, Cork
IRELAND

E-mail: a.morrison@ucc.ie

The well known advantages of CMOS, namely high reliability, low cost and potential for large scale integration, has meant there is currently an eagerness to produce a CMOS photoreceiver. The difficulty encountered with the development of such a receiver has been the development of a high sensitivity, high speed CMOS photodiode. The long absorption length of silicon ($2.5 - 15$ μm for $650 - 850$ nm light), combined with the shallow junction depths (< 1 μm) in CMOS technologies means carriers are generated in the substrate resulting in a diffusion tail which severely limits the bandwidth. If these bulk generated carriers are screened from the device (using SOI wafers), a higher speed is obtained but a very low responsivity results. This paper presents a CMOS compatible Geiger-mode avalanche photodiode (GMAP), developed for use in single photon counting, that eliminates the diffusion tail without loss of responsivity.

The shallow junction GMAP (see Figure 1) was fabricated with CMOS compatible processing steps and has a virtual guard ring structure that prevents edge breakdown. The enrichment doping was tailored to give the low (< 30 V breakdown voltage). Previous measurements on a GMAP with a 20 μm active area diameter and 3 μm overlap have revealed high responsivity (0.05 A/W, 0.44 A/W and 15.21 A/W at 5.0 V, 27.0 V and 27.4 V reverse bias respectively) [1] and impulse responses with the diode biased in the avalanche mode are presented here. The chip with the GMAP was mounted on standard FR4 1.6 mm PCB. Wirebonds were used to connect the on-chip anode and cathode bondpads to a grounded PCB bondpad and a 50 Ω transmission line respectively. The GMAP was reverse biased through a Mini-Circuits ($0.1 - 6000$ MHz) bias tee, which in turn was connected to a Tektronix TDS3052 500 MHz digital phosphor oscilloscope. The diodes were illuminated using 650 nm picosecond pulses (< 200 ps) at a repetition rate of 1 MHz from an IBH NanoLED pulsed diode excitation system. The GMAP impulse responses were measured and recorded on the scope for several reverse bias voltages (see Figures 2–4 for responses at 25.0 V, 26.0 V and 27.0 V reverse bias). Clearly, at low biases (≤ 26.0 V) the response has a diffusion tail and is diffusion limited, however, at higher biases (≥ 27.0 V) the tail disappears completely and a bandwidth of ≈ 616 MHz is obtained ($0.44/\tau$ where τ = full width at half maximum). The diffusion tail has been eliminated because at high reverse bias the doping profile of the GMAP allows for the spreading of the depletion region and the high electric field down below the junction. It is thought that the scope has limited the measurements here, and further measurements will be made on the GMAP and presented in the final paper.

In summary, a shallow junction, CMOS compatible diode has been shown to have a bandwidth of > 600 MHz at 27.0 V reverse bias. The diffusion tail normally apparent in CMOS photodiodes has been eliminated due to the spreading of the high electric field and no loss of responsivity has occurred. To the best of the authors' knowledge these are the first impulse response measurements made on GMAPs biased in the avalanche region.

References

[1] A.M. Moloney, *A CMOS Monolithically Integrated Photoreceiver Incorporating an Avalanche Photodiode*, Ph.D. thesis, University College Cork, April 2003.

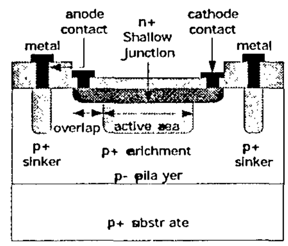

Figure 1: Virtual guard ring GMAP structure showing active area and overlap regions.

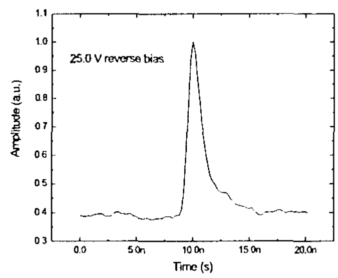

Figure 2: Impulse response of the GMAP at 25.0 V reverse bias.

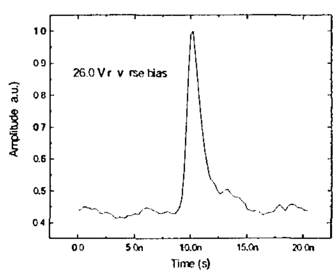

Figure 3: Impulse response of the GMAP at 26.0 V reverse bias.

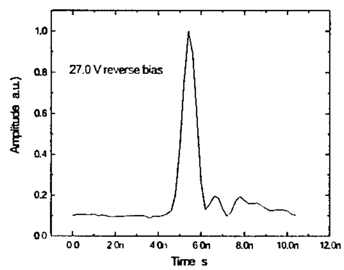

Figure 4: Impulse response of the GMAP at 27.0 V reverse bias.

NONLINEAR OPERATION OF 1D PHOTONIC CRYSTAL LASER*

A.Mossakowska-Wyszyńska,[1] T.Nazaruk[1] P.Szczepański[1,2]

[1]*Institute of Microelectronics and Optoelectronics, Warsaw University of Technology, Koszykowa 75 Str.,00-662 Warsaw, Poland*
E-mail: A.Mossakowska@elka.pw.edu.pl
[2]*National Institute of Telecommunications, Szachowa 1 Str., 04-894 Warsaw, Poland*

Photonic crystal structures have been the subject of intense research activity since Eli Yablonovitch pioneer work from 1987. Photonic crystals are one-, two- or three-dimensional dielectric (semiconductor or metal) structures of periodic spatial distribution of refractive indices. In photonic crystal exists a forbidden gap for electromagnetic waves, analogous to the electronic band gap in semiconductor. In semiconductors, the existence of periodic potential leads to the formation of band gaps as a result of Bragg's diffraction. The same analogy could be applied in photonic crystals. The presence of a periodic change in refractive index causes light waves to be subjected to the effects of Bragg's diffraction. This phenomenon forms a band gap (photonic band gap). Photonic crystal has many advantages such as: frequency range, where no electromagnetic eigenmode exists (photonic band gap), and optical gain, which is extremely intensified in the vicinity of the photonic band gap edge. It is also possible to: obtain photonic crystal with ultra high refractive index, control spontaneous emission in photonic crystal, modify the state density and group velocity, locate light by structure defects. Moreover, in the planar waveguide structures fabricated in photonic crystals, single mode propagation can be obtained (in contrast to classic waveguide structures with total reflection) in waveguides of very large cross section.

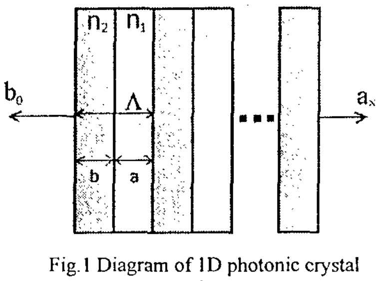

Fig.1 Diagram of 1D photonic crystal F-P laser.

Figure 1 shows schematically the investigated 1D photonic crystal laser structure, which consists of N elementary cells with alternating layers of different indices of reflection: first one with width b and refractive index n_2, and second with width a and refractive index n_1. We assume that the laser has at the ends two mirrors as it is in Fabry-Perot cavity. First mirror has reflection coefficient equals 1 and second has changeable reflection coefficient (for values between 0 and 1). Moreover, we make an assumption that the layers with width b are active medium of the laser and laser structure has at the ends active stripes, as it is indicated on figure 1.

We present semi analytical, approximate model of non-linear operation of 1D photonic crystal laser. In our theoretical model, we take into account the gain saturation effect, spatial hole burning effect, transverse and longitudinal field distribution. Our model, based on energy theory, allows to investigate in relatively easy way the influence of the real structure parameters such as photonic crystal geometry, losses as well as value of reflection coefficient of laser mirror on the small signal gain coefficient. With the help of this model, we obtained the laser characteristics, which reveal an optimal feedback strength for F-P cavity laser structure. This optimal strength provides maximal power efficiency for given pumping level.
PREFERENCE: Poster

* Project granted by the Polish State Committee for Scientific Research (KBN), project no 1280/T11/2003/25

ADVANCES IN PHOTOREFLECTANCE CHARACTERISATION OF EPITAXIAL DEVICE MATERIAL WAFERS

Martin E. Murtagh and Patrick V. Kelly, Optical Metrology Innovations Ltd., 2200 Cork Airport Business Park, Cork Airport, Co. Cork, Ireland.

Advances in the photoreflectance (PR) spectroscopy of epiwafer device material wafers are presented. PR is a laser pumped electro-absorptive modulation reflectance spectroscopy technique which probes the electric field modulated density-of-states (DOS). PR yields important band structural information including critical point type, interband transition energy levels, and resonances. Ternary and quaternary alloy mole fractions can be deduced from PR. Uniquely, as a consequence of its electro-optic character, PR can measure in-built surface and interfacial electric field strengths in the epiwafer structure. PR has traditionally been applied to heterojunction bipolar transistor (HBT) epiwafer characterisation. Pump intensity dependent PR results are presented. The emergence of wide variable angle of incidence PR has opened its application to VCSEL device material. Results from nominally 850nm and 980nm VCSELs, corresponding to cavity (top/bottom) emission between AlGaAs(AlAs) distributed Bragg reflector (DBR) stack mirrors, reveal the technologically important cavity resonance mode and ground state quantum well exciton structures.

Linewidth Enhancement Factor of Quantum Dot Lasers Emitting at 1310nm

Jan Muszalski[1], John Houlihan[2], Guillaume Huyet[2], Brian Corbett[3]

[1] *Institute of Electron Technology Al. Lotnikow 32/46, 02-668 Warsaw, Poland*
[2] *Department of Physic National University of Ireland, University College Cork, Cork, Ireland*
[3] *National Microelectronic Research Centre, "Lee Maltings", Prospect Row, Cork, Ireland.*

The linewidth enhancement factor (so called α factor) it is one of the most important parameters used to describe the properties of semiconductor lasers. It determines the frequency chirp under modulation, the antiguiding in narrow stripe lasers, self-focusing and filamentation in broad area devices. It is usually defined as $\alpha=2k_o(dn/dN)/(dg/dN)$ where N is the carrier concentration, n refractive index, g gain, and k_o is the wave vector in free space. It has been predicted that for quantum dot (QD) lasers α–parameter should close to zero, and initial measurements were encouraging[1]. However, in recent times reported values have varied considerably between 1 and 3 depending on material structure. Indeed, recent work at 980nm has shown on very high value of α equal to 4 [2]. In this paper, we discuss detailed measurements at 1310 nm which shows that the α–parameter depends strongly on the gain properties of the laser. We obtain a high value equal to 3.5 for short length high gain devices which decreases to 1.5 when the laser length is increased to 2mm.

In our experiment we have used the devices emitting in 1310 nm band. Those devices were fabricated both as single mode (3-5 micrometer ridge waveguide) and multimode (broad area 35 micrometer stripe width) in the transverse direction and cleaved to different resonator lengths (1, 1.5, 2 mm). All devices were fabricated from a heterostructure which consisted of a stack of 6 InAs QD layers grown using DWELL technology similar to [1]. The α-parameter was calculated directly from the refractive index and gain measurements performed using sub-threshold amplified spontaneous emission spectra taken for different current injections. The refractive index was calculated from the Fabry-Perot mode shifts and the gain using a standard Hakki-Paoli technique.

Measurements at different gain conditions were possible because the distributed mirror losses of long devices is much lower than for short ones and thus their threshold gains can differ considerably. The experimental data reveals that, for higher gain operation, the increase in α–parameter is a result of gain saturation i.e., a decrease in differential gain. For short devices (1mm) at high current excitation we have also observed the simultaneous emission from both the ground and exited states. In those devices the α–parameter was also measured for the excited state to be 1.5, which is much lower than the ground state measurement of 3.5.

[1] T.C. Newell, D.J. Bossart, A. Stinz, B. Fuchs and K.J. Malloy, IEEE Photon. Tech. Lett. 11 (12) 1527 (1999).
[2] Y. Tanguy, J. Muszalski, J. Houlihan, G. Huyet, E.J. Pearce, P.M. Smowton and M. Hopkinson, Opt. Commun. in press.

Marion Velly[1,2] and Patrice Féron[1]

1 Laboratoire d'Optronique, ENSSAT, Lannion, France.
2 Dept. of Applied Physics and Instrumentation, Cork Institute of Technology, Ireland.

Abstract

The purpose of this project is the characterisation of Erbium doped fluoride spherical glass microlasers. A microsphere with a diameter of around one hundred microns provides both the resonant cavity and the amplifying medium for lasing behaviour. Light propagates along the equator of the microsphere by repeated total internal reflections and it is confined inside a ring whose transverse dimension is of the order of the wavelength. This particular propagation mode is called a whispering gallery mode after the acoustical domain in which it was first studied. Considering this medium as being quasi-lossless, quality (Q)- factors of the order of 10^9 have been experimentally verified. By considering the small mode volume achievable, a very high energy density can be obtained. The aim of this project was to characterise the 3 micron Erbium transition, which may be of interest for medical applications. We also studied the 1.5 micron transition, which is the wavelength suited for telecommunication systems. To provide energy to the microsphere in order to permit the lasing effect, we chose to use the prism coupling method because it is a very selective coupling technique allowing a very "clean" excitation of gallery modes. This makes it possible to excite the most confined modes with a pump laser threshold of 600 µW. Whispering gallery modes properties are ideally suited for studying the fundamental physics of cavity electrodynamics, non-linear effects in optics with very low thresholds and they are also suited for applications in telecommunication systems and medical devices. This study contributes to the miniaturisation of optoelectronic components.

SOLAR ENERGY CONVERTERS ON THE BASIS OF a-Si_{1-x} Ge_x :H SOLID SOLUTION

B.A. Najafov
Institute of Radiation problems, National Academy of Sciences, Azerbaijan, 31a, H. Javid av., Baku, Az-1143, Azerbaijan,

V.R Figarov
Institute of Physics, National Academy of Sciences, Azerbaijan, 33, H. Javid av., Baku, Az-1143, Azerbaijan, e-mail: elmira@physics.ab.az

a-Si_{1-x} Ge_x :H solid solution amorphous films (with x = 0.4; 0.7, H=17at.%) were fabricated by the plasmochemical deposition method 1μm thick, at the substrate temperature of 200°C, the rate of deposition was 0.1A /s, and the distance between the target and the substrate was L ≈25cm. The dispersion process was conducted in a hydrogeneous plasmic medium, that had been obtained with the use of a magnetron and a RF field. Taken ESR spectra of a-Si_{1-x} Ge_x :H at 80K were asymmetric in form, inasmuch as they were composed of two kinds relating to free bonds of Si and Ge, respectively . At the same time the observed signal was not a simple superposition of the two signals (for Si and for Ge), since they violently interacted with each other and the resulting signal in the intervening interval aimed to assume the form of a sole line. Because of this the observed spectrum on the left and on the right could be depicted by a superposition of the two signal : with g-factor of g=2.004 ÷ 2.006 and the line width of 51-65 G and with g=2.018 ÷ 2.022 and 73-86 G relating to the silicon and germanium free bonds, respectively. In this way it could be evaluted densities of Si and Ge free bonds, taken separately. But in accordance with computation of molecular orbitals in a-Si_{1-x} Ge_x :H , the presence of atoms, adjacent to the orbitals, almost does not alter g-value of ESR-signals from both Si and Ge free bonds. By the IR absorption spectrum determining a number of Si-H bonds, and also a number of Ge-H bonds, it may assert that a number of Ge free bonds is 8-10 times larger than that of Si [1]. It is proved that in a-$Si_{1-x}Ge_x$: H films H atoms are mainly bound to Si atoms and so a total number of H is reduced with increasing of Ge content. That stands for the density of Ge free bonds decreases a number of H atoms, bound to Ge, but it does not a number of H atoms, bound to Si. This fact is also confirmed by ESR investigations. ESR investigations in a-Si_{1-x} Ge_x :H amorphous films with x=0 ÷15 at.% Si and in $Ge_{0.90}$ $Si_{0.10}$: H_x (x=23 at.%), fabricated by the vacuum evaporation and the plasmochemical deposition, have shown that the band gap, set up by strongly localized centres, is of 10^{19} ÷10^{20} cm^{-3} eV^{-1} order [2-3]. The localized centres are paramagnetic, and they probably define also the form of dependence of electrophysical properties of the material, σ (T) vs. $T^{-1/4}$, in low temperature ranges. Hence in a-Si_{1-x} Ge_x :H films by the signal intensity, it can be found the paramagnetic centre concentration, N_s,

$$N_s = \alpha N(\varepsilon_F)kT,$$

which unambiguously give a value of the density of states provided that the effective energy of correlation between two electrons in the band gap U is much less than kT (U << kT), N (ε_F) is the density of states near the Fermi level of 10^{18} $cm^{-3}eV^{-1}$ order, and $\alpha \approx 3$ [4]. In case of U >> kT, states lying below ε_F in U magnitude are paramagnetic independent of temperature. The study of influence γ- radiation on properties of the amorphous hydrogenated a-Si_{1-x} Ge_x :H enables one to get the valuable information on defects in the material. The investigation after γ-irradiation from a source at the irradiation dose of 10^{17} ÷10^{18} photon/cm^2 has revealed that quanta, passing through the a-Si_{1-x} Ge_x :H film, do not produce torn bonds (as it would be occurred ,e.g., under irradiation by the visible light). The results of the carried out studies makes it possible to maintain that a-Si_{1-x} Ge_x :H material involved is thermodynamically resistant and it is of important for manufacturing solar energy converters and IR receivers.

References

1.Najafov B.A. Proceedings of the 8-th conference on silicon-germanium alloys. Institute of Physics, Academy of Sciences, Uzbekistan, Tashkent, p.11, (1991).

Model for quantum dot lasers incorporating the $\alpha-$factor and external optical feedback

D. O'Brien, S.P. Hegarty, G. Huyet and A. Uskov.
Physics Department, National University of Ireland, University College, Cork, Ireland

April 2, 2004

1 Abstract

We present a model for quantum dot lasers that has been modified to incorporate effects arising from a non-zero value for the $\alpha-$factor and the effect of external optical feedback on this system. This work has been motivated by experimental results that indicate that quantum dot lasers exhibit an increased insensitivity to instabilities arising from external optical feedback. This insensitivity was measured on devices in which the $\alpha-$factor differed substantially from $\alpha = 0$, which was previously predicted for quantum dot lasers. Values of between 1 and 3 have been measured for the $\alpha-$factor at the gain peak for these devices. The exact physical origin of the $\alpha-$factor in quantum dot lasers is still unclear although some mechanisms including coulomb interaction in the dots and free carrier effects have been suggested as possible mechanisms. In the model presented here, we assume the refractive index of the device depends on the carrier densities in the well and/or dots. If we assume linear dependencies, the variation of the laser frequency with these densities reads $\delta\omega = \beta_1 N + \beta_2 \rho$. The coefficient β_1 describes the plasma effect from the carriers in the well, while β_2 describes the variations due to the population in the dots. If the dots are described by two-level atoms with symmetric line shape, then $\beta_2 = 0$ from the Kramers-Kronig relations. Coulomb interactions can lead to nonzero values for β_2. With $\beta_1 = 0$, $\delta\omega = \beta_2\rho$, with β_2 being the $\alpha-$factor in conventional rate equations. External optical feedback is modeled by the introduction of a time delay term on the field equation.

Using this model, the effect of external optical feedback in different operating regimes is explored, and a mechanism for the observed increased stability of these devices is explained.

Inorganic-organic hybrid material system for use in low cost optical waveguide component production

Shane O'Brien, R. Winfield, A. Connell, G. M. Crean

Photonics Group, NMRC, Lee Maltings, Cork

In the context of material development for optical waveguiding component applications, inorganic-organic hybrid materials offer new and exiting opportunities. A new 'inorganic-organic hybrid' waveguide material system is presented demonstrating tailored polymeric optical transmission properties combined with enhanced thermo-mechanical stability

This material is prepared by the sol-gel method and can be deposited by dip or spin-coating. Film thicknesses up to 25μm have been achieved in a single deposition, which is significant in minimizing the influence of inter-layer voids and/or inclusions on waveguide performance. It is demonstrated that the basic refractive index can be tailored over the range 1.48 to 1.515 with incorporation of diphenyl-dimethoxysilane in sol-gel formation. This enables precise adjustment of refractive index values to match those of glass or plastic fibres, thereby minimizing coupling losses that arise due to reflections. It is demonstrated that this novel materials system exhibits enhanced scratch resistance and thermo-mechanical properties, when compared to other inorganic-organic hybrid materials systems.

Mode Suppression in inhomogeneous Fabry-Perot Laser Cavities: a Transmission Matrix Approach

S. O'Brien and E. P. O'Reilly

NMRC, University College, Lee Maltings, Prospect Row, Cork, Ireland

Abstract:

The spectral purity of a ridge waveguide Fabry-Perot laser can be improved by patterning the effective refractive index seen by an optical mode propagating in the cavity. This can be achieved without additional regrowth steps by etching additional features into the laser ridge. Here we present a transmission matrix approach to first order in the effective index step from which we derive the threshold condition as a function of cavity mode index m. Our approach provides us with a simple recipe for the placement of these additional features in order to maximise the mode suppression. The optimal effective index pattern is shown to be related to that of a phase-shifted distributed feedback laser. Provided that cleaving can be performed to sufficient accuracy, our results indicate that devices with much improved spectral purity and at a substantially predetermined wavelength can be manufactured using this technique. We also discuss briefly how the technique should provide a straightforward path to mode suppression in longer wavelength Fabry-Perot lasers.

Near infrared photonic bandgaps and nonlinear effects in artificial magnetic metamaterials

S O'Brien[1], D McPeake[1], S A Ramakrishna[2] and J B Pendry[3]
[1]*NMRC, University College, Lee Maltings, Prospect Row, Cork, Ireland*
[2]*Department of Physics, Indian Institute of Technology, Kanpur, Kanpur - 208 016, India*
[3]*Condensed Matter Theory Group, The Blackett Laboratory, Imperial College, London SW7 2BZ, United Kingdom*

We examine the high frequency magnetic response of the split ring resonator (SSR) structure using numerical simulation and a simple physical model. The model reveals the importance of the inertial inductance due to the finite mass of the electrons in the metal forming the SSR. Limitations on the high frequency resonant response of the SSR due to the presence of this contribution to the inductance are discussed. We then describe and characterise an SSR photonic crystal metamaterial which is magnetically active in the near infrared region of the spectrum. The periodic array of modified metallodielectric SSR structures is numerically demonstrated to have a negative effective permeability at telecommunication wavelengths. Local electric fields in the structure can be many orders of magnitude larger than in free space thus allowing for enhanced nonlinear effects. We derive an expression for the change in the resonance frequency of the structure due to the Kerr nonlinear index change and calculate a characteristic magnetic field strength for the observation of bistable behaviour. Our results suggest that these structures have considerable potential for creating functional all optical elements.

A Kerr Mode-locked Semiconductor Laser: Design and Theory

Liam O' Faolain, Michael B. Flynn, Rab Wilson, Thomas F. Krauss.

email: jwwl@st-and.ac.uk
Ultrafast Photonics Collaboration, School of Physics and Astronomy, University of St Andrews, North Haugh, Fife, KY169SS, U.K.

In recent years, much time and effort has been spent in the search for a monolithic femtosecond diode laser. Such a device has many applications, particularly as a source for WDM in optical telecommunications. Currently available devices typically produce pulses of 1-2 ps duration, although pulses as short as 200 fs have been produced using an external cavity and external compression.

We propose a design for a monolithic semiconductor laser that is mode-locked by the Kerr effect. Such a laser would have a much improved ability to produce short pulsescompared with standard semiconductor lasers mode-locked using a saturable absorber.

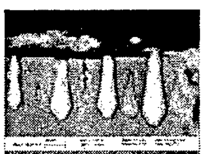

Figure 1: A scanning electron microscope image of a polymer infilled photonic crystal. The polymer is clearly shown to fill the etched features.

It has been shown that it is possible to fill photonic crystals with polymer, [1], see also fig.1. Therefore if a simple one dimensional photonic crystal is filled with a polymer which shows a strong Kerr coefficient [2], the resulting bandgap becomes dependent on the intensity of the incident light.

To acheive the maximum reflectivity change, we use a laser cavity defined by two asymmetric photonic crystal mirrors, one of which is polymer filled. For low light intensities, the overlap between the two mirror bandgaps is small, however a high intensity pulse may cause the bandgap of the polymer filled mirror to shift increasing the overall cavity reflectance. This effect behaves as a fast saturable absorber.

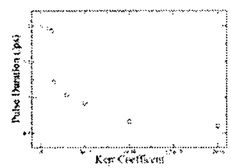

Figure 2: Pulse width with respect to Kerr coefficient.

We model such a device using a travelling wave rate equation model adapted and extended from that reported in [3]. Fig.2 shows the improvement in performance as a result of the incorporation of the polymer. Subpicosecond pulses may be produced at practical values of the Kerr coefficient.

Whereas as the proposed device is of a complex nature, requiring demanding fabrication, it is, to the best of our knowledge, the only such device, theoretical or experimental, which has the potential to overcome the considerable obstacles presently preventing the realisation of a true monolithic femtosecond diode laser.

References

[1] Ch. Schuller, F. Klopf, J. P. Reithmaier, M. Kamp and A. Forchel, *Appl. Phys. Lett.*, vol. 82, pp. 2767-2769, 2003.

[2] M. B. Marques, G. Assanto, G. I. Stegeman, G. R. Mohlmannn, E. W. P. Erdhuisen and W. H. G. Horsthuis, *Appl. Phys. Lett.*, vol. 58, pp. 2613-2615, 1991.

[3] M. Schell, M. Tsuchiya and T. Kamiya, *IEEE J. Quantum. Electron.*, vol. 32, pp. 1180-1190, 1996.

Diluted magnetic semiconductor (III-nitride) thin film growth using pulsed laser deposition

Donagh O'Mahony, Fintan McGee, James G. Lunney, M. Venkatasen and J.M.D. Coey

Physics Department, Trinity College, Dublin 2, Ireland.

Diluted magnetic semiconductor (DMS) growth has recently become an area of intense research with the aim of developing room temperature semiconductor-based spin-transport electronic (spintronic) for regulating the flow of spin-polarised current in magneto-optical devices [Ball, 2000]. Thin film growth of DMS materials involves doping a semiconductor like GaAs or GaN with small concentrations of a transition metal such as Mn or Fe. However, the equilibrium solubility of Mn in III-V semiconductors is less than 1 at. %, whereas higher concentrations (5 %) are predicted to be necessary to facilitate ferromagnetic behaviour in GaMnN [Dietl et al., 2000] and AlMnN [Litvinov and Dugaev, 2001] near room temperatures. Much interest has been generated by recent reports of high temperature ferromagnetism in various doped wide bandgap oxides grown by pulsed laser deposition (PLD), in particular, the observation of a giant Co moment in Co-doped tin oxide [Ogale et al., 2003]. Although, similar high temperature ferromagnetic behaviour has yet to be reported in PLD-grown magnetically doped nitrides, it seems that PLD is a promising technique for the growth these materials.
In this paper, we discuss the possibility of using PLD to achieve the 5% Mn concentration required for room-temperature ferromagnetism in Mn doped group III nitrides. In-situ optical reflectometry was used to monitor the growth rate and absorption characteristics of the Mn-doped films, while the structural phases were identified using X-ray diffraction analysis. The origin of room-temperature ferromagnetic behaviour observed in some of the films is also discussed.

Ball, P. (2000), *Nature*, **404**, 918 - 920.
Dietl, T., H. Ohno, F. Matsukura, J. Cibert and D. Ferrand (2000), *Science*, **287** (5455), 1019-1022.
Litvinov, V. I. and N. K. Dugaev (2001), *Phys. Rev. Lett.*, **86** (24), 5593-5596.

Ogale, S. B., R. J. Choudhary, J. P. Buban, S. E. Lofland, S. R. Shinde, S. N. Kale, V. N. Kulkarni, J. Higgins, C. Lanci, J. R. Simpson, N. D. Browning, S. Das Sarma, H. D. Drew, R. L. Greene and T. Venkatesan (2003), *Phys. Rev. Lett.*, **91** (7), 077205-077201.

Micro-optical Elements

Feidhlim T. O'Neill, Michael R. Gleeson, John V. Kelly, John T. Sheridan**

Department of Electrical and Electrical Engineering,

Faculty of Engineering and Architecture,

University College Dublin, National University of Ireland,

Belfield, D- 4,

Ireland.

**Corresponding author: john.sheridan@ucd.ie

Abstract

The development of many high-tech optical products require the use of micro-optical elements. The ability to produce such elements is therefore an enabling technology. At present there are a wide range of different fabrication methods each with their own advantages and disadvantages. In this paper a number of fabrication methods will be examined. The photoresist reflow method will be discussed in some detail, in particular the use of this method to produce aspheric lens arrays. The ability to produce aspheric lenses opens up a range of applications that include beam shaping, power transfer and fiber coupling.

Currently an experimental based iterative process is required to design and fabricate lens arrays using the photoresist reflow technique. This is due to the lack of a sufficiently accurate model. One model that has been proposed is the Curvature Correction Model, this model is based on first principles and has been shown in the literature to provide qualitative fits to the experimental lens profile data. In this paper we describe the use of a novel approach to reduce the search range for the Curvature Correction Coefficients thus greatly reducing the time required to obtain accurate numerical fits. We note that although this is a major improvement for the one dimensional case, it is most important in simplifying three dimensional case where the complexity of the problem of finding co-efficients is greatly increased.

In this paper we also report attempts to produce surface relief micro-optical elements by patterned exposure of a photopolymer recording material. This method may allow the fabrication of hybrid elements that combine the diffractive elements produced in the volume of the holographic material with the refractive elements possible by exploiting the surface relief pattern. Attempts to produce a fabrication system that allows the variation of the lens profile of a UV curable lens using an electric field will also be discussed.

High Performance Virtual Photonics

Gian-Luca Oppo
Department of Physics and Applied Physics,
University of Strathclyde

The development of new photonic devices is at the heart of the future expansion of communication systems. High performance and parallel computations are becoming crucial elements in virtual photonics where new devices are invented and tested for performance ahead of expensive prototypes. I will briefly review some of the recent progresses in virtual photonics using symmetric multi processing (SMP) atStrathclyde. Examples comprise models of broad area VCSEL, VECSEL, frequency up and down converters and the inclusion of noise and thermal effects. These examples show how fundamental science easily merges with photonic applications and technology in high performance numerical modelling.

Single mode wavelength specified Fabry-Perot lasers, obtained via the introduction of modal perturbations.

John Patchell, Dewi Jones, Brian Kelly and James O'Gorman

Eblana Photonics, Trinity College Enterprise Centre, Dublin 2, Ireland.

The wavelength spectra of ridge waveguide Fabry Perot lasers can be modified by perturbing the effective refractive index of the guided mode along very small sections of the laser cavity. One way of locally perturbing the effective index of the lasing mode is by etching features into the ridge waveguide such that each feature has a small overlap with the transverse field profile of the unperturbed mode, consequently most of the light in the laser cavity is unaffected by these perturbations. A proportion of the propagating light is however reflected at the boundaries between the perturbed and unperturbed sections. Suitable positioning of these interfaces allows the mirror loss spectrum of a Fabry Perot laser to be manipulated. In order to achieve single longitudinal mode emission, the mirror loss of a specified mode must be reduced below that of the other cavity modes. Here we briefly review one procedure for calculating the mirror loss spectra of devices containing such features. We then go on to describe a method for synthesising one-dimensional slot patterns, this technique allows the lasers emission wavelength to be specified to a high degree of accuracy. Furthermore, we discuss the use of evolutionary algorithms to design single longitudinal mode devices, which operate over a wide temperature range.

Microscopic Simulation of Intersubband Emitting Devices

M.F. Pereira
NMRC, University College Cork
Prospect Row, Lee Maltings, Cork, Ireland

Andreas Wacker
Department of Physics, University of Lund,
Box 118, 22100 Lund, Sweden

Intersubband emitting devices, like the quantum cascade laser (qcl) are now important devices in the infrared spectral region, with interesting perspectives for applications in the Thz regime.
Recent detailed comparisons between theory and experiments have clearly demonstrated that many body effects are required to explain the intersubband optical absorption of quantum wells.
However, the gain spectra of qcl structures have been explained relatively well without those effects.
Our nonequilibrium Keldysh Green's functions microscopic approach explains the apparent contradiction. Our method treats both transport and optics fully quantum mechanically, and is based on the self-consistent solution of the quantum kinetic equations under operating steady-state conditions. Scattering events that lead to the final nonequilibrium distributions are considered in the theory through selfenergies in the Dyson equation.
The many-body effects depend essentially in the occupations of the subbands and on the detailed Coulomb matrix elements that describe the overlap of elelectronic wavefunctions.
The combination of large population differences and occupation factors with large Coulomb matrix elements lead to strong Coulomb corrections on the THz region (absorption). However, in the mid-infra-red (gain) region, the Coulomb overlap integrals are small or the dominating gain transition. That explains the apparent contradiction, which requires the actual nonequilibrium distribution and realistic wavefunctions and Coulomb matrix elements, in contrast to simplifying approximations that are relatively successful for quantum wells, which fail in the more complex qcl superlattice scenario.

In summary, our fully quantum mechanical microscopic modeling of transport and optics of intersubband emitters demonstrates how to control the overall strength of Coulomb corrections by modifying the wavefunction overlap and thus the Coulomb matrix elements by means of the external bias. Our nonequilibrium simulations explain why Coulomb effects can be very large in the THz region and negligible for mid-infrared operation of quantum cascade lasers, and provide a basis for predictive simulations of new devices.

Wavelength Monitoring and Characterisation of a Sampled Grating DBR laser diode using Multiple Gas Absorption Lines.

R. Phelan, M. Lynch, J. F. Donegan and V. Weldon.
Semiconductor Photonics Group, Physics Department,
Trinity College Dublin, Dublin 2, Ireland

Abstract

Tuneable lasers are important components for next generation wavelength division multiplexing fibre optic networks. The wide tuning range and ability for fast wavelength switching make SGDBR lasers especially attractive for multi-channel DWDM networks. To manage the channel wavelength of DWDM systems, wavelength-monitoring techniques such as the use of arrayed-waveguide grating [1], fiber grating [2], active-layer junction voltage detection [3], and etalon [4] have been reported. In addition to these techniques with their characteristic advantages and disadvantages, the use of multiple gas absorption lines for wavelength monitoring offers the highest degree of accuracy. The gas absorption lines have a typical FWHM of a few hundred MHz at low pressure, and their wavelength dependence on temperature is such that, active temperature control and stabilisation, which is necessary for other methods, is not required.

The characterisation and control of the SGDBR laser diode is rather complex. Tuning the laser to a particular wavelength with a specific output power requires the adjustment of four control currents. We have investigated the use of multiple gases to provide unique wavelength identifiers to characterise the device and provide monitoring of the lasing wavelength. We have shown that the tuning behaviour of the SGDBR can be characterised using a combination of reference gases without any other form of wavelength measurement.

[1] M. Teshima, M.Koga, and K. Sato, "Performance of multiwavelength simultaneous monitoring circuit employing arrayed-waveguide grating," J. Lightwave Technol., vol. 14, pp. 2277–2285, Oct. 1996.
[2] Y. Park, S. Lee, Chang, and C. Chae, "A novel wavelength stabilization scheme using a fiber grating for WDM transmission," IEEE Photon. Technol. Lett., vol. 10, pp. 1446–1448, Oct. 1998.
[3] S. Lee, Y. Hsu, and C. Pien, "High-resolution wavelength monitoring using differential/ratio detection of junction voltage across a diode laser," IEEE Photon. Technol. Lett., vol. 13, pp. 872–874, Aug. 2001.
[4] H. Nasu, "25-GHz-Spacing wavelength-monitor integrated DFB laser module for DWDM applications", IEEE Photon. Technol. Lett., vol. 15, pp. 293–295, Feb. 2003.

Pump-probe studies of non-linear polarization rotation in semiconductor optical amplifiers

S. Philippe[a], B. Kennedy[b], M. Martinez-Rosas[ac], A. L. Bradley[a], P. Landais[b].
a) Physics Department, Trinity College Dublin.
b) School of Electronic Engineering, Dublin City University.
c) UABC, Ensenada, Mexico.

Ultra fast switching and gating applications can be achieved by taking advantage of the various non-linear effects exhibited by semiconductor optical amplifiers (SOAs). All optical signal processing has been achieved with configurations based on different non-linearities, such as cross-gain/cross-phase modulation and four-wave mixing. We focus on the less studied non-linear polarisation rotation[1]. Applications, such as logic functions and wavelength conversion, based on this effect have been proposed[2].

The device under test is a commercially available component, it is a 1.5-mm long bulk InGaAsP active region surrounded by InP. This structure was grown by MOCVD and it is quoted as having low polarisation dependent gain. Both facets are anti-reflection (AR) coated, with a tilted output of 12° to reduce the Fabry-Perot resonances due to the residual reflectivity of the facets. The experimental set-up is in free space, allowing optimum control, preservation and analysis of the state of polarisation of the injected and collected signals. In previous measurements we have shown that both gain discrepancy between the transverse electric (TE) and transverse magnetic (TM) axes of the waveguide and birefringence due to different values of the refractive indices along these axes contribute to the nonlinear polarization rotation in this device [3].

A contra-propagation pump-probe experiment has been undertaken to investigate the impact of the pump power and pump polarization state on the polarization state of the probe signal. The input polarisation states of both pump and probe signals can be independently controlled. As can be seen in the figure below, the polarization state of the probe at the output is relatively independent of the polarization state of the pump. However, there is modification of both the ellipticity and orientation of the probe polarization as the injected pump power increases. In the example shown, for an input probe beam with a linear polarization state at 45^0, the ellipticity of output probe signal is strongly dependent on the pump power. At low pump power the probe polarization state is approximately circular and as the pump power increases the probe polarization state tends toward a linear polarization state. The orientation of the probe polarization state changes initially and then remains relatively constant. These results have been analysed in the context of optical switching applications and the optimum operating conditions will be discussed.

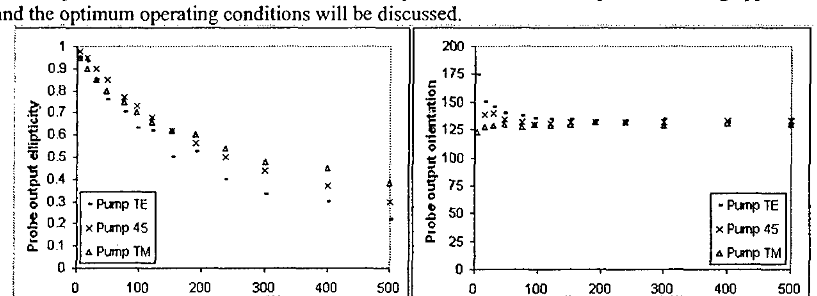

[1] Manning, R.J., Antonopoulos, A., Le Roux, R., and Kelly, A.E., "Experimental measurement of nonlinear polarization rotation in semiconductor optical amplifiers", Electronics Lett. 37, 4, pp. 229-231 (2001).
[2] Soto, H., Erasme, D., and Guekos, G.: 'Cross polarization modulation in semiconductor optical amplifiers,' IEEE Photon. Technol. Lett., 11, pp. 970–972 (1999).
[3] Kennedy, B.F., Philippe, S., Landais, P., Bradley, A.L., Soto, H., "Experimental investigation of polarisation rotation in semiconductor optical amplifiers", IEE Proceeding – Optoelectronics (accepted for publication) April (2004).

Vertical-cavity semiconductor devices for fluorescence spectroscopy

P.A. Porta and H.D. Summers

School of Physics and Astronomy,
Cardiff University, 5, The Parade
Cardiff, CF24 3YB, Wales, UK.

The integration of a partially coherent light source and a sensitive detector within the same semiconductor wafer is a further step toward the realization of miniaturised optical biochips for DNA analysis and cytometry.
We present a novel vertical-cavity semiconductor device called α-RCLED capable of generating optical radiation to pump fluorescent labelling dyes in forward bias mode and detecting their fluorescence emission when operated in reverse bias mode.

The structure and the criteria chosen to design these devices, their emission and detection properties are presented and discussed in detail. We demonstrate also the possibility to grow the top DBR mirror to behave as an optical low pass filter: radiation with wavelength shorter than 660 nm will be absorbed and only the fluorescence emission to be measured will pass through and reach the detection layer. This particular top DBR mirror has to be removed by chemical etching when the devices are operated as emitters.

These devices can find useful application in lab-on-a-chip technology to provide non-invasive, non contact biochemical analysis on the micron scale such as identification and quantification of DNA molecules. They have also great potential to produce integrated high- sensitive miniatured sensors for areas such as genomics and proteomics.

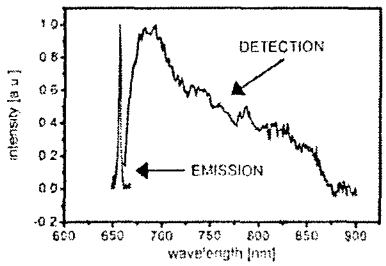

Optical emission spectrum and long-wavelength responsivity of an α-RCLED.

3D Photonic Crystal Structures by Holographic Lithography

O. M. Roche, J. Scrimgeour, E. R. Dedman, D. N. Sharp, A. J. Turberfield
University of Oxford, Department of Physics, Parks Road, Oxford OX1 3PU, UK

C. F. Blanford, R. G. Denning
University of Oxford, Department of Chemistry, South Parks Road, Oxford OX1 3QR, UK

A photonic crystal is a dielectric microstructure with a periodic variation in refractive index. A photonic bandgap is a range of frequencies where no electromagnetic modes can propagate in the crystal. Structural defects in the photonic crystal can result in spatially localized electromagnetic modes at frequencies within the bandgap. The aim of our research is to fabricate 3D photonic crystals for the visible and near IR-spectra, to characterise the structures, and to introduce defects in a controlled manner.

Holographic lithography is a technology for the fabrication of 3D photonic crystals with the sub-micron periodicity required for optical and near IR-wavelength operation. It is a technique that allows the lattice and basis to be designed [1]. In holographic lithography the interference pattern generated at the intersection of four coherent laser beams is used to expose a thin film of photoresist. Highly exposed photoresist is rendered insoluble while unexposed areas are dissolved away leaving a polymeric photonic crystal with interconnected air-voids (see figure 1 below left).

The ultimate goal of our research is to produce integrated optical devices with our photonic crystals. In order to realise this we must first create passive structures, such as waveguides, by introducing defects in the defined periodic lattice. By carefully engineering the defects we will be able to produce waveguides and microcavities within the crystal. We use two-photon absorption at the high intensity focus of a laser to write defects point-by-point into the crystal. To align the defect complex with a lattice already generated by holographic lithography, confocal fluorescent microscopy is used (see figure 2 below right).

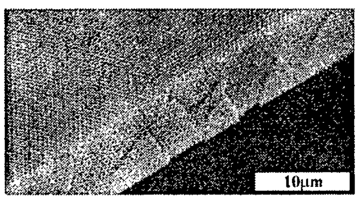

Figure 1: SEM image of a structure generated with an fcc interference pattern.

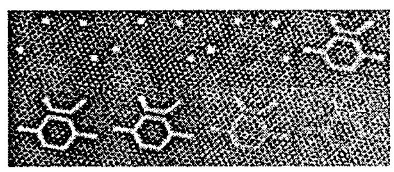

Figure 2: Confocal images of photoacid density revealing a latent image of the test structure, written within and aligned to the 3D photonic crystal.

[1] M. Campbell, D. N. Sharp, M. T. Harrison, R. G. Denning and A. J. Turberfield. Fabrication of photonic crystals for the visible spectrum by holographic lithography. Nature **404**, 53 (2000)

Dispersion measurements across broad wavelength ranges by low-coherence interferometry

J. H. Rothwell, D. F. Murphy, M. AlHourani and D. A. Flavin,
Optics Research Group, Waterford Institute of Technology, Waterford, Ireland

The measurement of dispersion is of vital interest in a number of fields including ultrafast laser systems, characterisation of propagation properties of new photonic materials, Optical Coherence Tomography, and chirped Bragg gratings.

Straightforward cross-correlation interferometry, using either low-coherence sources filtered at a sequence of wavelengths or tunable sources, has long been used to measure low-order dispersion—in this case, the processing of the discreet measurements for the optical path delay for a range of specific wavelengths yield the group delay and dispersion characterisation across the range of wavelengths. Recently more and sophisticated efficient schemes, based on measurement of the phase of the Fourier transform of the low-coherence interferogram have been shown to yield dispersion information for the full spectral range of the low-coherence source [1,2]. Similar approaches have been applied in fibre optic sensing [3].

In this paper we concentrate on the recent developments, in the application of dispersive Fourier transform spectrometry (DFTS) to the measurement of group velocity and group velocity dispersion, at the Optics Research Group of WIT. We have developed interferometric structures based on both single bulk-optic Michelson interferometers and on tandem interferometers. The latter are combinations of a local reference bulk-optic Michelson with a remote fibre optic Michelson, and facilitate remote measurements.

In all cases the interferometers are illuminated by low-coherence sources. Both superluminescent diodes and thermal sources have been used—the latter allow measurements over a range of a few hundred nm, despite the limitations imposed by the coupling of such spatially-multimoded sources to single-mode fibre.

The critical information on the wavelength dependence of the propagation constant of the lightwave material under test is determined from the phases of the Fourier transform of the low-coherence interferograms which are captured. Curve fitting has been shown to produce accurate measurement of the derivatives of this propagation constant to fourth-order, corresponding to group velocity dispersion measurements to third-order. Results will be presented for measurements on the borosilicate and SF ranges of lightwave glasses.

We have refined the approach so that measurements can be undertaken based solely on the Fresnel reflections at the facets of the lightwave sample under test [4]. In a parallel development, measurement of the dispersion coefficients, without *a priori* measurement of the thickness of the sample, has been made possible.

Accurate measurements of the higher orders of dispersion—given that, by their nature, they are derivatives of the initial phase measurement—require a number of refinements to maximise the accuracy of the initial measurement. We have developed various approaches to overcome accuracy degradation,—in particular we deal with the Hilbert transform approach to correcting for nonlinearity in the scanning of the optical delay. Our approaches also exhibit a marked immunity to the residual phase imbalances within the interferometers.

References

[1] S. Diddams and J-C. Diels, "Dispersion measurements with white-light interferometry," *J. Opt. Soc. Am. B*, 13, 6, p. 1120, 1996

[2] D.A. Flavin, R McBride and J. D. C. Jones, "Dispersion of birefringence and differential group delay in polarization-maintaining fiber", *Optics Letters*, 27, 12, p. 1010, 2002.

[3] D. F. Murphy and D. A. Flavin, "Dispersion-insensitive measurement of thickness and group refractive index by low-coherence interferometry," *Applied Optics*. 39, 25, p. 4607, 2000.

[4] J. H. Rothwell and D. A. Flavin, "Dispersion measurement by white-light interferometry based on Fresnel reflections", Presented at the European Conference on Lasers and Electo-Optics (CLEO-Europe), Munich, June 2003

Measured limitations to Transfer Matrix modelling

Brendan Roycroft, Brian Corbett
NMRC, Lee Maltings, Cork, Ireland. e-mail: Brendan.Roycroft@nmrc.ie

Abstract:

Transfer matrix modelling is a very well understood and widely used technique, and can be used to calculate reflection, transmission and absorption spectra of multilayer structures. However, it assumes spatially coherent plane waves with infinite coherence lengths, and these assumptions have limited validity for incoherent sources such as LEDs. We measure reflectivity and emission spectra for various 500 nm and 650 nm emission resonant cavity LEDs, and determine the conditions when transfer matrix modelling is and is not valid. In particular, we find the limited temporal coherence of LEDs produces results in disagreement with the transfer matrix model for longer cavities even at relatively small angles. The point at which disagreement occurs allows us to make an estimate of the coherence length. The consequent effect on emission has implications for estimates of extraction efficiency and internal efficiency, due to the integration over all angles.

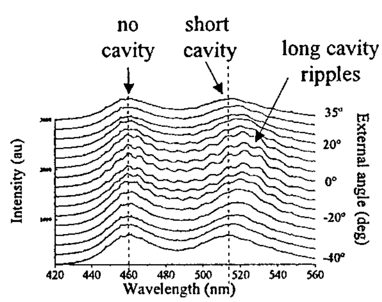

Figure 1 Emission spectra from a compound microcavity at various collection angles, showing three different components, a) no cavity, b) short cavity showing coherence to over 40° external angle, c) long cavity which loses coherence at 20° external angle

NEW AGE FIBER CRYSTALS

Philip Russell
Department of Physics, University of Bath

Photonic crystal fibres (PCFs) have been the focus of increasing scientific and technological interest since the first working example was reported in 1996. Although superficially similar to a conventional optical fibre, PCF has a unique microstructure, consisting of an array of microscopic holes (i.e., channels) running along its entire length. These holes act as optical barriers or scatterers, which suitably arranged can 'corral' light within a central core (either hollow or made of solid glass). The holes can range in diameter from ~25 nm to 50_m. Although most PCF is formed in pure silica glass, it has also recently been made using polymers and non-silica glasses, where it is difficult to find compatible core and cladding materials suitable for conventional total internal reflection guidance. PCF supports two guidance mechanisms: total internal reflection, in which case the core must have a higher average refractive index than the holey cladding; and a two-dimensional photonic bandgap, when the index of the core is uncritical - it can be hollow or filled with material. Light can be controlled and transformed in these fibres with unprecedented freedom, allowing for example the guiding of light in a hollow core (with losses as low as 1.7 dB/km at 1550 nm), the creation of highly nonlinear solid cores with anomalous dispersion in the visible and the design of fibres that support only one transverse spatial mode at all wavelengths. The PCF concept has ushered in a new and more versatile era of fibre optics, with a multitude of different applications spanning many areas of science. See reviews in Science 299 (358-362) 2003 and Nature 424 (847-851) 2003.

Optical signal processing in switching and transmission systems

Kristian E. Stubkjaer,
Technical Univ. of Denmark,
DK-2800 Lyngby, Denmark,
stubkjaer@adm.dtu.dk

Abstract:

The progress in component technologies have enabled more and more advanced optical systems. Today, work in the laboratories has reached the level where simple optical signal processing is important for the further advancement of switching and transmission systems. The development of systems with higher bit rates beyond the capabilities of electronics requires fast optical processes. Likewise high capacity optical network nodes require optical signal processing in both wavelength and time dimension. Especially, packet type all-optical networks need optical signal processing at the bit level putting new demands on speed capabilities and power consumption of the all-optical building blocks that we want to employ.

The presentation will review some of the interesting developments we have seen for all-optical time demultiplexing, wavelength conversion, 2R and 3R regeneration, label swapping, clock recovery, packet routing, and all-optical logic functions.

Clearly, the further advancement of all-optical signal processing depends on the development of new advanced materials and components with wavelength scale features for the efficient handling of the photons. Focus is especially on the development of Photonic Bandgap structures and quantum dot materials that hold promise for fast and compact devices. The presentation will also focus on these aspects.

Self-consistent solution of Schrödinger and Poisson equations applied to investigations of III-V heterostructures and lasers

Michał Szymański, Mariusz Zbroszczyk

Institute of Electron Technology, Al. Lotników 32/46, 02-668 Warsaw, Poland

Recent, dynamic development of sophisticated epitaxial techniques enables growth of low-dimensional, multi-layer, modulation-doped semiconductor structures of excellent quality. These structures are used for producing different opto- and microelectronic devices like lasers, detectors or transistors. However understanding their optical and transport properties requires advanced modelling techniques taking into account quantum effects. In this work we present software for finding the self-consistent solution of the one-dimensional Schrödinger-Poisson equations. Our numerical tools are based on finite-difference method with non-uniform mesh. The iterative procedure consists of the following steps. The Schrödinger equation is solved for electron, heavy and light holes independently. Using the Fermi-Dirac statistic, the condition of charge neutrality of the crystal and bisection method, we calculate the Fermi level energy. Then the free carrier density is found. By solving the Poisson equation, we find the electric potential, which allows us to modify the conduction and valence bands previously assumed and start the next iteration. Sufficiently small changes of electric potential stop the calculations.

We apply our software for investigating different MBE-grown III-V devices. Example results for HEMT structure are shown in Fig. 1. For InGaAs/GaAs or InGaAlAs/GaAs heterostructures we calculate electron and hole energy levels and compare the results with photoluminescence measurements held in our laboratory. For InGaAs/GaAs or InGaAlAs/GaAs lasers we calculate gain in the active region and compare the results with measurements found in the literature.

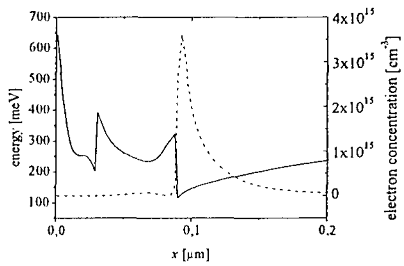

Fig. 1 Conduction band edge and electron density across MBE-grown AlGaAs/GaAs HEMT.

Gain Recovery Acceleration in Semiconductor Optical Ampli?ers Employing a Holding Beam

G. Talli [a] and M. J. Adams [b]

[a] Department of Physics, University College Cork, Ireland.
[b] Department of Electronic Systems Engineering, University of Essex, United Kingdom.
E-mail: giuseppe.talli@ucc.ie

For many applications of semiconductor optical ampli?ers (SOAs) in high speed networks a fast gain recovery is required. A possible way to reduce the recovery time of SOAs is the use of a holding beam in a scheme usually called a three-wavelength device (TWD) [1]. The use of a holding beam has been proposed for applications in all-optical switching [1] and wavelength conversion [2] to improve the performance of SOAs. Recently a variation of the TWD scheme has been proposed where the holding beam wavelength is chosen at the SOA transparency point [3].

The gain recovery of SOAs employing a holding beam has been studied both experimentally and theoretically [1], [3]–[9]. Numerical results presented in the literature show that the gain recovery when the holding beam is propagating in the same direction as the saturating pulse can be signi?cantly different from the case when the the holding beam is propagating in the opposite direction [9], [10]. However, to the best of our knowledge, a direct comparison between the gain recovery in co- and counter-propagating con?guration has never been analysed experimentally.

The gain recovery of an SOA was characterized with a holding beam injected in co- and counter-propagating con?gurations. Two different sets of gain recovery measurements were performed using two different lasers to generate the holding beam, a tunable laser and a commercial 1490 *nm* pump laser. In the ?rst set-up the use of the tunable laser allowed the measurement of the gain recovery for various holding beam wavelengths in the gain region of the device. On the other hand, using the 1490 *nm* laser we could analyse the effect of injecting a strong holding beam near the transparency point of the SOA.

As expected from the numerical studies presented in the literature [9], [10], an overshoot is present in the gain recovery measured for the counter-propagating con?guration, but it is absent in the co-propagating one thus causing a slower gain recovery. For all the conditions analysed in the measurements the recovery time of the counter-propagating con?guration is shorter than the co-propagating one due to the presence of the overshoot in the gain recovery.

The difference measured in the recovery time between the two con?gurations is more pronounced with the holding beam wavelength near the transparency. The recovery time for the counter-propagating con?guration decreases when the injected power is increased, as previously reported [7]. On the contrary, when the injected power increases the recovery time for the co-propagating con?guration increases [9]. This behaviour is analysed experimentally and numerically. The increase in the recovery time observed for the co-propagating con?guration is explained and it is found to be related to the suppression of the gain overshoot.

REFERENCES

[1] R. J. Manning and D. A. O. Davies, "Three-wavelength device for all-optical signal processing," *Optics Letters*, vol. 19, pp. 889–891, June 1994.
[2] M. Asghari, I. H. White, and R. V. Penty, "Wavelength conversion using semiconductor optical amplifi ers," *Journal of Lightwave Technology*, vol. 15, pp. 1181–1190, July 1997.
[3] M. A. Dupertuis, J. L. Pleumeekers, T. P. Hessler, P. E. Selbmann, B. Deveaud, B. Dagens, and J. Y. Emery, "Extremely fast high-gain and low-current SOA by optical speed-up at transparency," *IEEE Photonics Technology Letters*, vol. 12, pp. 1453–1455, November 2000.
[4] R. J. Manning, D. A. O. Davies, and J. K. Lucek, "Recovery rates in semiconductor laser amplifi ers: optical and electrical bias dependencies," *Electronics Letters*, vol. 30, pp. 1233–1234, July 1994.
[5] R. Gutierrez-Castrejon, L. Schares, L. Occhi, and G. Guekos, "Modeling and measurement of longitudinal gain dynamics in saturated semiconductor optical amplifi ers of different length," *IEEE Journal of Quantum Electronics*, vol. 36, pp. 1476–1484, December 2000.
[6] M. T. Hill, E. Tangdiongga, H. de Waardt, G. D. Khoe, and H. J. S. Dorren, "Carrier recovery time in semiconductor optical amplifi ers that employ holding beams," *Optics Letters*, vol. 27, pp. 1625–1627, September 2002.
[7] J. L. Pleumeekers, M. Kauer, K. Dreyer, C. Burrus, A. G. Dentai, S. Shunk, J. Leuthold, and C. H. Joyner, "Acceleration of gain recovery in semiconductor optical amplifi ers by optical injection near transparency wavelength," *IEEE Photonics Technology Letters*, vol. 14, pp. 12–14, January 2002.
[8] T. P. Hessler, M.-A. Dupertuis, B. Deveaud, J.-Y. Emery, and B. Dagens, "Experimental demonstration of optical speed-up at transparency in semiconductor optical amplifi ers," in *2002 IEEE/LEOS Summer Topical*, pp. TuK2-23 –TuK2-24, July 2002.
[9] G. Talli and M. J. Adams, "Gain dynamics of semiconductor optical amplifi ers and three-wavelength devices," *IEEE Journal of Quantum Electronics*, vol. 39, pp. 1305–1313, October 2003.
[10] F. Ginovart and J. C. Simon, "Gain dynamics studies of a semiconductor optical amplifi er," *Journal Of Optics A-Pure And Applied Optics*, vol. 4, pp. 283–287, May 2002.

Mode Competition in Quantum Dot Semiconductor Lasers

Yann Tanguy, John Houlihan and G.Huyet
Physics department, National University of Ireland, University College Cork, Ireland.

The mode competitions in quantum dots ridge waveguide lasers at 1.3 um is analysed experimentaly, in particular when simultaneous lasing in the ground and excited states is observed. The two states have well defined and different wavelengths. In order to characterise the possible coupling mechanisms some correlation measurements are performed, within the 50 MHz bandwidth where most of the noise from the mode competitions is present. This involves correlating the timetraces of spectrally resolved longitudinal modes, or groups of such longitudinal modes, or even the total light from each lasing state, ground or excited. The power spectra of the timetraces are not linear and peak at different frequencies, which may depend on the observed state or whether the input is a single mode or the total light from the state. We describe and try to explain the different interactions between such non-linear oscillators.

Thulium doped ZBLAN fibre ring-cavity amplifier

S. Tessarin[a], M. Lynch[a], A. Bavard[a], J.F. Donegan[a], G. Mazé[b]

[a] Semiconductor Photonics Group, Physics Department, Trinity College, Dublin 2, Ireland
[b] Le Verre Fluoré, Campus Ker Lann, F-35170 France.

ABSTRACT

New optical fibre amplifiers are key components in extending the operation of fibre networks to new wavelengths in response to the fast growth of data traffic.

Thulium doped fibres in low phonon energy hosts are recognized as an interesting candidate for covering the wavelength region between 1.45 µm to 1.50 µm. Low phonon energy glasses, such as heavy metal fluoride glasses, are crucial for the development of high gain rare-earth thulium fibre amplifiers, since in silica hosts Thulium is affected by strong non-radiative relaxation which reduces the obtainable performance. The realization of an efficient Thulium fluoride fibre amplifier has been prevented by the longer lifetime of the terminating level compared to the upper level of the transition.

Several solutions have been proposed in the past such as an upconversion pumping scheme [1], where fast depopulation of the terminating level has been achieved pumping an excited state absorption transition. Another solution is codoping with Holmium where the terminating level is depopulated by resonant transfer to the Holmium neighbor ions [2].

CW cascade operation at 1.47 µm and 1.88 µm transition in Tm^{3+} doped fluoride fibre laser has been extensively studied in the recent years [3,4] and used for achieving simultaneous oscillation at the two wavelengths; this mechanism can be extended to obtain signal amplification in the region 1.45 µm-1.50 µm. We will present a new amplifier based on the previously mentioned cascade operation. The amplifier has an all-fibre ring cavity configuration; the feedback for achieving oscillation at 1.88 µm is obtained by two Y-couplers with a transmission windows centered at 1.9 µm. A model based on the rate equations for the relevant levels has been solved using standard numerical techniques. The measured amplifier performance has been compared with model results and used to predict the characteristics of an optimised amplifier. The performance of the optimised version has been simulated for various pumping schemes.

[1] T. Komukai, T. Yamamoto, T. Sugawa, Y. Miyajima, *1.47 µm band Tm^{3+} doped fluoride fibre amplifier using a 1.064 µm upconversion pumping scheme,* Electronics Letters Vol.29, N. 1, 1993, pp. 110-112

[2] M. Percival, D. Szebesta, S. T. Davey , N. A. Swain, T. A. King, *Thulium sensitized holmium-doped cw fluoride fibre laser of high efficiency,* Electronics Letters Vol.28, N.24, 1992, pp.2231-2232

[3] M. Percival, D. Szebesta, S. T. Davey, *Highly efficient cw cascade operation of 1.47 µm and 1.82 µm transition in Tm^{3+} doped fluoride fibre laser,* Electronics Letters Vol.28, N.22, 1992, pp. 2063-2065

[4] R. Allen, L. Esterowitz, I Aggarwal, *An efficient 1.46 µm Tm^{3+} fiber laser via a Cascade Process,* IEEE Journal of Quantum Electronics, Vol.29, N. 2, 1993, pp. 303-306

Novel erbium doped waveguide amplifiers

R.R.Thomson, H.T.Bookey, S.Campbell, N.M.Bell, A.K.Kar, D.T.Reid. †
S.Shen, A.Jha. ‡
M.Martino. ◊
Navin Suyal. ♦

Physics, School of engineering and physical sciences, Heriot Watt University, Edinburgh, EH14 4AS. †
Institute for materials research, University of Leeds, Leeds, LS2 9JT. ‡
Dipartimento di fisica, Universita di Lecce, Lecce, Italy. ◊
Exxelis Ltd, Rosebank Park Livingston, EH54 7EJ. ♦

As the demand for high bandwidth applications such as video-on-demand and broadcast TV increases, the bit rate of Local Area Networks (LANs) and Metropolitan Area Networks (MANs) must also increase. This increase in the LAN and MAN bit rates is driving research into low cost network components such as splitters, multiplexers and optical amplifiers. In order to meet space requirements, it is essential that these components can be integrated into one Photonic Integrated Circuit (PIC). The state-of-the-art in optical amplifiers (Raman, EDFA) are not suitable for optical integration due to their physical nature and power requirements. Over recent years the Erbium Doped Waveguide Amplifier (EDWA) has attracted increasing research interest. It is clear however that there is much scope for improvement in both device manufacture and device operation.

Various technologies including Plasma Enhanced Chemical Vapour Deposition (PECVD), ion exchange and RF sputtering have being employed to create the erbium doped waveguides. At present we are investigating two routes to deposit the erbium doped glass layer that forms the core of the waveguide structure. The first method we are investigating is Pulsed Laser Deposition (PLD), the second is sol-gel.

PLD involves the ablation of a target by a pulsed laser. The ablation produces a plume of the target material. A thin film of the target material is then formed by placing a substrate in the path of the plume. Using PLD we were able to produce thin films of novel silicate and tellurite erbium doped glasses. The targets used in this deposition process exhibit attractive properties such as high fluorescence lifetime (>10 ms), high rare earth dopant levels (1.0 mole%), large gain bandwidth (>35 nm FWHM) and the ability to produce near 100% population inversion as demonstrated in fibres drawn from the same glasses. PLD should maintain the stoicheometry of the glass between bulk and film and hence preserve these glass properties. Using femtosecond machining, ridge waveguides were created in the erbium doped glass film by ablating material either side of the desired waveguide core region. These waveguides produced a broad fluorescence spectrum similar to that of the bulk glass when pumped at 980nm. The waveguides also exhibited a wavelength dependent insertion loss that showed a clear erbium absorption profile in the 1524-1570 nm range.

Sol-gel is a room temperature chemical process whereby thin glass films can be produced by mixing the desired precursors in a solvent to produce a "sol". By spin coating the sol onto a substrate and subsequent heating, high quality glass films can be formed. Using a sol-gel route we were able to deposit erbium doped silica glass films 5-6 μm thick in a single deposition without cracking. After the film was etched and clad, the waveguides exhibited saturated relative gains of up to 1 dBcm $^{-1}$ and passive losses as low as 0.3 dBcm $^{-1}$. Time resolved studies of the fluorescence decay of the erbium $^{4}I_{13/2}$ transition revealed pump power dependent fluorescence lifetimes due to ion-ion interactions. High pump power regime fluorescence lifetimes of up to 4.3 ms were observed.

Optically Pumped Semiconductor Disk Lasers

Peter Unger
Abteilung Optoelektronik, Universität Ulm

I will present the basic physical principles and some practical device implementations of optically pumped semiconductor disk lasers. This novel laser unifies the benefits of solid-state thin-disk lasers and Vertical-Cavity Surface-Emitting Lasers (VCSELs). The undoped epitaxial structure consists of a Bragg mirror and a resonant gain region which is optically pumped by a broad-area laser diode. The second mirror is an external concave dielectric mirror resulting in a stable concentric resonator configuration enforcing single-mode operation. The whole concept is scalable allowing high optical output powers. Due to the external mirror, additional elements can be positioned inside the laser cavity like nonlinear crystals to achieve frequency doubling. Devices are presented which emit in the blue and the orange-yellow wavelength range.

Marion Velly[1,2] and Patrice Féron[1]

1 Laboratoire d'Optronique, ENSSAT, Lannion, France.

2 Dept. of Applied Physics and Instrumentation, Cork Institute of Technology, Ireland.

Abstract

The purpose of this project is the characterisation of Erbium doped fluoride spherical glass microlasers. A microsphere with a diameter of around one hundred microns provides both the resonant cavity and the amplifying medium for lasing behaviour. Light propagates along the equator of the microsphere by repeated total internal reflections and it is confined inside a ring whose transverse dimension is of the order of the wavelength. This particular propagation mode is called a whispering gallery mode after the acoustical domain in which it was first studied. Considering this medium as being quasi-lossless, quality (Q)- factors of the order of 10^9 have been experimentally verified. By considering the small mode volume achievable, a very high energy density can be obtained. The aim of this project was to characterise the 3 micron Erbium transition, which may be of interest for medical applications. We also studied the 1.5 micron transition, which is the wavelength suited for telecommunication systems. To provide energy to the microsphere in order to permit the lasing effect, we chose to use the prism coupling method because it is a very selective coupling technique allowing a very "clean" excitation of gallery modes. This makes it possible to excite the most confined modes with a pump laser threshold of 600 μW. Whispering gallery modes properties are ideally suited for studying the fundamental physics of cavity electrodynamics, non-linear effects in optics with very low thresholds and they are also suited for applications in telecommunication systems and medical devices. This study contributes to the miniaturisation of optoelectronic components.

High-Brightness Semiconductor Lasers

James N. Walpole

Retired from Lincoln Laboratory, Massachusetts Institute of Technology, Lexington, MA 02420-9108

ABSTRACT

Several types of semiconductor lasers have been demonstrated that provide CW power levels in the 1-W class with single-spatial-mode, diffraction-limited, or nearly diffraction-limited, beams. These include phased-locked arrays of anti-guided diode lasers, tapered lasers and amplifiers, grating-confined distributed-feedback lasers (or α-DFB lasers), broadened waveguide lasers, and large-diameter vertical-cavity lasers operating in an external cavity. The advantages and disadvantages of these devices relative to one another will be briefly reviewed. Also discussed is the use of semiconductor arrays to pump solid-state and fiber lasers, producing high brightness lasers with good overall conversion efficiency. The remainder of the paper will emphasize the recently introduced slab-coupled-optical-waveguide laser, a high-power, high-brightness semiconductor laser source that emits light in a single-spatial, lowest-order mode that is nearly circular in cross section and has a modal diameter of several micrometers. Such lasers have been demonstrated in InGaAs-InP materials, emitting near 1.3-_m wavelength, and in AlGaAs-InGaAs-GaAs materials, emitting at several wavelengths in the range between 915 and 980 nm. CW output power over 1 W has been obtained in diffraction-limited beams with over 80% coupling efficiency to single-mode optical fibers. This coupling is achieved by simple butt coupling of the fiber directly to the laser without the use of optical lenses.

Temperature maps of GaAs/AlGaAs quantum cascade-laser facets measured by micro-thermoreflectance

Dorota Wawer, Anna Wójcik-Jedlińska, Tomasz Ochalski, Tomasz Piwoński, Maciej Bugajski
Institute of Electron Technology, Al. Lotników 32/46, 02-668 Warsaw, Poland

Hideaki Page
Thales Research and Technology, Domaine de Corbeville, 91 404 Orsay Cedex, France

Quantum cascade (QC) lasers are characterized by large number of interfaces, high applied voltages and the high losses, which results in high thermal resistance and large electrical powers dissipated in this devices. This appears to be limiting factor for achieving cw lasing at room temperatures. Recently it has been shown that buried waveguide QC lasers can operate at 300K which confirms potential of QC lasers as practical devices[1]. For the industrial use of QC lasers, however, the better understanding of thermal management in this devices is needed. One of the major challenges is to optimize their design and identify all thermally induced effects which may influence their performance. In particular, direct methods of probing temperature distribution in crucial elements of QC laser would be very helpful.

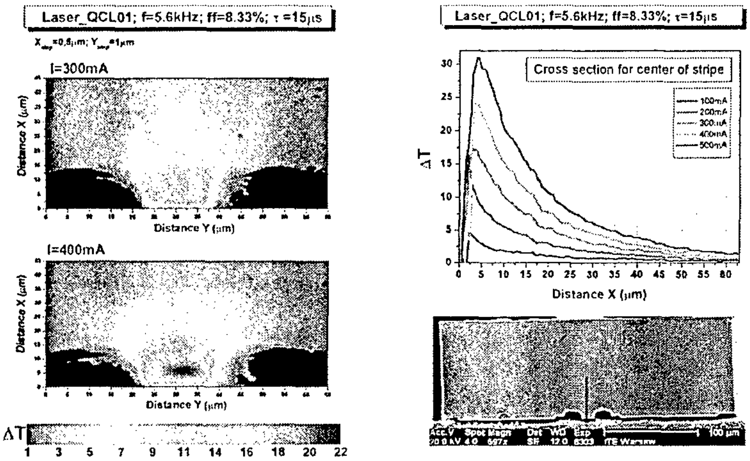

Fig. 1. The maps of temperature distribution at the front facet of QC laser (left) and the linear scans of the temperature taken along the symmetry axis of the structure (right)

In this work, we use spatially resolved thermoreflectance to measure temperature distribution over the facet of pulsed operated QC lasers. The measurements are done at 300K for the wide range of supply currents. The thermoreflectance is a modulation technique

relaying on the periodic temperature change of the laser due to the current self-heating. The periodic temperature change of the laser induces variation of semiconductor refractive index and consequently modulates probe beam reflectivity. The technique has a spatial resolution of about ~ 1μm and temperature differences of a degree can be measured[2]. The method allows the investigation of thermal resistance of devices and evaluation of different mounting techniques. It also gives an insight into distribution and relative importance of heat sources within the laser.

An example of the maps of temperature distribution at the front facet of quantum cascade laser is shown in Fig.1. The maps were taken at different supply currents (100 - 500 mA) at room temperature. The devices were mounted epi-layer down on copper-tungsten (CuW) heat sinks and soldered onto copper mounts. We also show linear scans of the temperature taken along the symmetry axis of the system. The hottest area overlaps with the active region and the maximum temperature attained is proportional to electrical power.

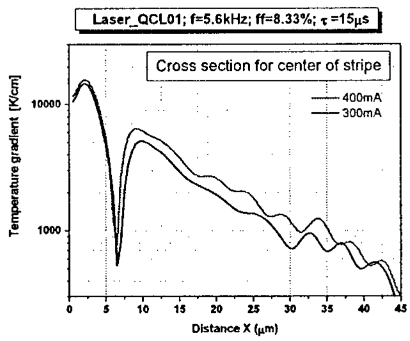

Fig. 2. Temperature gradient in the laser along the symmetry axis of the structure

The heat dissipation in the active region is poor and large temperature gradients are observed in the device comparing to standard quantum well lasers (see Fig.2). This produces thermally induced stress field in the ridge region[3].

1. M. Beck, D.Hofstetter, T.Aellen, J.Faist, U.Oesterle, M.Ilegems, E.Gini, H.Melchior, Science **295**, 301 (2002)
2. M. Bugajski, T. Ochalski, T. Piwoński, D. Wawer, B. Mroziewicz, B. Corbett, E. Deichsel Int. Workshop on GaAs based lasers for 1.3 – 1.5 μm wavelength range, April 24 – 26, 2003, Wrocław, Poland
3. V. Spagnolo, G.Scamarcio, D.Marano, H.Page, C.Sintori, Appl.Phys.Lett., **82**, 4639 (2003)

Noise Transfer Characteristics and Pulse Shaping in SOA-Based Regenerators

Rod Webb, Photonic Systems Group, UCC.

Signal regenerators and other all-optical logic devices utilising the cross-phase modulation in a semiconductor optical amplifier (SOA) together with an interferometer continue to be promising components for many applications in high-speed communication systems. In these devices, the recovery time of the nonlinear response is long compared typical signal pulse widths, thus the output depends on the integrated optical energy received at the input. SOA-based regenerators differ significantly therefore from those using much faster nonlinear effects – in silica fibre, for example – where the nonlinear phase change may be regarded as being proportional to the instantaneous signal power. Nevertheless, the model described here is believed to be the first to include the effect of an integrated response on the noise transfer characteristics of the regenerator.

The phase delay of an SOA is a function of the carrier density and, on a timescale short compared to the recovery lifetime, changes are proportional to the integrated input energy. High-speed operation is obtained with differential schemes that convert the phase difference measured over a short time-window to an amplitude difference using an interferometer. Hence, an ideal SOA-based regenerator may be modelled as an integrator operating over the time-window, followed by the phase to output power transfer characteristic of the interferometer, multiplied in turn by the CW probe power or optical clock waveform. The calculation of the integrated optical energy must include the beat noise terms caused by mixing between the input signal and amplified spontaneous emission (ASE) components from the preceding amplifiers, just as when calculating the electrical noise from a detector.

Simulations of the transmission of noisy signals through successive regenerator spans have been carried out for both 2R (re-amplifying and reshaping) and 3R (retiming) regenerators. The results show how the noise, jitter and number of errors accumulate with the number of spans and how the pulse shape evolves. It emerges that 2R regeneration can be sufficient for 10 or more spans.

Diffractive optical elements and waveguides fabricated by Hg lamp induced scission

R Winfield, M Meister and G Crean
Photonics Group, NMRC. Lee Maltings, Prospect Row, Cork.

A photo induced scission technique has been developed for patterning PMMA (polymethyl methacrylate) substrates. This has been used as a technique for locally increasing the solubility of the polymer. It can also be used to modify the refractive index in the exposed areas over a range 1.490 – 1.495. In this report we show that large area (100 cm^2) can be processed easily using a mercury lamp system optimised for emission at 254nm. The process has the advantage of using highly stable fully cured PMMA in sheet form.

We present results on the fabrication of two photonic components: a diffractive optical element and a monomode waveguide. We show a typical example of a fabricated DOEs reconstructed using a HeNe laser at 633 nm. We also show transmission measurements of linear monomode waveguides.

A New Model for VCSELs with Laterally Non-Uniform Parameters

T.C. Woo, J. Sarma, F. Causa
Dept. of Electronic & Electrical Eng.,Univ. of Bath, Bath – BA2 7AY, U.K.
Email: t.c.woo@bath.ac.uk, j.sarma@bath.ac.uk, f.causa@bath.ac.uk

Abstract:

In the pursuit to achieve single mode (wavelength) semiconductor laser operation the earliest design by K.Iga was to produce a relatively short cavity length device that was structured to emit vertically, [1]. Although such Vertical Cavity Surface Emitting Lasers (VCSELs) were expected to produce single wavelength operation, experimental results often showed otherwise, [2]. Further experiments established the role of higher order transverse modes as the cause of multiple wavelength output [3], and theoretical models provided quantitative evidence of modal gain and/or modal reflectivity as mechanisms for lasing mode selection, [4,5]. VCSELs have subsequently undergone various stages of development to provide for robust, single mode operation with proton-implanted [6] and, more recently, oxide aperture devices, [7], yielding the best operational characteristics.

As a consequence of the above developments, however, the resulting awkward geometries pose considerable difficulties with respect to device modelling. Although purely numerical methods (e.g. Finite Element analysis) are most frequently used for the purpose, this paper presents a quasi-analytic (Q-A) modelling scheme based on the function expansion method, [8]. Even though Q-A models can sometimes be less accurate than purely numerical methods, the former are attractive since they tend to allow for a much better 'feel' for the physics of the device and hence are more amenable to designing for improved and/or new device characteristics. The particularly important feature of the present Q-A procedure is that it can account for diffraction-type and guided optical field propagation in the same device - e.g., the oxide aperture in the VCSEL produces diffracting fields while, further along the device, temperature distribution can create a radial index profile which may result in guided wave propagation ,Fig.1. Hence the model applies to a large category of VCSEL structures.

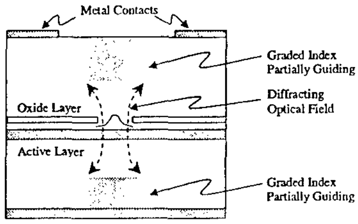

Fig.1

The model to be presented in the paper is based on the use of Laguerre-Gauss Functions (LG- F), [9], to expand the optical field, [10]. Other researchers have used the Laguerre-Gauss Beams (LG-B) as the expansion function set, [11], but the LG-Fs permit a far more convenient and simpler formulation even for inhomogenous media, thus enabling the development of realistic models. Indeed, the correspondingly, general inversion population (carrier) distribution is also represented by a LG-F expansion, [12], in the model and both, radial and azimuthal variations for the optical field and the carriers are self-consistently accounted for. Results obtained from the model that has only radial variations are shown in Figs.2,3 for an oxide aperture device. Note that these are self-consistent solutions, for a specified injection current (density), corresponding to the optical field (intensity) and carrier profiles that emerge from the model after convergence has been achieved. Results from the general model (with radial and azimuthal variations) will be presented at the conference.

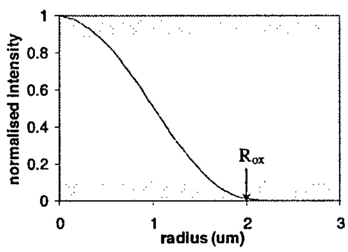

Fig.2

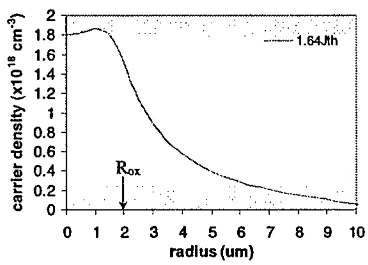

Fig.3

References:

[1] K.Iga, F.Koyama & S.Kinoshita, IEEE Jl.Qtm.Eletm, vol.24, no.9, p.1845, Sept 1988.

[2] C.J.Chang-Hasnain, M.Orenstein, V.V.Lehmen, L.T.Florez, J.P.Harbison & N.G.Stoffel, Appl.Phys.Lett, vol.57, no.3, p.218, July 1990.

[3] Y.A.Wu, C.J.Chang-Hasnain & R.Nabiev, IEEE Photon.Tech.Lett, vol.6, no.8, p.924, Aug 1994.

[4] C.H.Chong & J.Sarma, Proc.Soc.Photo-Opt.Intstrum.Eng., vol 2146, p.397, 1994.

[5] D.I.Babic, Y.Chung, N.Dagli, & J.E.Bowers, IEEE Jl.Qtm.Electrn, vol.29, no.6, p.1950, June 1993.

[6] M.Orenstein, N.G.Stoffel, A.C.Von Lehmen, J.P.Harbison & L.T.Florez, Appl.Phys.Lett, vol.59, no.1, p..31,July 1991.

[7] M.Grabherr, R.Jager, R.Michalzik, B.Weigl, G.Reiner & K.J.Ebeling, IEEE Photon. Tech. Lett., vol.9, no.10, p.1304, Oct 1997.

[8] D.Marcuse, Theory of Dielectric Optical Waveguides, 2nd ed, Academic Press Inc, San Diego,1991.

[9] M.Abramowitz & A.Stegun, Handbook of Mathematical Functions, Dover Pub. Inc., New York,1965.

[10] T.C.Woo, J.Sarma & F.Causa, IEE Proc-Circuits Devices Syst. vol.150, no.6, p.542, Dec 2003.

[11] S.A.Riyopoulos, D.Dialetis, J.Liu & B.Riely, IEEE J. Selected Topics in Qtm.Electrn, vol.7, no.2, p.312, March/April 2001.

[12] T.C.Woo, J.Sarma & F.Causa, 'A Versatile Model for VCSELs', European Semiconductor Laser Workshop, Turin,19-20 Sept. 2003.

Plasmonics: Optical Frequencies but with X-ray Wavelengths

Eli Yablonovitch
UCLA Electrical Engineering Department, 420 Westwood Plaza, Los Angeles, CA 90095-1594

Optical frequency electromagnetic waves, running in close proximity to a metal surface, can have surprisingly shortwave-lengths, as short as 1nm. This opens the door to 1nm imaging, including plasmon lenses, and other in-plane optical components. In effect plasmon waves experience a high effective refractive index, n>100, and can form a type of 'immersion objective' to a conventional optical system. This is only the beginning of new science & technology that is manifested in the 'plasmon regime'. There are many other examples that represent major new nano-meter opportunities, new circuits, and new opto-electronic components.

Light Transmission Through Subwavelength Apertures

Armis R. Zakharian[†], Masud Mansuripur,* and Jerome V. Moloney[†,*]

[†]Department of Mathematics and *Optical Sciences Center
University of Arizona, Tucson, AZ 85721 <armis@acms.arizona.edu>

When optical apertures shrink to dimensions that are comparable or smaller than a wavelength, polarization effects become important, as exemplified by the case of transmission through an elliptical aperture in a thin metallic film: whereas in the case of normal incidence with polarization (i.e., E-field vector) parallel to the long axis of the ellipse there is negligible transmission, when the incident polarization is rotated 90° (i.e., oriented parallel to the short axis of the ellipse), the aperture will transmit a substantial fraction of the incident light. This paper presents the results of computer simulations based on the *Finite Difference Time Domain* (FDTD) method for an elliptical aperture in a thin metallic film under illumination by a normally incident plane wave. Both cases of incident polarization parallel to the long and short axes of the ellipse are considered, and we develop an intuitive description of the behavior of the electromagnetic fields in each case. This study finds application in near-field optical recording.

Plane wave reflection from a (highly conducting) flat mirror. Figure 1(a) shows the case of a normally incident plane wave on a perfect conductor (yellow slab at the bottom). The incident beam induces a surface current I_s in the conductor, which creates equal-amplitude plane waves propagating in the ±Z-directions. In the half-space below the conductor, the induced and incident plane-waves cancel each other out. In the half-space above the conductor, interference between the incident and reflected beams creates standing-wave fringes of the electric-field E and the magnetic field B. The B-field is strongest at the surface of the conductor, reversing sign at intervals of $\Delta z = \lambda/2$, where its adjacent peaks are located. The peaks of the E-field, also located at $\lambda/2$ intervals, are staggered relative to the B-field peaks, thus coinciding with planes of vanishing magnetic field. At the upper surface of the conductor, where the E-field is zero, the B-field is sustained by the surface current I_s. (Although I_s is shown antiparallel to the standing-wave's E-field at $\Delta z = \lambda/4$, in reality I_s is 90° behind this E-field, reaching maximum when the E-field immediately above the surface is going through zero on its way to the peak.) In the half-space above the conductor, absent any electrical charges and currents, the E-field is sustained by the time-variations of the B-field ($\nabla \times \boldsymbol{E} = -\partial \boldsymbol{B}/\partial t$), and vice-versa ($\nabla \times \boldsymbol{B} = \partial \boldsymbol{D}/\partial t$).

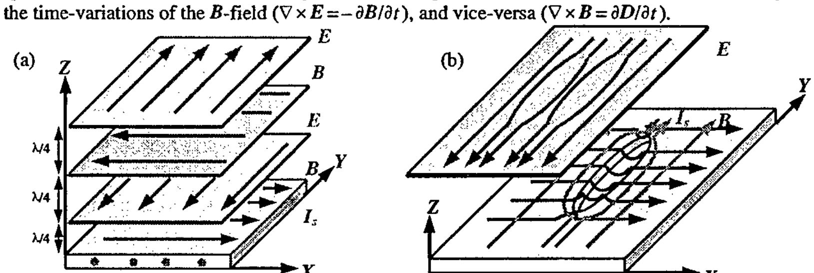

Figure 1. (a) Normally incident plane-wave on a perfect conductor (yellow slab) induces a surface current I_s, which radiates two equal-amplitude plane waves in ±Z-directions. (b) A small elliptical

aperture, having major axis parallel to the surface current I_s, distorts the current distribution by diverting its path to avoid the hole.

Elliptical aperture illuminated with plane-wave polarized along the long axis. The presence of a small (subwavelength) elliptical aperture in the system of Fig. 1(a) distorts the surface current I_s in the vicinity of the aperture by diverting the current's path to avoid the hole, as shown in Fig. 1(b). The *B*-field lines within the fringe immediately above the mirror surface bend in such a way as to remain more or less perpendicular to the lines of I_s, thus bending toward the center of the aperture. The *B*-lines above the aperture, lacking support from an underlying surface current, drop into the hole on the left side and come up again on the right side.

The *E*-field in and around the aperture is redistributed in a way that would support the *B*-field (through Maxwell's curl equations), but, because parallel *E*-field cannot exist on conducting surfaces, it must also stay away from the long side-walls of the hole. Figure 1(b) shows a possible way for the *E*-lines just above the aperture to dodge the side-walls and concentrate near the center, as they drop toward and into the hole from above.

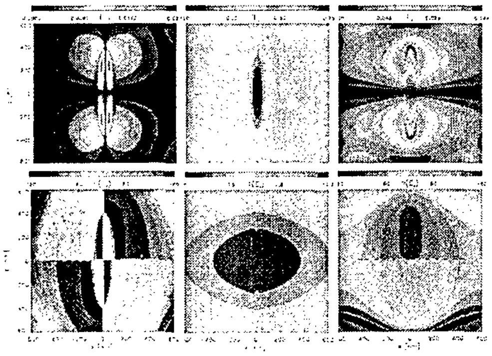

Figure 2. Computed plots of E_x, E_y, E_z in the XY-plane located 20 nm above the top surface of the conductor in the system of Fig. 1(b). Top row: magnitude, bottom row: phase.

Aside from the incident beam, which is fixed at the outset, all other radiation in the system of Fig. 1(b) is generated by the surface currents I_s (and the charges deposited by I_s around the sharp corners of the aperture). The same is true of the system of Fig. 1(a), with its uniform current confined to the upper surface of the conductor. Any differences between the radiation fields in the systems of Figs. 1(a) and 1(b) must therefore arise from the difference between the two surface current distributions. Subtracting the (uniform) surface current of Fig. 1(a) from that of Fig. 1(b) yields two loops of current circulating in opposite directions, as well as positive and negative charges in those regions where the divergence of the local current is non-zero. These circulating currents are equivalent to a pair of oppositely oriented magnetic dipoles (i.e., a magnetic quadruple), and the charges localized on the aperture's sharp corners give rise to an oscillating electric dipole. The main source of radiation through the aperture of Fig. 1(b) seems to be the magnetic quadruple; the induced electric dipole in this system is relatively weak and plays only a secondary role, namely, canceling the electromagnetic field radiated inside the metallic film by the quadruple. In general, quadrupolar sources are weak radiators; this explains the weakness of transmission through an elliptical aperture when the incident beam's *E*-field is parallel to the major axis of the ellipse.

Figure 2 shows computed plots of E_x, E_y, E_z in the XY-plane located just 20 nm above the surface of the conductor in the system of Fig. 1(b). The simulated conductor was a 124 nm-thick film of silver ($n + ik = 0.226 + i\,6.99$ at $\lambda = 1.0\,\mu m$) having an 800 nm-long, 100 nm-wide elliptical aperture. The magnitude of each field component is shown in the top row of Fig. 2, and the corresponding phase profile appears below it. (The main utility of the phase distribution is to indicate the relative orientation of the various field components.) The field distribution depicted in Fig. 2 is consistent with the qualitative behavior sketched in Fig. 1(b). The E_x component bends the central field lines toward the center of the aperture, and pushes the peripheral lines further way, thus ensuring that the long side-walls repel the parallel E-field. The E_y component is strengthened near the center of the aperture because the field lines are pushed upward and squeezed toward the center. Finally, the E_z component is consistent with the presence of electric charges of opposite sign at and around the sharp corners of the aperture. These pictures are consistent with the presence of a weak electric dipole and a magnetic quadruple within the elliptical hole.

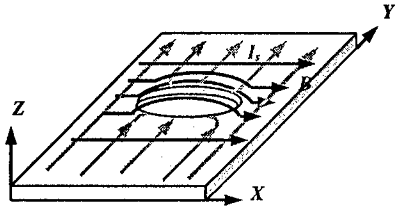

Figure 3. When the incident E-field is parallel to the minor axis of an elliptical aperture, the surface current I_s deposits charges at and around the long side-walls of the aperture.

Elliptical aperture illuminated with plane-wave polarized along the short axis. When the incident E-field is parallel to the minor axis of an elliptical aperture, the surface currents I_s deposit charges on and around the long side-walls of the aperture, as shown in Fig. 3. These charges, which proceed to radiate as an oscillating electric dipole, create a circulating magnetic field around the ellipse's minor axis that pushes the incident B-lines upward and sideways. The induced electrical charges (both on the surfaces near the aperture and on the long side-walls inside the hole) create oscillating E-fields in the short gap between these walls and also in the regions immediately above and below the aperture. The time rate of change of this field, $\partial D/\partial t$, which is equivalent to an electrical current J across the gap, creates circulating magnetic fields that wrap around the (oscillating) electric dipoles.

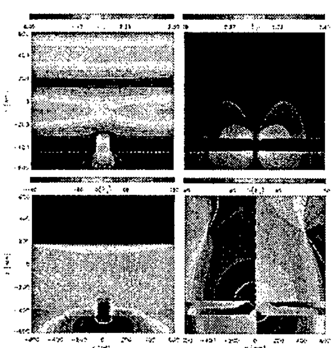

Figure 4. Amplitude and phase of E_y, E_z in the central YZ-plane in the system of Fig. 3.

Figure 4 shows that inside and below the aperture E_y is strong, and has reversed its direction compared to the E-field immediately above the aperture; its energy appears to have been extracted from the E-fringe directly above the hole. The distribution of E_z shows the presence of electric charges on the conductor's surfaces; these charges have the same sign on the top and bottom surfaces on either side of the hole, but their sign is reversed in going from the left-side to the right-side. All in all, an elliptical aperture with the incident E-field parallel to its short axis is a much stronger transmitter than the same aperture when its long-axis is parallel to the incident E-field.

Silicon-on-insulator photonic crystal guides, filters, planar micro-cavities and light extractors

Marc Zelsmann, NMRC

Photonic crystals, i.e. periodic dielectric structures, allow the control of light. For example, propagation of photons can be suppressed in certain directions and for frequencies contained in what is called the photonic band gap. This work report on the conception, fabrication and characterization of guides, filters, planar micro-cavities and light extractors based on two-dimensional silicon-on-insulator (SOI) photonic crystals.
In a first part, we focus on passive structures. An original optical bench was build in order to perform transmission measurements on a wide wavelength range (1.1 to 1.7 µm). Monolayer waveguides, mirrors and unidimensional cavities are investigated.
The second part concerns the out-of-plane light emission from photonic crystal structures. Confinement of photons in planar micro-cavities and light extraction properties of particular points on the photonic crystal band diagram are studied. Both approaches are investigated on SOIsubstrates and on a new kind of substrates, called "SODBR substrates", developed especially for our applications and composed of a monocrystalline silicon layer bonded on a buried distributed Bragg reflector. On SOI substrate, a light extraction efficiency higher than 45 % have been measured on one side and in a reduced solid angle.
All the results presented are systematically compared to FDTD (Finite Difference Time Domain) simulations and to calculated band diagrams.